Computational studies on formation and intermolecular [1+2] cycloadditions of nitrilimines

Sima Mehrpajouh

A Thesis

In the Department
of
Chemistry and Biochemistry

Presented in Partial Fulfillment of the Requirements
For the Degree of Master of Science (Chemistry) at
Concordia University

Montreal, Quebec, Canada

December 2012

CONCORDIA UNIVERSITY
School of Graduate Studies

This is to certify that the thesis prepared

By: Sima Mehrpajouh_____

Entitled: Computational studies on formation and intermolecular [1+2] cycloadditions of nitrilimines_____

and submitted in partial fulfillment of the requirements for the degree of

Master of Science_____

complies with the regulations of the University and meets the accepted standards with respect to originality and quality.

Signed by the final examining committee:

Dr. Georges Dénès_____ Chair

Dr. Pat Forgione_____ Examiner

Dr. Ann. M. English _____ Examiner

Dr. Heidi M. Muchall_____ Supervisor

Dr. Gilles H. Peslherbe_____ Supervisor

Approved by _____
Chair of Department or Graduate Program Director

_____
Dean of Faculty

Date _____

Abstract

Computational studies on formation and intermolecular [1+2] cycloadditions of nitrilimines

Sima Mehrpajouh, M.Sc. Chemistry
Concordia University, 2012

2,5-disubstituted tetrazoles decompose thermally to give nitrilimines (R^1–CNN–R^2), whose electronic structure widely varies with the substituents R^1 and R^2. In particular, for R^1, R^2 = H, the carbenic contribution to the resonance structure is small, while for NH_2-disubstitution Natural Resonance Theory predicts 70% carbene character. This has large implications for the reactivities of substituted nitrilimines. The goal of this work is to identify nitrilimines with large carbenic contributions to their resonance structure that can undergo [1+2] cycloaddition reactions with unsaturated systems, in contrast to the common [3+2] cycloadditions of nitrilimines with only a small carbenic character.

In this study, twelve tetrazoles known in the literature have been analyzed with respect to changes in geometry and orbital interactions. A Natural Bond Orbital analysis of the corresponding nitrilimines indicates that several possess an electron lone pair on carbon, which could be indicative of a sizeable carbenic contribution to the resonance structure. Based on this finding, the decomposition of the respective tetrazoles has been investigated. We have shown that, depending on the substituents, decomposition is either stepwise or concerted: C-substituted tetrazoles with electron donating groups follow a concerted pathway while electron withdrawing groups promote a stepwise path.

Nitrilimines have been widely used in 1,3-dipolar ([3+2]) cycloadditions, in which they add to a dipolarophile, typically an alkene or alkyne, to form five-membered heterocyclic rings. In fact, all nitrilimines studied experimentally to date have been

shown to undergo [3+2] cycloaddition reactions and their mechanism has been extensively studied in the past. On the other hand, nitrilimines can be described through a carbenic valence-bond structure, and while intermolecular carbenic reactions from nitrilimines are unknown, intramolecular reaction products from ortho-vinyl MeCOO–CNN–Ph and Ph–CNN–Ph that seem to have followed two typical carbene reaction mechanisms, [1+2] cycloaddition and C–H insertion, have been reported. In an attempt to promote the intermolecular [1+2] cycloaddition, reactions of F–CNN–F and NH_2–CNN–NH_2, both possessing substantial carbenic character, with ethene and electron-poor alkenes were compared to those for the unsubstituted H–CNN–H with smaller carbene character. The intermolecular [1+2] reaction is observed for H–CNN–H and F–CNN–F with tetrafluoroethene. NH_2–CNN–NH_2, as a nucleophilic species and possibly a stable carbene, does not tend to react with alkenes. To render these findings feasible for experiments, the carbenic character of readily accessible nitrilimines was determined from natural resonance theory.

Nitrilimines with even a small carbenic character can undergo [1+2] cycloaddition with tetrafluoroethene. For example, COOH–CNN–OH and CHO–CNN–OH, with as little as 13% carbenic character, undergo [1+2] cycloaddition preferentially (B3LYP/6-31+G(d)).

Dedication

To my parents and my husband, Mostafa.

Acknowledgement

I would like to thank my supervisors, Dr. Heidi M. Muchall, and Dr. Gilles H. Peslherbe for providing me with this opportunity to work in their research group. I would also like to thank my committee members, Dr. Pat Forgione and Dr. Ann M. English for their advice during this study.

Thanks and appreciation is extended to my colleagues in the lab for their help and their friendship: Soran Jahangiri, Stephen Boateng, Pradeep R. Varadwaj, Xijun Wang, and Maria Shadrina. A special note of appreciation goes to my friend, Soran Jahangiri, for the time and effort he put into giving me feedback on this work.

I wish to acknowledge the financial support from Concordia University. Calculations were performed at the computational facilities of Centre for Research in Molecular Modeling (CERMM).

I would like to express my deepest thanks and love to my family for their constant love and support:

To my husband, Mostafa, who is everything for me and without his love and understanding I would not be able to make it.

To my loving mother, who has given me so much, thanks for her faith in me and for teaching me that I should never surrender.

To my sister and brother, who unconditionally encourage me and also they have stood by me through the hard times and over miles.

Table of Contents

List of figures

List of tables

List of schemes

Glossary

B3LYP	Becke's three-parameter hybrid exchange/Lee-Yang-Parr correlation functional
PBE0	Perdew, Burke and Ernzerhof/ a parameter free density functional model
DFT	Density functional theory
NBO	Natural Bond Orbital
NRT	Natural Resonance Theory
PES	Potential energy surface
TS	Transition state
ZPVE	Zero-point vibrational energy
IR	Infrared
UV	Ultra-violet

Chapter 1.

Nitrilimines; General Background

1.1. Nitrilimine, a 1,3-dipole

1,3-dipoles are defined as possessing an **a-b-c** connection, where atom **a** possesses a formal positive charge (electron sextet) due to an incomplete valence shell and atom **c** carries a negative charge owing to an unshared electron pair. Atom **b**, on the other hand, has an unshared electron pair and its bond with atom **a** could be either single or double according to the sextet structure. Since the sextet structures are unstable, atom **b** plays a major role in the stabilization of 1,3-dipoles by sharing electrons with atom **a** and forming an additional bond, resulting in an octet structure for atom **a**. Atom **b** is usually either nitrogen or oxygen, and atoms **a** and **c** are carbon, nitrogen or oxygen (Scheme 1-1).[1]

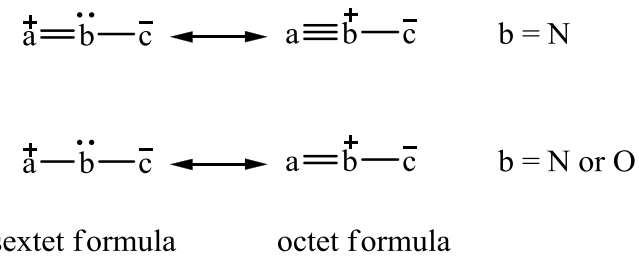

Scheme 1-1. 1,3-dipoles with single or double bond and internal octet stabilization.

The importance of 1,3-dipolar compounds is their ability to form heterocyclic 5-membered rings. 1,3-dipoles could react with any dipolarophile, double or triple bond,

and lose charges to form a 5-membered ring. Normally, such a reaction proceeds in a concerted fashion, and the combination of 1,3-dipoles with multiple bond systems is then called a 1,3-dipolar cycloaddition reaction. Scheme 1-2 shows the general design of a 1,3-dipolar reaction.[1] In general, 1,3-dipoles are classified into two groups: 1,3-dipoles with a single bond such as nitrones, ozone, and nitro compounds, and 1,3-dipoles with a double bond, namely nitrile ylides, nitrilimines, and azides.[1] Nitrilimines are the subject of our interest in the current work.

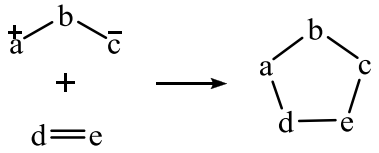

Scheme 1-2. General design of 1,3-dipolar cycloadditions.

Nitrilimines are a class of organic compounds that possess the general sequence $R^1CN\text{-}NR^2$ where an imine is bonded to the N-terminus of a nitrile. Nitrilimines have been widely used in 1,3-dipolar cycloadditions[1] in which they add to a dipolarophile, typically an alkene or alkyne, to form 5-membered heterocyclic rings. Nitrilimine, H–CNN–H, itself is an unstable isomer of diazomethane,[2] which can undergo rearrangement to form carbodiimide,[3-5] intramolecular cyclization[6-9] or fragmentations to nitriles and nitrenes.[4] Since nitrilimines contain an electron sextet on the carbon atom, they are not stable and are well-known as reactive intermediates.[3-5, 10] This restricts the nitrilimine characterization techniques to infrared (IR) and ultraviolet (UV) spectroscopies in 85K matrix,[3, 4] mass spectrometry,[3] and real-time photoelectron spectroscopy[10] in the gas phase. Alternatively, nitrilimines are inferred from their characteristic reactions.[1, 11-13]

Since nitrilimines have been used to produce heterocyclic compounds, several studies have been devoted to the preparation and isolation of nitrilimines (discussed in section 1.3). Nitrilimines were first generated by Huisgen and co-workers in 1959 by thermal decomposition of 2,5-disubstituted tetrazoles[13] and by base-induced elimination of hydrogen halide from hydrazonoyl halides.[14] The formation of nitrilimines was detected by characteristic reactions in which the alkenes, alkynes and nitriles added in situ to the former nitrilimines.

1.2. Electronic Structure of Nitrilimines

The structure of the parent nitrilimine (H–CNN–H) has been explored in several computational studies during the past decades.[15-24] Nitrilimines, as a conclusion of these studies, are described by six valence-bond structures,[1, 20-22, 24] propargylic, allenic, 1,3-dipolar, carbenic, reverse 1,3-dipolar, and hypervalent (Scheme 1-3).

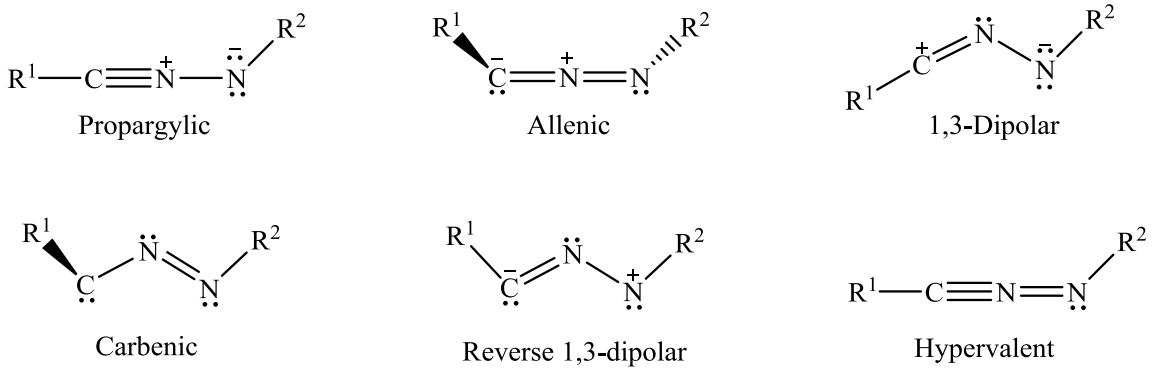

Scheme 1-3. Valence-bond structures of nitrilimines.

The propargylic structure was first reported as a lowest-energy conformation of nitrilimine with planar geometry,[2, 15, 16, 19, 20] until Houk and co-workers claimed that the

nonplanar allenic structure is another stable conformation of nitrilimine with similar energy to the propargylic structure.[15, 16] Further investigations revealed that the nonplanar allenic structure is prefered over the propargylic structure through employing high-level ab initio calculations.[24] Information obtained from X-ray crystallography demonstrated that stable nitrilimines have a bent and nonplanar geometry corresponding to the allenic structure.[11] However, electron-withdrawing substituents can change the geometry to represent the propargylic structure.[24]

The carbenic structure of nitrilimine was proposed by Huisgen as an uncommon structure, and it was proposed that its contribution in reactions should be negligible.[1] This structure consists of a sextet neutral carbon atom with an unshared electron pair.

The hypervalent structure was proposed by Pople and co-workers using the Hartree-Fock computational method.[20] In principle, the valence bond structures for 1,3-dipoles include as hypervalent structure with completely formed double and triple bonds, in which the central nitrogen is allocated more than its normal complement of valence electrons.[20] The hypervalent structure could exist if nitrogen expands the coordination, which has not been observed for the nitrogen atom.

Previous studies in our group indicated that among the six valence-bond structures of nitrilimines, propargylic, allenic, 1,3-dipolar and carbenic are the only four necessary to describe the electronic structure of nitrilimines.[22]

1.3. Generation of Nitrilimines

There are several different ways by which nitrilimines can be generated. These are introduced in the following section.

1.3.1. From Decomposition of Tetrazoles

Decomposition of tetrazoles has been one of the most common methods to produce nitrilimines. The decomposition can be carried out thermally in solution or by vacuum flash pyrolysis in the gas phase.

1.3.1.1. Thermal Decomposition

Huisgen reported that nitrilimines are intermediates in the thermal decomposition of 2,5-disubstituted tetrazoles.[13] According to structural and electronic relationships, nitrilimines (in general) are analogous to azides and nitrile oxides and have not been isolated due to their high reactivity. Based on the substituents, thermolysis of tetrazoles occurs at 150 °C (2-methyl-5-phenyltetrazole) or 200 °C (2,5-diphenyltetrazole).[13] Nitrilimines as an intermediate in these decompositions were suggested from 1,3-addition products in the presence of reagents carrying double bonds. As can be seen in Fig. 1-1, the decomposition of 2,5-diphenyltetrazole in benzonitrile gives 1,3,5-triphenyl-1,2,4-triazole in 63% yield, and in dicyclopentadiene, the tetracyclic compound is obtained in 68% yield; both compounds are suggested to be the result of reaction between nitrilimine and the unsaturated species.[13]

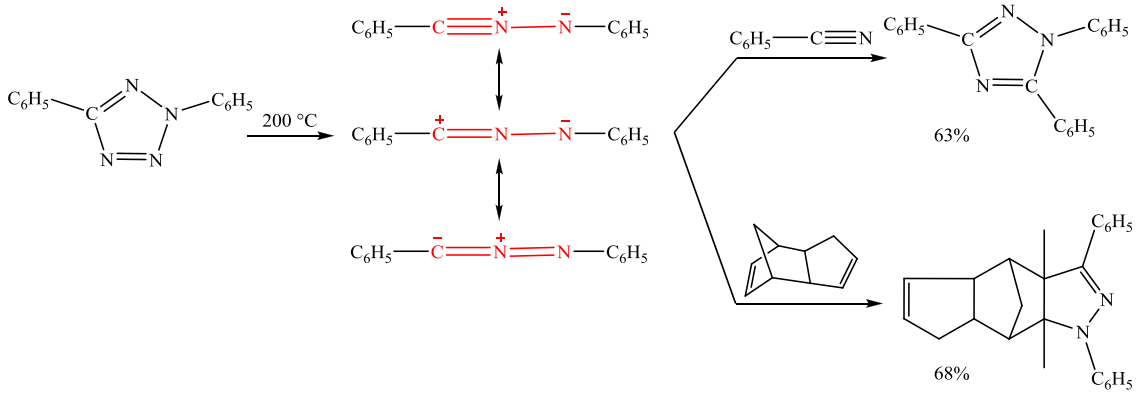

Figure 1-1. Thermal decomposition of 2,5-diphenyl tetrazole and cycloaddition in the presence of dipolarophiles.

1.3.1.2. Flash Vacuum Pyrolysis

A nitrilimine was produced in the gas phase by flash vacuum pyrolysis of C-phenyl-2-trimethylsilyltetrazole at 710 K and 10^{-3} Torr.[3] The nitrilimine could be obtained as a solid at 77 K and appears stable at this low temperature, although it disappears once the temperature is elevated to 170K (Fig 1-2). However, the 5-membered ring yields in the presence of alkyne in this temperature.

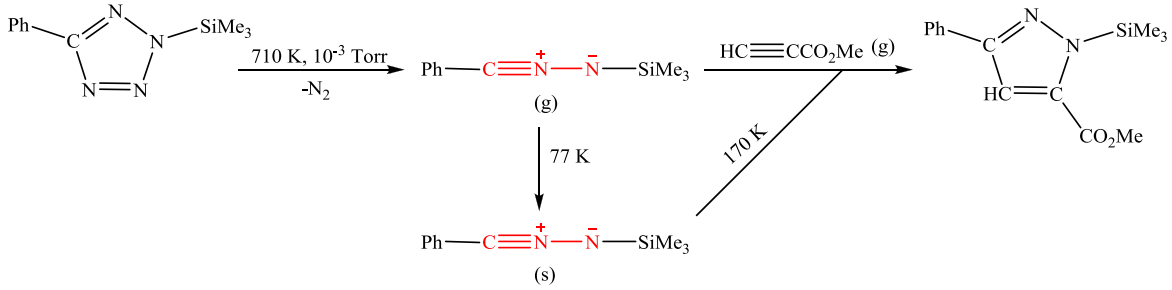

Figure 1-2. Flash vacuum pyrolysis of C-phenyl-2-trimethylsilyltetrazole.

1.3.2. From Base-induced Elimination of Hydrogen Halide from Hydrazonoyl Halides

In order to avoid the high temperature required for the decomposition of tetrazoles, treatment of carboxylic acid hydrazide halides with bases was employed to generate nitrilimines at room temperature.[13, 25] Figure 1-3 shows the preparation of nitrilimines from N-(α-chlorobenzylidene)-N'-phenylhydrazine by 1,3-elimination of hydrogen chloride. In the presence of ethyl phenyl propiolate, the corresponding nitrilimine undergoes 1,3-dipolar cycloaddition to form pyrazole drivatives.[14]

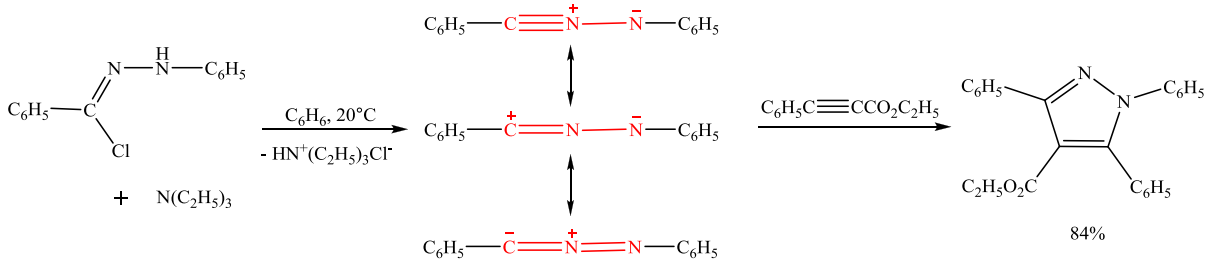

Figure 1-3. Elimination of hydrogen halide from hydrazonoyl halides to form nitrilimine.

1.3.3. From Elimination of Carbon Dioxide from 1,3,4-Oxadiazolin-5-ones

Flash vacuum pyrolysis of N-allyl-substituted 1,3,4-oxadiazolin-5-ones generates a nitrilimine along with carbon dioxide.[26] The pyrolysis occurs at 500-700 °C at 10^{-2} Torr. The nitrilimine undergoes rearrangement to a diazoalkene via a 3,3-sigmatropic shift and forms the carbene species by releasing nitrogen (Fig. 1-4).

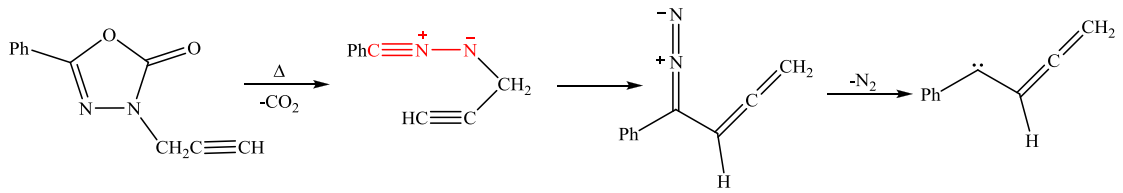

Figure 1-4. Elimination of carbon dioxide from 1,3,4-oxadiazolin-5-ones to form a nitrilimine.

1.3.4. From Thermolysis of a Substituted 1,3,4,2-Oxadiazaphosphole

The thermal decomposition of 3-phenyl-5-trifluoromethyl-2,3-dihydro-1,3,4,2-oxadiazaphosphole at 140 °C for 24h gives the corresponding nitrilimine, which forms the mixture of heterocyclic compounds (73% yield) in the presence of styrene (Fig. 1-5).[27] Tanaka claimed that this route is advantageous since the decomposition occurs at low temperature and under neutral conditions.

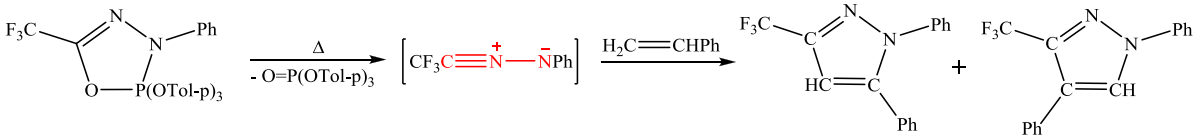

Figure 1-5. Formation of a nitrilimine by thermolysis of a 1,3,4,2-oxadiazaphosphole.

1.3.5. From Lithiated Diazo Derivatives

Figure 1-6 shows that the lithium salt of thiophosphinediazomethane reacts with alkylchlorophosphines to give nitrilimines, which undergo cyclization in the presence of olefins at room temperature. The nitrilimine is stable and its melting point is 100 °C without decomposition.[28]

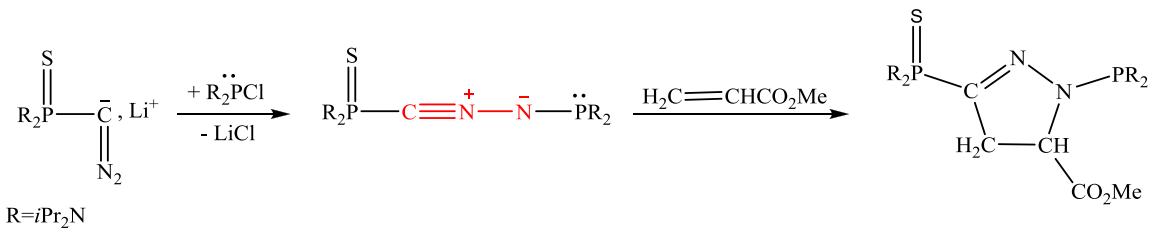

Figure 1-6. Generation of nitrilimines from lithiated diazo derivatives.

Moreover, the reaction of the lithium salt of triisopropylsilyldiazomethane with triisopropyl chloride occurs at around –100 ºC in dry tetrahydrofurane in the presence of crown ether and generates the corresponding nitrilimine, which is stable and can be purified at 90-100 °C without noticeable decomposition.[29] Stable nitrilimines can be synthesized by using hindered diazo lithium salts.[29-33]

The nitrilimine shown in Fig. 1-6, with phosphorus substitution and with 85% isolated yield, was the first stable nitrilimine generated by Bertrand and co-workers in 1988.[28] It undergoes 1,3-dipolar cycloadditions in the presence of unsaturated compounds such as methyl acrylate or methyl propiolate at room temperature. The stability of phosphorus-substituted nitrilimines is probably due to the bulky substituents and steric effects as well as the delocalization of charges over two phosphorus atoms.[28] The group also generated a C- and N-silylated nitrilimine that was stable enough to be isolated and purified by distillation at 90-100 °C, with no noticeable decomposition (80% yield).[29] The nitrilimine reacts at room temperature in the presence of a large excess of alkenes to form 5-membered heterocyclic compounds.

1.3.6. From Hydrazones

C-Bromo-N-phenylnitrilimine is generated in situ at –5 °C by reaction of the corresponding hydrazone with N-bromosuccinimide (NBS) in dimethylformamide

(DMF) and triethylamine (TEA) and undergoes 1,3-addition in the presence of alkynes (Fig. 1-7).[34]

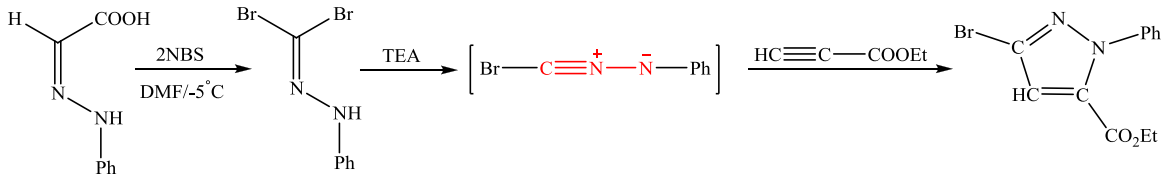

Figure 1-7. Synthesis of a bromonitrilimine.

1.4. Reactions of Nitrilimines

Depending on the substituents, nitrilimines can undergo cycloaddition to heterocyclic compounds[1, 6, 12, 35, 36] or thermally rearrange to azines by a 1,4-hydrogen shift[5] or to diazo compounds by a 1,3 sigmatropic shift.[26, 32, 37, 38] In addition, nitrilimines can dimerize to either bis(azo)ethenes[39, 40] or 1,4-dihydro-1,2,4,5-tetrazines[41, 42] in the absence of dipolarophiles.

1.4.1. Cycloaddition

Cycloaddition reactions are mostly classified based on the size of the ring formed. As an example, 4- and 6-membered rings are formed by thermal or photochemical formation from alkenes ([2+2]) and in Diels-Alder reactions ([4+2]), respectively. 5-membered rings are produced by [3+2] cycloadditions, also known as 1,3-dipolar cycloaddition, which cannot possibly occur with octet-stabilized reactants.[1] The carbene-type cycloaddition is an example of formation of 3-membered rings ([1+2]). Since nitrilimines could only undergo [3+2] and [1+2] cycloadditions, here we briefly explain these reactions.

1.4.1.1. 1,3-Dipolar ([3+2]) Cycloaddition

In terms of the 1,3-dipolar cycloaddition, treatment of nitrilimines with different dipolarophiles such as alkenes, alkynes, carbonyls, and nitriles has been widely studied in the 2000s.[43-56] Aside from these studies on their synthetic usefulness, a number of studies have been devoted to the mechanism and stereochemistry of 1,3-dipolar cycloadditions. In the following section, we introduce the 1,3-dipolar cycloaddition of nitrilimines with some dipolarophiles, the mechanism, and stereochemistry of this reaction.

1.4.1.1.1. Addition to Alkenes and Alkynes

The reaction between nitrilimines and alkenes produces pyrazoline, a heterocyclic 5-membered ring containing three carbon atoms, two adjacent nitrogen atoms, and one double bond in the ring. The general reaction is shown in Scheme 1-4. The reaction of nitrilimines with alkynes generates pyrazoles, compounds containing an aromatic heterocyclic ring composed of three carbon atoms and two nitrogen atoms in adjacent positions (Scheme 1-5). Huisgen demonstrated that a substituted pyrazole is obtained in 84% yield by decomposition of the corresponding tetrazole in the presence of ethyl phenylpropiolate (Scheme 1-6).[13] It was also found that nitrilimines react with disubstituted olefins, but the cycloaddition fails with tri- and tetraalkylated ethenes.[1]

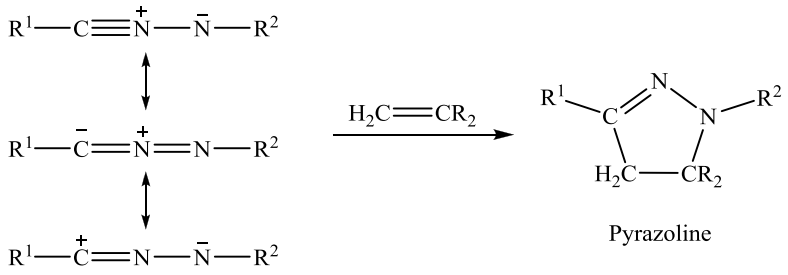

Scheme 1-4. A pyrazoline, a product of the 1,3-dipolar cycloaddition between a nitrilimine and an alkene.

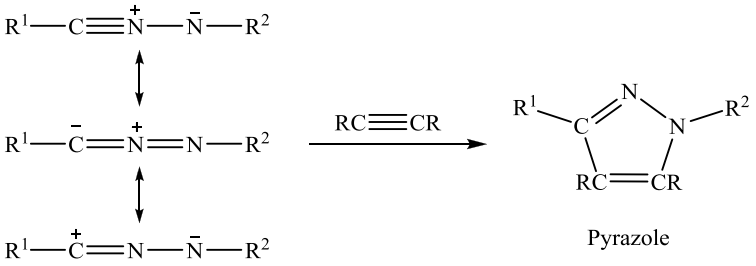

Scheme 1-5. A pyrazole, a product of the 1,3-dipolar cycloaddition between a nitrilimine and an alkyne.

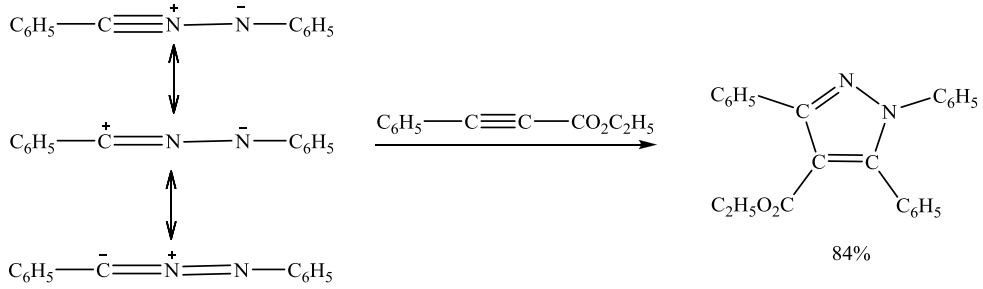

Scheme 1-6. Formation of diphenylnitrilimine and 1,3-dipolar cycloaddition with ethylphenylpropiolate.

1.4.1.1.2. Addition to Carbonyls and Thiocarbonyls

Since nitrilimines are not restricted to be added to CC multiple bonds, compounds with a C=O or C=S group can act as a dipolarophile. For example, diphenylnitrilimine with benzaldehyde gives a substituted oxadiazoline, regardless how the nitrilimine is

generated, by thermolysis of diphenyltetrazole or using substituted phenylhydrazine (Fig. 1-8).[13] Since the mechanism of Diels-Alder and 1,3-dipolar cycloaddition reactions are closely related, Huisgen claimed that good dienophiles could be active dipolarophiles, and vice versa.[1] However, there are exceptions like the C=S double bond, which shows slight dienophile character whereas it is highly reactive as a dipolarophile.[1] For example, diphenylnitrilimine in the presence of carbon disulfides leads to formation of spiranes. Moreover, monoadducts at the C=S double bond were obtained with diphenylnitrilimine in 58% yield (Fig. 1-9).

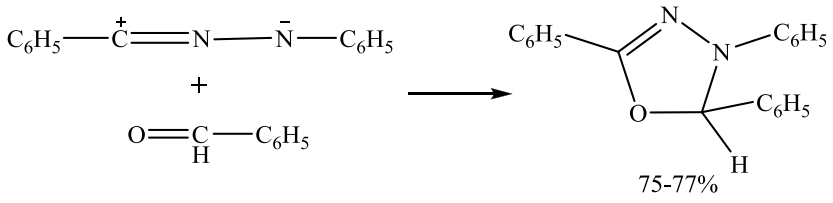

Figure 1-8. 1,3-Dipolar cycloaddition with diphenylnitrilimine and a carbonyl as dipolarophile.

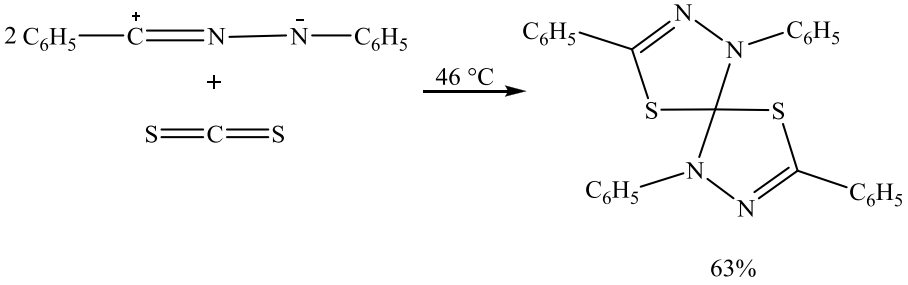

Figure 1-9. 1,3-Dipolar cycloaddition with diphenylnitrilimine and CS_2 as dipolarophile.

For the question of regiochemistry, formation of a bond between the nitrogen of the nitrilimine and a nitrogen, oxygen or sulfur atom of the dipolarophile is unfavourable due

to the fact that additions to hetero-multiple bonds occur in order to form the most stable new σ-bonds.[1] 1,3-Dipolar cycloadditions can also happen intramolecularly (Fig. 1-10).[6]

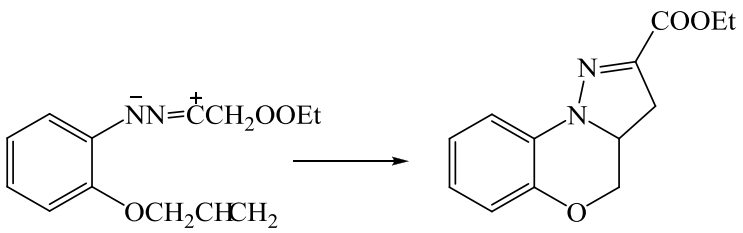

Figure 1-10. Intramolecular 1,3-dipolar cycloaddition of a nitrilimine.

1.4.1.1.3. Mechanism of the 1,3-Dipolar Cycloaddition

The mechanism of 1,3-dipolar cycloaddition is concerted and stereoselective.[12, 57] A concerted addition is described in terms of molecular orbitals indicating delocalization of four π-electrons of the allyl anion type (four π-electrons in three parallel p-orbitals) at centers C and N, reacting with the π-bond of the dipolarophile (Fig. 1-11).[12] Accordingly, a biradical mechanism cannot be applied. Regarding the stereoselectivity of the 1,3-dipolar addition with geometrically isomeric alkenes, the kinetic study showed that the trans-isomer is more highly reactive than the cis one.[12] During the addition, the olefinic (double bond) carbon atoms change hybridization from sp^2 to sp^3, and consequently, the bond angle from 120° to 109°. This results in an increase in the van der Waals repulsion in the case of the cis-alkene, with a higher activation energy to cycloaddition in contrast to that for the trans-isomer. Figure 1-12 shows the steric changes occurring during the cycloaddition of a 1,3-dipole, **a-b-c**, with a 1,2-disubstituted ethane (larger parenthesis represents the larger repulsion betweens substituents).

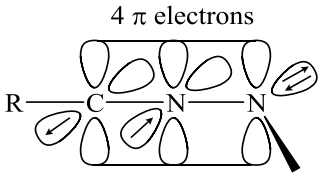

Figure 1-11. Delocalization of four π-electrons of the allyl anion type.

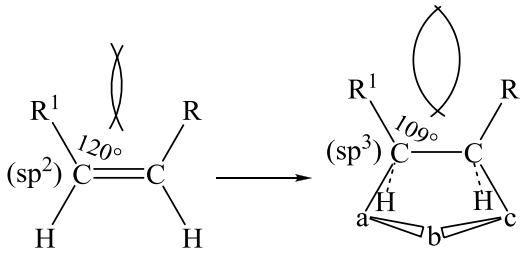

Figure 1-12. Steric changes occurring during the cycloaddition of a 1,3-dipole, a-b-c, with a 1,2-disubstituted ethene.

1.4.1.2. Carbene-type 1,1-Cycloaddition ([1+2] cycloaddition)

It has been suggested that the electron-deficient carbon atom of specific nitrilimines should react with a neighbouring ethylenic function to form a cyclopropane derivative (Fig. 1-13).[7] This conclusion seemed supported by the fact that the endo isomer was formed, implying retention of stereochemistry in the addition, as it would be observed for a singlet carbene. In a recent study, Muchall showed that this is not definitely [1+2] cycloaddition and she proposed to describe this reaction as a 1,7-electrocyclization.[58] Similar 1,1-cycloadditions have been reported for nitrile oxides[59] and ylides.[60]

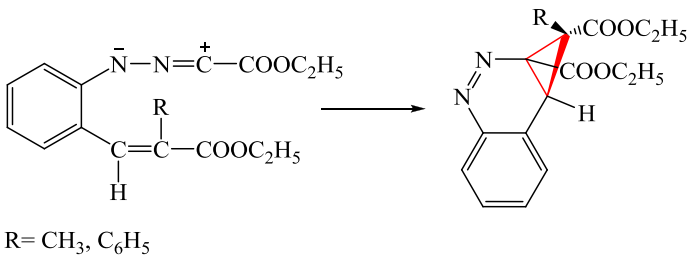

Figure 1-13. Proposed intramolecular carbene-type 1,1-cycloaddition of a nitrilimine.

Nitrilimine has been described as a 'flexible' molecule that can accept its geometry depending on the nature of the reaction.[16] According to Caramella and Houk studies, nitrilimine adopts a planar geometry in the presence of an electrophilic reagent resulting in an increase in the HOMO energy. On the other hand, nucleophilic reagents promote the bent structure by lowering the nitrilimine LUMO energy. It was reported that nitrilimines are resonance hybrids of bent dipolar and carbene structures, and undergo intramolecular cyclization with the formation of indazoles in the absence of trapping agents.[9] Studies on 1,1-cycloaddition of nitrilimine has been followed until it was found that the reaction of substituted hydrazone with base gives a 91% yield of the corresponding 7-membered ring.[61, 62] Nitrilimine is an intermediate in this reaction and the 3-membered ring is generated by intramolecular 1,1-cycloaddition of the corresponding nitrilimine with the neighbouring double bond which is eventually converted to a 7-membered ring. The 1,1-addition product was noticeably suppressed in the presence of excess alkene due to the fact that 1,1-cycloaddtion occurs once the attack by double bond is constrained to occur perpendicular to the plane of nitrilimine which is unfavourable in terms of energy in contrast to intermolecular addition with the normal "two-plane" orientation.

1.4.2. 1,4-Hydrogen Shift

1,4-hydrogen shift for nitrilimines can occur once the intramolecular cycloaddition is inhibited (e.g. with alkyl groups as N-substituents).[5] It was found that azines and carbodi-imides are the only primary rearrangement products of N-alkyl nitrilimines. The supportive ab initio calculations on unsubstituted nitrilimine revealed that carbodi-imide is more stable than the parent nitrilimine (HCNNH) in terms of energy (Fig. 1-14).

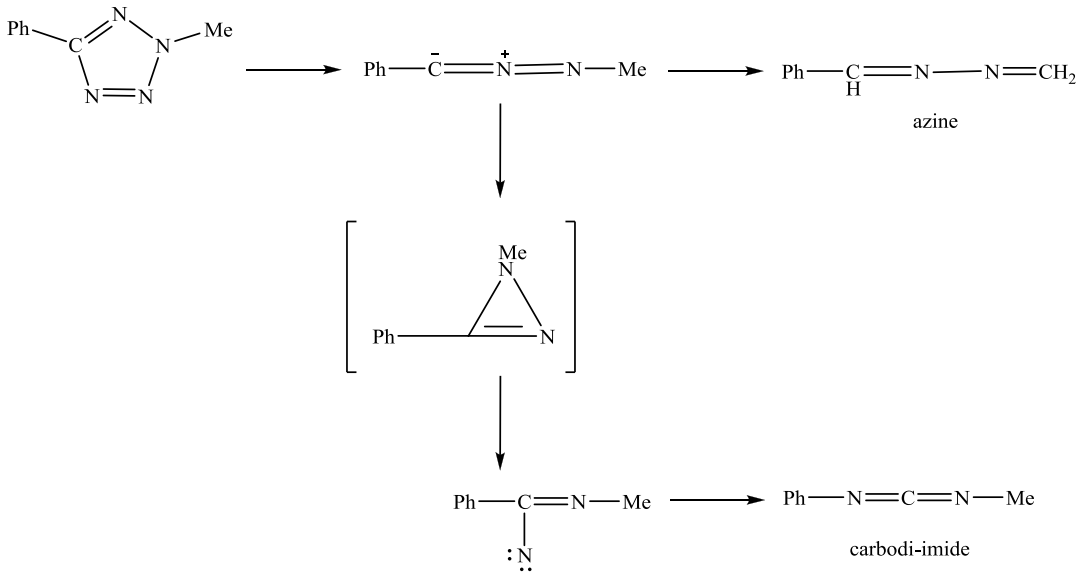

Figure 1-14. 1,4-Hydrogen shift in a nitrilimine.

1.4.3. Sigmatropic Shift

Nitrilimines generated by flash vacuum pyrolysis of N-allyl-substituted 1,3,4-oxadiazolin-5-ones undergo a 3,3-sigmatropic shift to give a rearranged diazoalkene.[37, 63] A carbene is generated as a further intermediate by loss of nitrogen which provides an explanation for the variety of products formed (Fig. 1-15). The analogous nitrile-N-imide

in Fig. 1-16 undergoes a corresponding 1,3-sigmatropic benzyl shift to give the diazoalkane.[38]

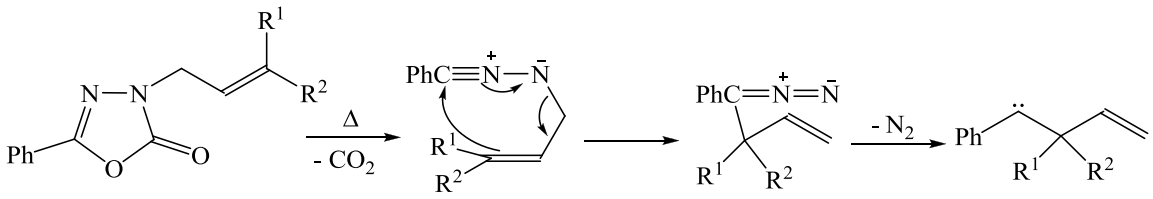

Figure 1-15. 3,3-Sigmatropic shift in a nitrilimines.

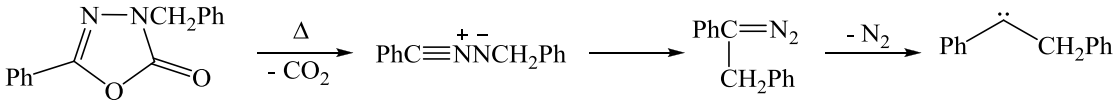

Figure 1-16. 1,3-Sigmatropic benzyl shift in a nitrilimine.

1.4.4. Dimerization

Since the reactivity of most nitrilimines is so great, these 1,3-dipoles can undergo dimerization in the absence of dipolarophiles. Dimerization can occur via either head-to-tail, i.e., [3+3], interaction to give 1,4-dihydro-1,2,4,5-tetrazine derivatives[41, 42] (Fig. 1-17) or carbene attack to give bis(azo)ethenes (Fig. 1-18).[39, 40]

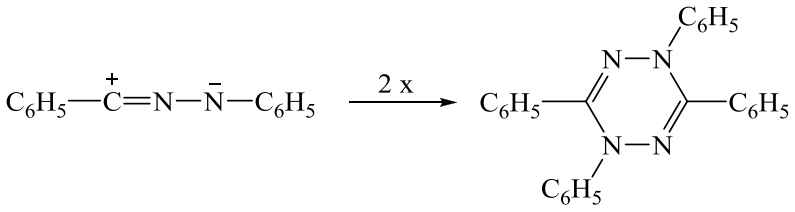

Figure 1-17. Head-to-tail dimerization of nitrilimines.

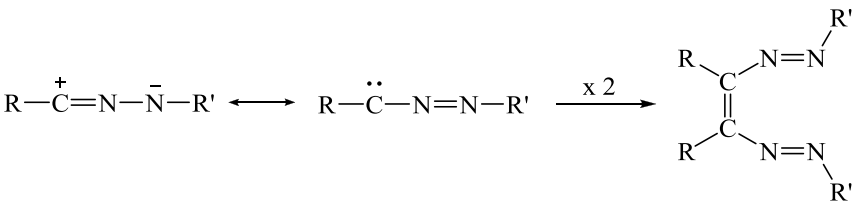

Figure 1-18. Carbene dimers of nitrilimines.

1.5. Observation of Nitrilimines

Direct observation has not been reported for unstable nitrilimines generated thermally in solution.[4] In order to observe nitrilimines in thermal reactions, it was claimed that their generation would have to be carried out in the gas-phase with short contact times and isolation at low-temperaure, in other words, through flash-vacuum thermolysis.[3] However, N-aryl substituted nitrilimines in the gas phase cyclize readily to form indazoles, and consequently, they could not be observed directly. Similarly, N-methyl and related nitrilimines have been reported to isomerize to azines and carbodiimides.[5] Wentrup and Fischer indicated the existance of discrete N-silylated nitrilimines with a nonisomerizing N-substituent, and they provided the identity of the N-silylated isolated nitrilimine by co-condensing it at 77 K with an alkyne as a trapping agent.[3] The N-silylated nitrilimines were observed in an IR spectrum at 77 K, whereas the product spectrum was obtained at 170 K.[3] It was suggested that the stability of nitrilimines is strongly dependent on the steric hindrance provided by the nitrogen substituents.[32] Certainly, one way to kinetically stabilize a nitrilimine is to protect the highly reactive center by bulky substituents. It has been shown that certain specific substituents stabilize

nitrilimines in the crystal or liquid states.[28-34, 64, 65] In particular, it was reported that heteroatom substituents such as B, Si and P at carbon or nitrogen rendered nitrilimines stable at room temperature.[29, 66] These nitrilimines were prepared by the reaction of lithiated diazo compounds with electrophiles.

1.6. Application of Nitrilimines

Nitrilimines are mostly used in the pharmaceutical industry as intermediates in the synthesis of drugs and medicines. In the following section, we shortly introduce a number of applications of nitrilimines.

Substituted pyrazoles are generated through reactions of nitrilimines as 1,3-dipoles with dipolarophiles. The pyrazole is the main core structure of many drugs, such as Celebrex (Celecoxib),[67, 68] used in the treatment of osteoarthritis or acute pain, and Rimonabant,[69] a high-potency cannabinoid type-1 (CB1) receptor inverse agonist, as a treatment for obesity. Furthermore, the pyrazole is the structural motif of many highly potent inhibitors of coagulation factor Xa.[67, 70] Among them, Rivaroxaban and Apixaban were selected for clinical development for the prevention and treatment of thrombotic diseases.[71]

A large number of pyrazole derivatives have antimicrobial and antiviral,[72] hypoglycemic,[73] and anticancer activities.[74] For example, 3-substituted pyrazolo[5,1-c][1,4]benzoxazines and pyrazolo[1,5-a][1,4]benzodiazepin-6(4H)-ones[75] were synthesized by intramolecular 1,3-dipolar cycloaddition from a nitrilimine with an alkyne to form the desired product.

The nitrilimine generated by halohydrazones can be used directly to react with dipolarophiles to give specific pyrazoles having fungicidal activities against Corynespora cassiicola.[76] Synthesis is shown in Fig. 1-19.

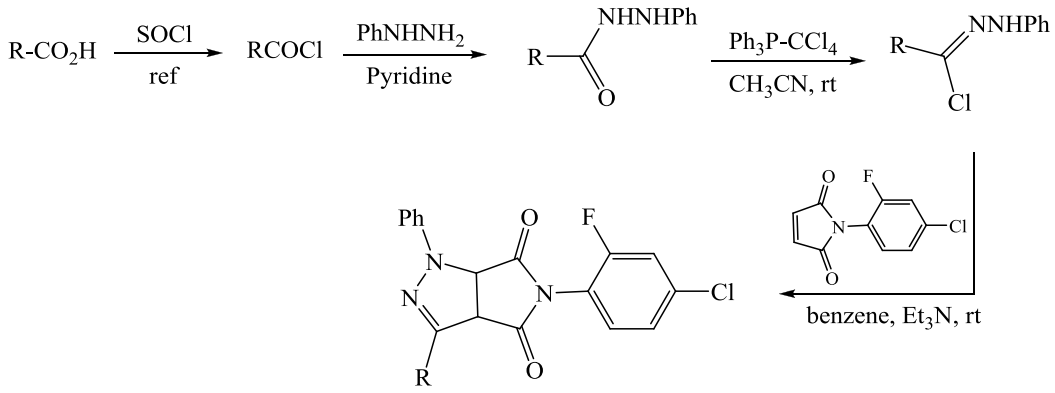

Figure 1-19. Synthesis of pyrazole derivatives having fungicidal activities.

1,3,5-trisubstituted 1,2,4-triazole derivatives are synthesized via 1,3-dipolar cycloaddition of nitrilimines by reacting oximes with hydrazonoyl hydrochlorides and triethylamine as a base.[77] 1,2,4-Triazole is an important class of heterocyclic compound in the biological activity of many pharmaceutically active compounds that show significant antifungal,[78, 79] anti-inflammatory,[80] antiasthmatic,[81] antiproliferative,[82, 83] and hypotonic activities.[84]

Cycloadditions of appropriate nitrilimines have been employed to synthesize tricyclic β-lactams (Fig. 1-20).[85-88] With their potency and broad range of antibacterial activity, tricyclic β-lactam and its derivatives have been used in the clinical treatment of microbial infections.[89-91]

[1,4]Benzodiazepin-6-one derivatives are synthesized via intramolecular nitrilimine cycloaddition to the cyano group (Fig. 1-21).[92] [1,4]Benzodiazepines and their oxo

derivatives have anti-convulsant and anti-anxiety activities. Several triazolobenzo-diazepines such as triazolam[93] and estazolam[94] were found to be effective in the treatment of some central nervous system (CNS) disturbances.

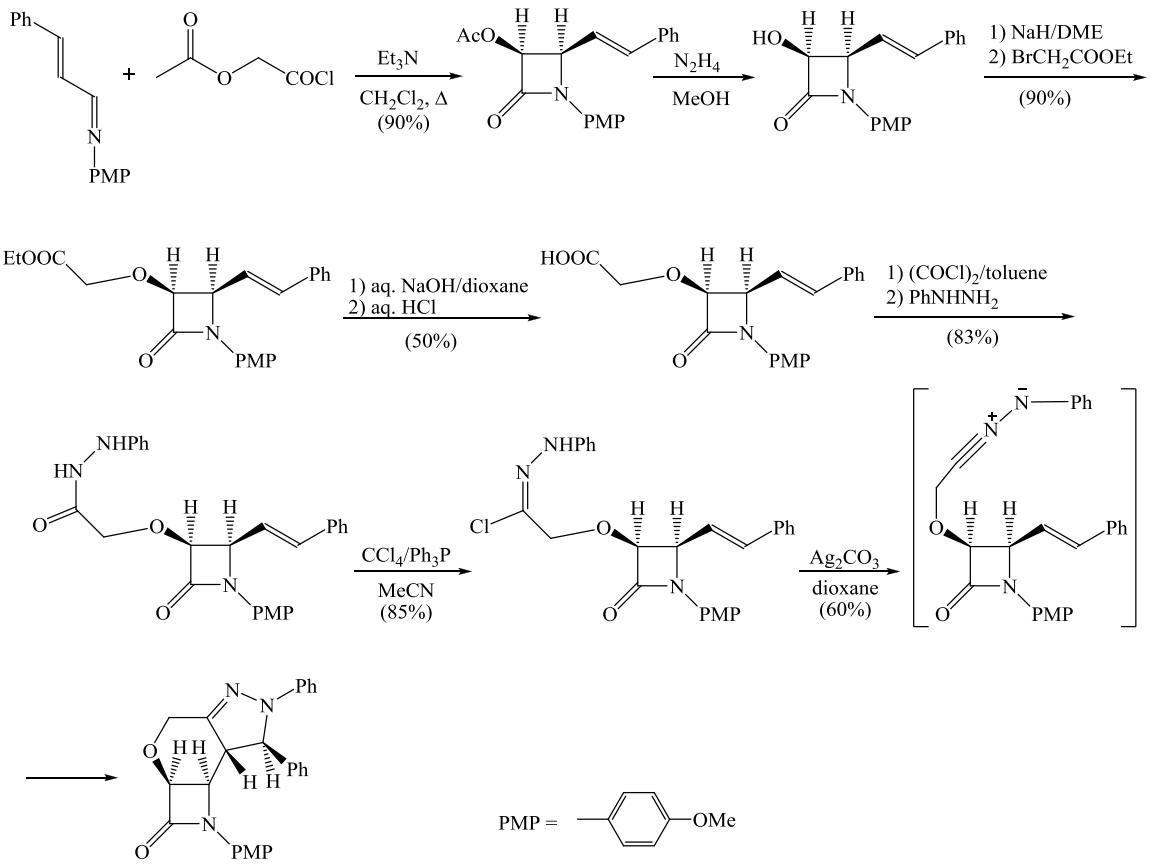

Figure 1-20. Synthesis of tricyclic β-lactams from nitrilimines.

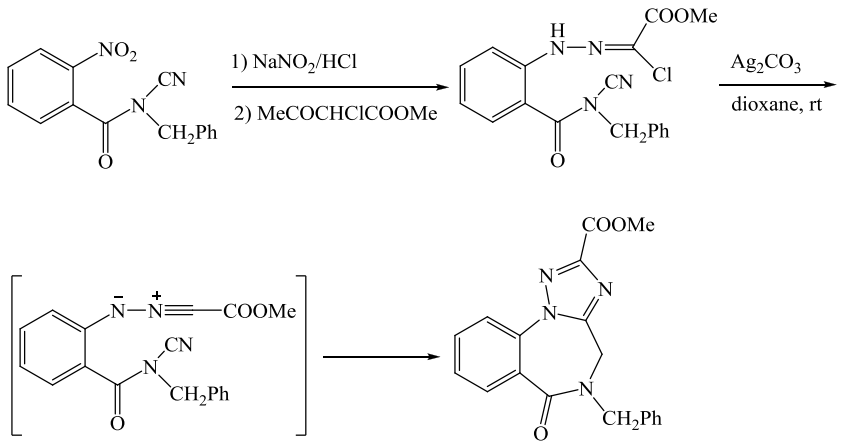

Figure 1-21. Synthesis of [1,4]benzodiazepin-6-ones.

Nitrilimines are important reagents in organic syntheses especially in 1,3-dipolar cycloaddition reactions to produce heterocyclic compounds. Since the thermolysis of tetrazoles is one of the common ways to generate nitrilimines, in this thesis, the decomposition of tetrazoles is examined computationally, and therefore, tetrazole is briefly introduced in the following section.

1.7. Tetrazole

Tetrazoles are heterocyclic 5-membered unsaturated rings consisting of one carbon and four nitrogen atoms. They have an aromatic character and contain four nitrogen atoms in a ring. In general, tetrazoles and 5-substituted tetrazoles are heterocyclic N-H acids although they behave as weak organic bases when dissolved in mineral acids.[95, 96]

Two tautomeric forms, 1-H and 2-H (Fig. 1-22), were proposed for tetrazole and 5-substituted tetrazoles, and various characterization methods such as NMR and IR spectroscopy were used to investigate these tautomeric forms.[97, 98] Both forms have been

observed[97-105] and X-ray crystallography results showed that tetrazole exists as the 1-H tautomer in the solid state.[106] In solution, there is an equilibrium between the tautomers that is very sensitive to the solvent and the nature of substituents.[107, 108] It was found both experimentally and theoretically that the 2H-tetrazole is the preferred tautomer in the gas phase being 4-6 kJ mol^{-1} more stable than 1H-tetrazole.[108-117] The formation enthalpy of 2H-tetrazole in the gas phase was reported to be 1.5-2 kcal mol^{-1} lower than that of 1H-tetrazole.[117]

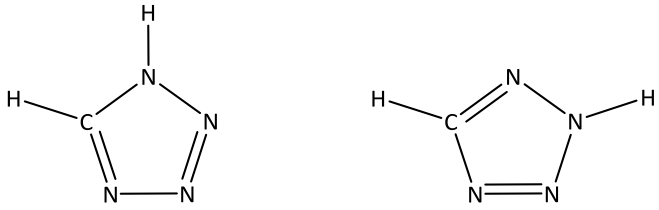

Figure 1-22. Tetrazole tautomers.

Tetrazoles have been widely used in medicine.[118-121] As an example, one type of cephalosporin contains the sodium salt of the 1H-tetrazole which is more active than antibiotics of the penicillin series.[120] Some compounds, synthesized using a tetrazole series, show antiallergenic activity.[119] Moreover, tetrazoles have applications in biochemistry and biology.[122, 123] 1-arylsulfonyltetrazoles are used as condensing agents to synthesize polynucleotides.[124] Another application of tetrazoles is in agriculture where esters of 2-tetrazolylscetic acids are used as regulators for the growth of fruit plants.[125]

1.7.1. Generation of Tetrazoles

The first derivative of tetrazole was prepared by Bladin in 1885 when he could generate phenylcyanotetrazole during the reaction of nitrous acid with

dicyanophenylhydrazin.[126] Later on in 1892, he prepared the tetrazole itself starting with a carboxylic acid produced from the phenylcyanotetrazole.[127] The simplest synthesis of tetrazole was obtained by Dimroth and Fester in 1910, employing the direct combination of hydrogen cyanide and hydrazoic acid in alcoholic solution at 100 ºC (Fig. 1-23).[128] The alkaline hydrolysis of ethyl tetrazole-5-carboxylate followed by decarboxylation at 90 °C is another way to obtain tetrazole in good yield.[96]

Generation of tetrazole derivatives has been studied from the 1960s until present and compounds such as 5-monosubstituted tetrazoles,[129-132] 1,5-disubstituted tetrazoles,[133-138] and 2,5-disubstituted tetrazoles[139-142] have been produced in different ways by many researchers.

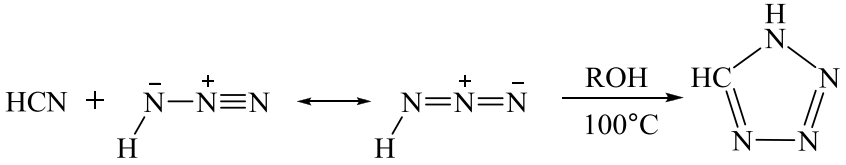

Figure 1-23. Synthesis of tetrazole itself, in its 1-H tautomeric form.

1.7.2. Reaction of Tetrazoles

Theoretically, if nitrogen is released, the thermolysis of the unsubstituted 2H-tetrazole results in the primary ring fragmentation product H–CNN–H.[111, 116, 143]

Tetrazoles alkylate and acylate on N1 or N2 depending on the substituent at C5.[144, 145] The formation of mixtures is the usual outcome for alkylation. An example of tetrazole alkylation is provided in Fig. 1-24. In general, electron-donating substituents at the tetrazole 5-position promote alkylation on the N1 position while electron-withdrawing groups cause N2-alkylation.[146] 1-substituted tetrazoles can undergo a metallation process.

C-Lithiation of 1-substituted tetrazoles occurs readily depending on the 1-substituents but lithio compounds tend to decompose (Fig. 1-25).[147]

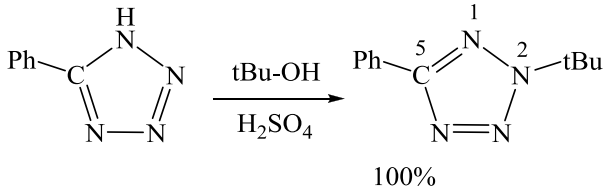

Figure 1-24. Alkylation of tetrazoles.

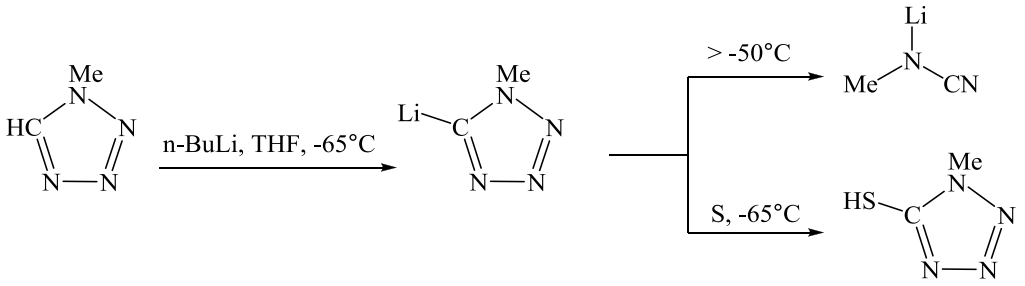

Figure 1-25. Metallation of tetrazoles.

Thermolysis of tetrazole is accomplished by studying the substituent effects on the mechanism of decomposition. Therefore, in the following section, substituent constants are briefly explained.

1.8. Substituent Constants

Substituent effects are defined as changes on a reaction or property due to substituent variations in the unaffected part of the molecule. These are classified into steric and electronic effects. Steric effects are related to spatial arrangement of atoms in molecules. Electronic effects, in contrast, embody inductive and resonance influences due to the

electrostatic effects transmitted through σ bonds and transmission of electron density through the π system of molecules, respectively.

Since the early 1900s, chemists were interested in analyzing the mechanism of organic reactions through substituent effects. A significant progress in these analyses was made in 1935 by Hammett providing the Hammett equation (Eq. 1-1),[148] which is expressed as:

— Eq. 1-1

where and are the reaction rate constant of substituted and unsubstituted reactants, respectively, is a substituent constant dependent on the specific substituent, and is a reaction constant dependent on the type of reaction. The substituent constant was obtained using ionization constants of benzoic acids in water. The reaction constant was defined as unity when measurements were performed in water at 25 °C.

Hammett σ constants have been mostly employed with benzene derivatives, although good correlation is obtained with heterocyclic systems.[149] Since the effect of each substituents can be obtained by difference of changes in Gibbs free energy (ΔG) for ionization constants of substituted benzoic acids with those of the parent compounds and any changes in structure cause proportional changes in the activation free energy ($\Delta G^{\ddagger}$) for all such reactions, the Hammett equation is well-known as a linear free energy relationship expression[150] and hence can be employed for any reactions with two aromatic reactants differing only in the type of substituents.

The σ constant depends on the substituent position; it is different for meta (σ_m) and para (σ_p) substitution. Sigma constants for the ortho position cannot be obtained because

of steric effects. However, the Hammett equation mostly fails where substituents are directly conjugated with the reaction center, exerting effects known as "through resonance".[151] Substituents possessing electron lone pairs fall into this category. They impart greater activity than their expected σ values due to the conjugative interaction of the substituent lone pair with the aryl ring. As a result, the Hammett equation deviates from the desired linearity. To overcome this issue, modified constants such as σ^+ were proposed by Brown and Okamoto.[152, 153] The modified σ^+ was defined by the solvolysis of cumyl chlorides at 25 °C in aqueous acetone. Several studies were performed to define constants for radical reactions,[154, 155] but none of these was successful in the correlation analysis. In general, σ or σ^+ correlate reasonably well in radical reactions.

The steric effect of substituents, E_s, was assessed by Taft[156] in the form of Eq. 1-2:

— Eq. 1-2

where refers to the reaction rate constants for acid hydrolysis of esters X-CH_2COOR. To do this, the electronic effect of substituents and was set zero for the hydrolysis of formate as a reference. For many substituents, the values of cannot be obtained due to the instability of the substituted esters under the condition of acid hydrolysis. Charton proposed values that are related to the van der Waals radii of substituents.[157-160] In his work, Charton tried to avoid the use of any particular chemical reaction using the expression in Eq. 1-3:

Eq. 1-3

where is the minimum van der Waals radius for symmetrical top substituents X, and is the van der Waals radius for hydrogen. Rates of esterification of substituted carboxylic acids with methanol or ethanol were correlated with the ν constants using the equation 1-4 which is the modified version of the Taft's equation.

Eq. 1-4

In the present work, Hammett constants were employed to investigate the substituent effects on the decomposition of tetrazoles. In addition, introductory topics such as thermal decomposition of 2H-tetrazoles and reaction of nitrilimines are treated in the following three individual chapters.

Chapter 2.

Objectives and Organization of Thesis

The main goal of this thesis is to investigate the intermolecular carbene-type cycloaddition ([1+2]) reactions of the parent nitrilimine and disubstituted nitrilimines having different carbenic character in terms of resonance weights. For this purpose, computational studies are to be performed on a series of nitrilimines to obtain a substantial understanding of their carbenic weight as well as their behaviour in the cycloaddition reactions in the presence of ethene and tetrafluoroethene.

The first task is to identify the specific tetrazoles which are known in the literature to have the possibility of the synthesis or even purchase of the tetrazoles as reactants.

The thermolysis of 2,5-disubstituted tetrazoles as a common method of the generation of nitrilimines is necessary to be investigated. Moreover, the substituent effect on the thermolysis of tetrazoles needs to be established. It is important to determine the contribution of carbenic character of the generated nitrilimines to predict the possibility of [1+2] cycloaddition reactions. Only nitrilimines with substantial carbene contributions to their electronic structure will be investigated further.

The [3+2] and [1+2] cycloaddition reactions of suited nitrilimines will be explored. Nitrilimines with different carbenic character are used to determine which one promotes the [1+2] cycloaddition reaction. Tetrafluoroethene will be employed to investigate the effect of an electron-poor alkene on the pathway of cycloaddition.

For geometry optimizations, frequency calculations and intrinsic reaction coordinates, the Gaussian program package will be employed. For detailed analyses of electronic

structures, Natural Bond Orbital (NBO) and Natural Resonance Theory (NRT) methods will be used. All additional data important for discussions for Chapters 3, 4, and 5 are covered in Appendices A, B and C, respectively.

This manuscript-based thesis is organized in a way to follow the goals and tasks presented above. Chapter 3 presents the formation of nitrilimines by thermal decomposition of 2,5-disubstituted tetrazoles. Chapter 4 is dedicated to the electronic structures of nitrilimines. The possible intermolecular [1+2] cycloaddition reactions of nitrilimines, contrasted with their [3+2] reactions, are presented in Chapter 5. The general conclusions of the thesis are addressed in Chapter 6.

None of the work has been published as of the thesis defense date.

Chapter 3.

Formation of Nitrilimines; Decomposition of 2H- and 2,5-Disubstituted Tetrazoles

3.1. Introduction

Nitrilimines are important reagents in organic syntheses, especially in 1,3-dipolar cycloaddition reactions to produce heterocyclic compounds.[1, 6, 9, 12, 35] Ways by which nitrilimines are generated include the decomposition of tetrazoles,[3, 13] base-induced elimination of hydrogen halide from hydrazonoyl halides,[13, 14] lithiated diazo derivatives reacting with alkylchlorophosphine,[28-32, 161] thermolysis of substituted 1,3,4,2-oxadiazaphospholes,[27] elimination of carbon dioxide from 1,3,4-oxadiazolin-5-ones,[26] and the reaction of hydrazone with N-bromosuccinimide in dimethylformamide and triethylamine.[34] Among these, the thermolysis of 2H- and 2,5-disubstituted tetrazoles is one of the common ways in the generation of nitrilimines, owing to the facile elimination of N_2 under simple experimental conditions at mild temperatures.

Thermal decomposition of an unsubstituted tetrazole[162, 163] as well as of 5-substituted tetrazole derivatives[164-168] in gas phase and melt has been the subject of many experimental and theoretical studies, and it is found that the thermolysis products profoundly depend on the reaction conditions or, more precisely, on the tetrazole annular tautomerism, i.e., on the presence of 1H- and 2H-forms (Fig. 3-1).[97, 98] In the solid state, as shown through X-ray diffraction, the 1H-form is present.[106] In a melt, the tautomeric form is unknown, but the final products of tetrazole thermolysis are N_2, H_2 and HCN as

well as "other gaseous products" and an unidentified polymer.[163] In solution, an equilibrium exists between the two tautomers, which is sensitive to the nature of the solvent.[97, 99, 100, 102, 104-106] Finally, in the gas phase, the 2H-tetrazole is predominant,[108-117] and generation of HCNNH has been shown through matrix isolation of the products (as well as photolysis of matrix-deposited tetrazole).[169]

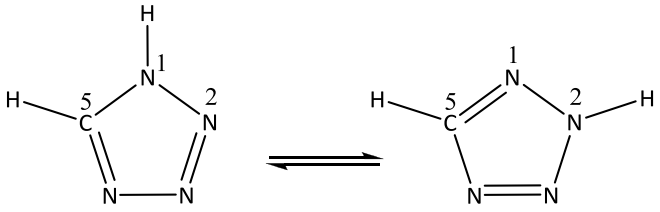

Figure 3-1. Tautomerism in the unsubstituted tetrazole.

The experimental data regarding the primary reaction of the thermolysis of tetrazole are incomplete and contradictory,[110, 162, 163, 170] mainly due to the involvement of short-lived intermediates and difficulties in the detection of some intermediates and products (e.g. nitrogen is inactive in the IR). To overcome these shortcomings as well as several experimental obstacles in the detection of intermediates and products, quantum chemical calculations have been used to study the thermolysis of tetrazoles.[108-117] Theoretically, if nitrogen is released, the thermolysis of the unsubstituted 2H-tetrazole results in the primary ring fragmentation product H–CNN–H.[111, 116, 143] Such a simple retro-[3+2]-cycloaddition involving two bond-breaking processes has been proposed for 2H-tetrazole decomposition, with the formation of a nitrilimine.[143]

Since 2,5-disubstituted tetrazoles do not undergo tautomerism, they could be a wise choice to work with to generate nitrilmines experimentally. The thermolysis of 2,5-

disubstituted tetrazoles results in the formation of disubstituted nitrilimines accompanied by the elimination of nitrogen (Fig. 3-2). The thermal decomposition of 2,5-diphenyltetrazole was first studied by Huisgen who succeeded to generate the nitrilimine intermediate and trap it using benzonitrile to give 1,3,5-triphenyl-1,2,4-triazole.[13] The kinetics of thermal decomposition of 2,5-diaryltetrazoles (with meta and para substitution and a range of substituents) were determined by Hong and Baldwin.[140, 171] The results of their studies suggested an unsymmetrical activated complex, although their results did not allow a decision between a concerted or a non-concerted process. In general, electron-deficient substituents on nitrogen result in an increase in the rate of decomposition,[14, 140, 171] whereas on carbon, electron-donating groups facilitate the process.[172] Overall, substituents on nitrogen have a more significant influence on the decomposition rate than those on carbon.[14, 171] Whereas the thermolysis mechanism of 2,5-disubstituted tetrazoles does not seem to have received attention, a computational study on the thermal decomposition of 5-nitro-1H-tetrazole has been published.[116] As expected from bond dissociation energies, decomposition is initiated through N–N bond cleavage. The proposed mechanism is stepwise and the calculated activation energy for N–N bond cleavage is 25.85 kcal mol^{-1} whereas it is 69.25 kcal mol^{-1} for an initial C–N bond breaking.[116] This finding is consistent with the experimental data; the bond dissociation energy, BDE, for N–N bond is ca. 170 kJ mol^{-1} while it is ca. 308 kJ mol^{-1} for C–N bond.[173] Consequently, the N–N bond cleaves first in the thermal decomposition of tetrazoles.

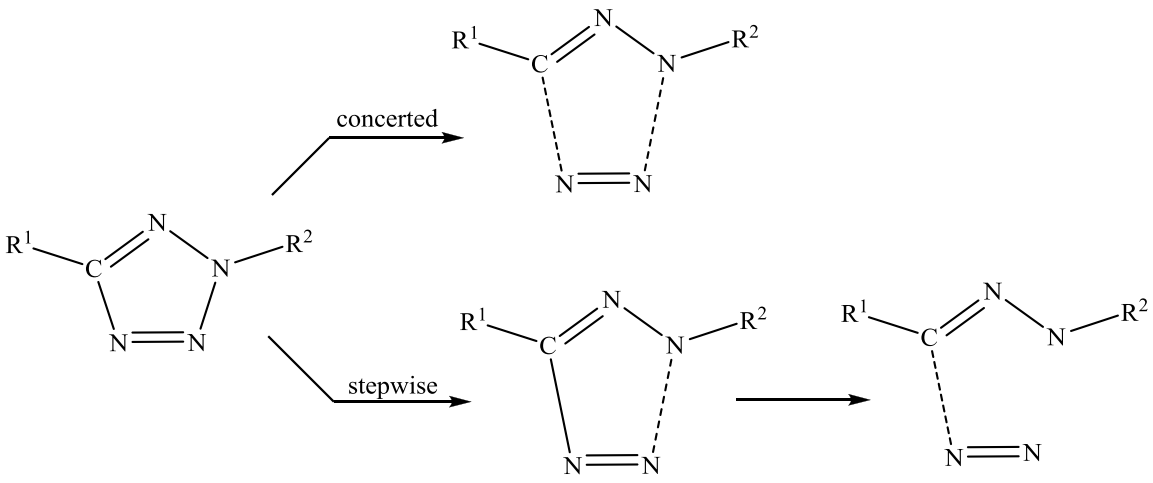

Figure 3-2. Schematic decomposition of 2,5-disubstituted tetrazoles.

In the following, we examine those 2,5-disubstituted tetrazoles known in the literature for which a natural bond orbital (NBO) analysis of the corresponding nitrilimines indicates an electron lone pair on carbon, and for which a natural resonance theory (NRT) analysis indicates a sizeable carbenic contribution to the electronic structure. First, and due to their aromatic character, we examine the substituent effects on the tetrazole geometry with special attention to the N–N bond to be fragmented. This is followed by a study on tetrazole thermal decomposition, again with respect to possible substituents effects.

3.2. Computational Details

All calculations were performed using the Gaussian 03[174] and Gaussian 09[175] packages of programs. Geometry optimizations of the tetrazoles and their transition states for decomposition were carried out using the Becke 3-parameter Lee-Yang-Parr (B3LYP)[176-179] hybrid density functional with the 6-31+G(d) basis set. Vibrational

analyses were used to characterize the nature of the stationary points. Energies are reported including zero point vibrational corrections. Restricted and unrestricted calculations on the transition state structures and intermediates returned the same energies, implying the absence of further stable diradical species. The intrinsic reaction coordinate (IRC) procedure[180, 181] was applied to transition states to verify the proposed reaction path. Orbital interactions in the parent molecules were evaluated using the NBO analysis[182] as implemented in Gaussian.

3.3. Results and Discussion

3.3.1. Substituent Effects in Tetrazoles

Twelve tetrazoles known in the literature have been analyzed with respect to changes in geometry and orbital interactions. Since the decomposition of tetrazoles is initiated through N2–N3 bond cleavage, the effect of substituents is examined on the N2–N3 bond length. The data in Table 3-1 are ordered from the shortest to the longest bond length to illustrate the importance of the substituent effect and the possibility that a long bond breaks more readily than a short bond. The table demonstrates that Δr_{NN} over the series is small, 0.034 Å, and it could be concluded that the N2–N3 bond is not noticeably influenced by substituents, yet all changes are significant. In all cases, the C5–N4 bond is longer than the N2–N3 bond and the N3–N4 bond varies in the range of 1.305 Å to 1.329 Å (it is 1.10 Å in the isolated N_2). On the other hand, for example, calculated bond lengths of 2-methyl-5-nitrotetrazole are compared with the data from X-ray diffraction. Results demonstrate that the C5–N4 bond in both calculated and X-ray data is longer than the N2–N3 bond (Table 3-1). The N3–N4 bond length obtained by X-ray diffraction and

DFT calculation is 1.317 and 1.308 Å respectively, which it is therefore shorter than either C5–N4 or N2–N3 bonds. In addition, the C5N1N2 bond angle obtained computationally (100.5°) is very similar to that obtained by X-ray diffraction, 99.9°. Therefore, this comparison shows a general agreement between the calculated and experimental data and validates the chosen model chemistry.

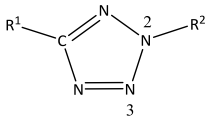

Table 3-1. Selected bond lengths (Å) for disubstituted tetrazoles.[a]

R^1	R^2	N2-N3	N3-N4	N4-C5
F	F	1.306	1.329	1.340
H	H	1.311	1.311	1.357
NH_2	NH_2	1.318	1.322	1.357
OCH_3	CH_3	1.322	1.320	1.354
CH_3	CH_3	1.328	1.312	1.360
NH_2	NCH_2	1.329	1.305	1.370
COOH	OH	1.329	1.316	1.352
$NHSiMe_3$	$SiMe_3$	1.330	1.312	1.366
CHO	OH	1.331	1.316	1.354
SCH_3	SO_2NMe_2	1.332	1.310	1.367
$OSiMe_3$	$SiMe_3$	1.334	1.313	1.361
NO_2	NH_2	1.335	1.316	1.340
Ph	Ph	1.338	1.305	1.366
NO_2	CH_3	1.340	1.308	1.346

[a] R^1 is C-substitution, R^2 N-substitution. [b] Experimental data for 2-methyl-5-nitrotetrazole[183]: N2-N3; 1.329(2), N3-N4; 1.317(2), N4-C5; 1.331(2).

Since tetrazoles are aromatic compounds, the substituent effects can be examined by a Hammett plot. Figures 3-3 and 3-4 show the plots of N2–N3 bond distance as a function of the Hammett substituent constant σ^+ for C- and N-substituent, respectively, of the disubstituted tetrazoles. As can be seen from these graphs, correlations are not found

between the data, probably as a direct cause of di-substitution. We therefore investigated the effect of each substituent separately in two series of mono-substituted tetrazoles, where the substituents were chosen according to those found in the disubstituted tetrazoles (Figs. 3-5 and 3-6). Data points for H and CH_3 are omitted, because neither those tetrazoles nor their nitrilimines were carried over into the following studies. Moreover, only substituents with known Hammett constants could be analyzed, and those such as $NHSiMe_3$ and $OSiMe_3$ were excluded.

As can be seen from Fig. 3-5, for C-substituted tetrazoles, there is indeed a decent correlation between the N2–N3 bond length and Hammett σ^+, with a positive slope. Thus, electron donating groups on carbon such as NH_2, OCH_3 and SCH_3 lead to a shorter N2–N3 bond whereas electron withdrawing groups such as NO_2 cause an increase in its length. As thermolysis of tetrazoles is initiated through N2–N3 bond cleavage, electron withdrawing substituents on carbon might therefore be expected to show lower activation energies to decomposition. Our findings are accord with experimental data have been carried out by Baldwin and Hong.[140] C-substituents with electron withdrawing groups delocalize positive charge of transition state complex rather than tetrazole and hence accelerate the rate of decomposition.[140] According to the trend in bond N2-N3 lengths, it is expected that a tetrazole with a Ph-C-substituent decomposes more readily than one with CH_3-C-substituents while experimental results demonstrated that activation energy for N-methyl tetrazoles with Ph- and CH_3-C-substituents are almost the same, 42 kcal mol^{-1}.[184] In contrast to the variation of substituents on carbon, N-substituted tetrazoles do not exhibit a correlation between N2–N3 bond length and Hammett σ^+ (Fig. 3-6). Substituents may affect the N2–N3 bond distance in two ways, through π- and σ-effects;

σ-effects should be more dominant for N2-substitution. These are not captured by Hammett substituent constants, though. While it cannot be claimed that σ-effects are more important than π-effects, clearly it is N2-substitution that prevents Hammett correlations for the N2–N3 bond in the disubstituted tetrazoles (Figs. 3-3 and 3-4). Therefore, it could be concluded that both effects are important to express the stability of tetrazoles although the prediction of stability of tetrazoles could be interpreted by σ-effect; electron donating groups on carbon stabilize tetrazoles rather than those with electron withdrawing groups.

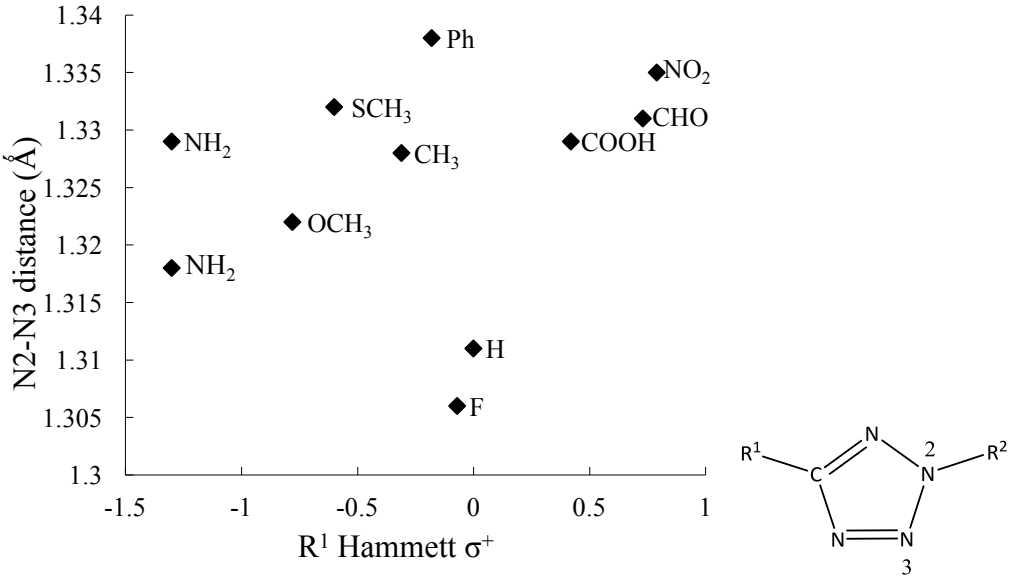

Figure 3-3. Variation of the N2–N3 bond length versus R^1 Hammett substituent constant, for disubstituted tetrazoles.

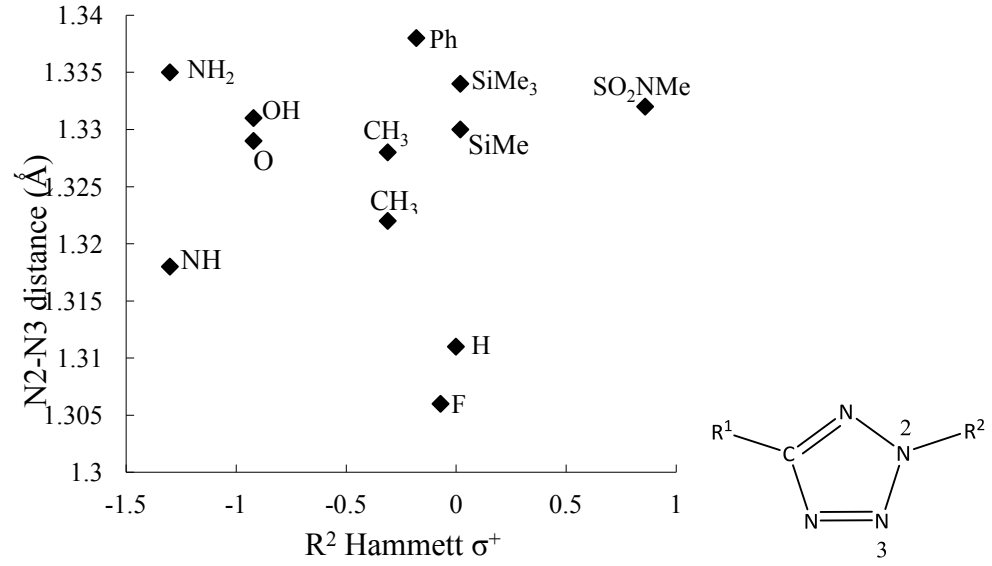

Figure 3-4. Variation of the N2–N3 bond length versus R^2 Hammett substituent constant, for disubstituted tetrazoles.

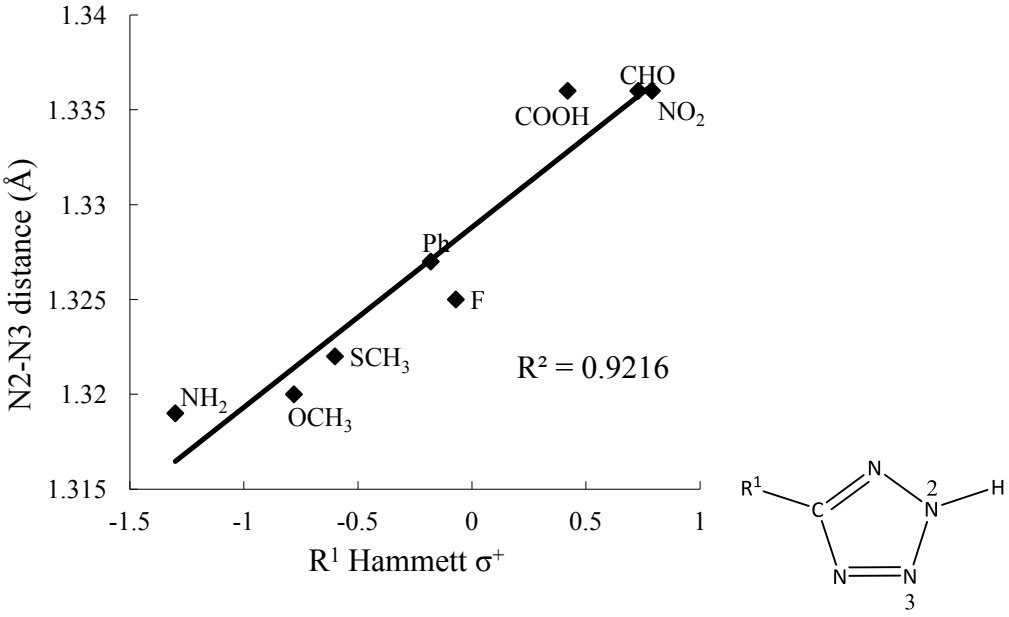

Figure 3-5. Variation of the N2–N3 bond length versus R^1 Hammett substituent constant, for C-substituted tetrazoles.

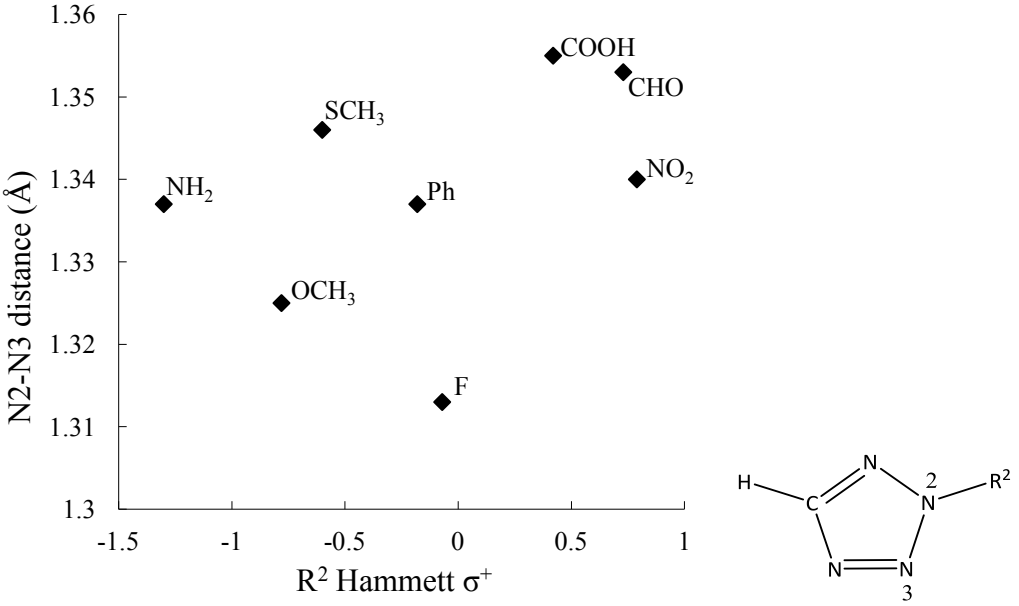

Figure 3-6. Variation of the N2–N3 bond length versus R^2 Hammett substituent constant, for N2-substituted tetrazoles.

That the π-effect is operating in both C- and di-substituted tetrazoles can be shown through NBO analyses. Depending on the specific substituent, two dominant orbital interactions, n-π* or π-π*, need to be considered between a substituent on carbon and the aromatic ring; in the NBO analysis, it is the π_{CN} system that interacts with the substituent. In terms of stabilization energy to plot the graph, the orbital interaction energy between the lone pair of a substituent such as NH_2 and OCH_3 and the empty π^* orbital of the C=N bond was used (Table 3-2). For substituents with a π system, two possibilities exit to employ stabilization energies, the energy of the orbital interaction between the π orbital of a substituent ($\pi_{C=O}$ in COOH, for example) and the π^* orbital of the C=N bond or vice versa. Both interactions indeed influence the stability of a molecule although we use the interaction energy of π_{sub}-π^*_{CN} in order to determine the direct effect of substituents on stability of tetrazoles. To illustrate the π-effect, the stabilization (interaction) energies are

plotted as a function of Hammett σ^+ for disubstituted (Fig. 3-7) and C-substituted (Fig. 3-8) tetrazoles. The figures demonstrate that there is a good correlation between stabilization energy and Hammett constant for both tetrazoles. In other words, it seems that the tetrazole ring π-system, as represented in the NBO analysis by the C=N bond, is influenced the same way, regardless of N-substitution.

Table 3-2. Selected orbital interaction energies (kcal mol^{-1}) for disubstituted and C-substituted tetrazoles

		Stabilization energy		
R^1	R^2	n_{Sub}-π^*_{CN}	π_{CN}-π^*_{Sub}	π_{Sub}-π^*_{CN}
Disubstituted tetrazoles				
NH_2	NH_2	36.79		
F	F	27.80		
OCH_3	CH_3	28.24		
NH2	$NHCH_2$	39.24		
SCH_3	SO_2NMe_2	28.02		
COOH	OH		4.76	13.19
CHO	OH		6.30	11.23
Ph	Ph		24.32	8.26
NO_2	NH_2		6.02	12.14
C-Substituted tetrazoles				
NH_2	H	38.16		
F	H	27.11		
OCH_3	H	42.29		
SCH_3	H	27.90		
COOH	H		5.46	13.43
CHO	H		5.79	9.45
Ph	H		24.57	8.33
NO_2	H		6.04	12.38

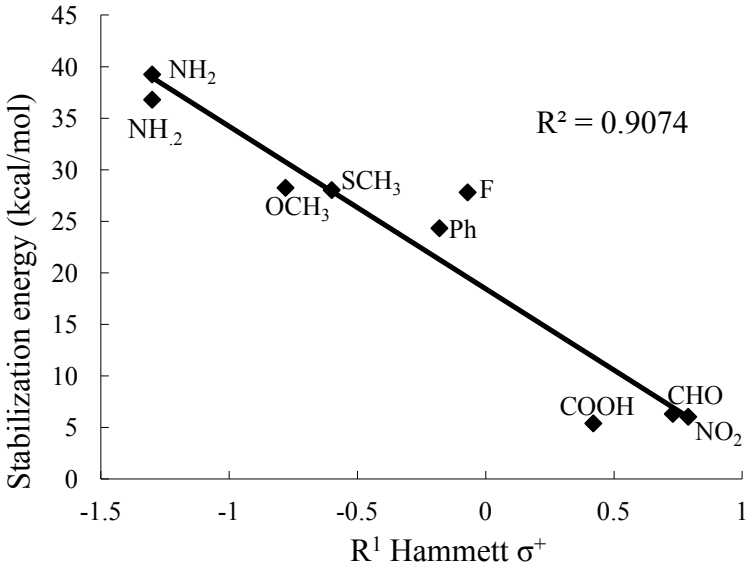

Figure 3-7. Variation of the stabilization energy with R^1 Hammett substituent constant, for disubstituted tetrazoles.

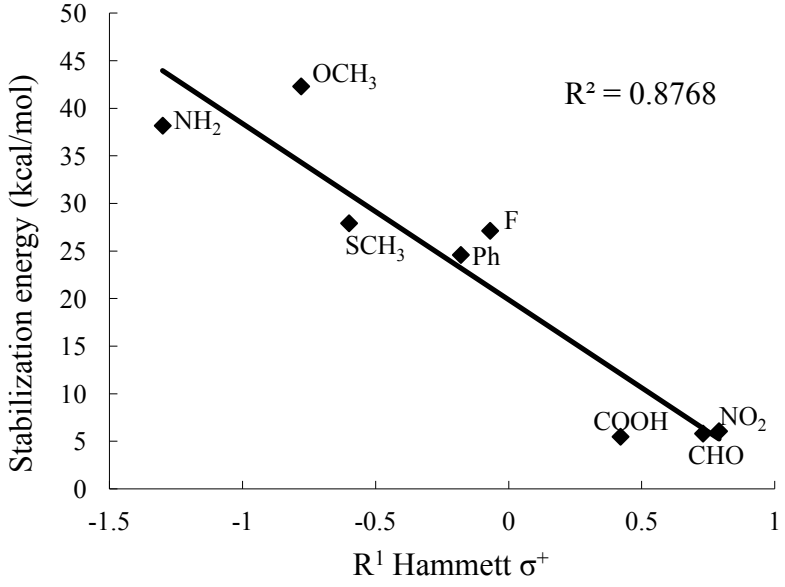

Figure 3-8. Variation of the stabilization energy versus R^1 Hammett substituent constant, for C-substituted tetrazoles.

3.3.2. Decomposition of Tetrazoles

3.3.2.1. Unsubstituted tetrazole

From the various detailed experimental studies on substituent effects, it seems that the N2–N3 bond cleaves first when a tetrazole decomposes.[110, 111, 143, 162, 163, 166, 169] The reaction then continues by the release of N_2 through C5–N4 bond breaking (Fig. 3-2). Considerable efforts have been devoted to the experimental analysis of decomposition of the unsubstituted tetrazole.[40, 110, 162, 163, 166, 185, 186] Lesnikovich et al.[162, 163, 166] reported that thermal decomposition of the 1H-tetrazole occurred through the open-ring azido form, yielding the corresponding nitrene by release of N_2, whereas the 2H-tetrazole decomposes through N–N bond breaking to form the nitrilimine via elimination of N_2. Moreover, other products such as HCN,[110, 162, 163, 166, 169] NH_2CN (cyanamide), CH_2N_2 (diazomethane),[110, 169] and HN=C=NH (carbodiimide)[169] have been reported as products in tetrazole decomposition experimentally. On the other hand, computational studies on the decomposition of the unsubstituted tetrazole have not been widely considered.[111, 143] da Silva and Bozzelli[143] proposed a retro-[3+2]-cycloaddition as a mechanism of 1H- and 2H-tetrazole decomposition. The mechanism proposed for 1H-tetrazole decomposition is stepwise, in which NHCNH and N_2 are produced, whereas the concerted mechanism is proposed for 2H-tetrazole decomposition yielding NHNCH and N_2. Since the unsubstituted tetrazole decomposition is a good reference to compare and determine the effect of the various substituents on tetrazole decomposition, in the following section, we examine the mechanism of decomposition of 2H-tetrazole as well as selected disubstituted tetrazoles.

Decomposition is initiated through N2–N3 bond cleavage, with the corresponding transition state TS1, and the calculated energy barrier for this cleavage is 37.4 kcal mol^{-1}. The thermal decomposition is followed by the release of N_2 in TS2, with a barrier of 42.1 kcal mol^{-1} (Fig. 3-10). As the N3–N4 bond length in the intermediate is 1.13 Å (compared to 1.10 Å in N_2 and 1.311 Å in the tetrazole), N_2 released is facilitated since it is already 'preformed' in the intermediate.

From a visual inspection, for TS1, the unique imaginary vibration mode corresponds to N2–N3 bond cleavage only. For confirmation, the intrinsic reaction coordinate (IRC) was obtained, i.e., the minimum-energy path that connects a transition state to its reactant(s) and product(s). The IRC path for TS1 is shown in Fig. 3-9.

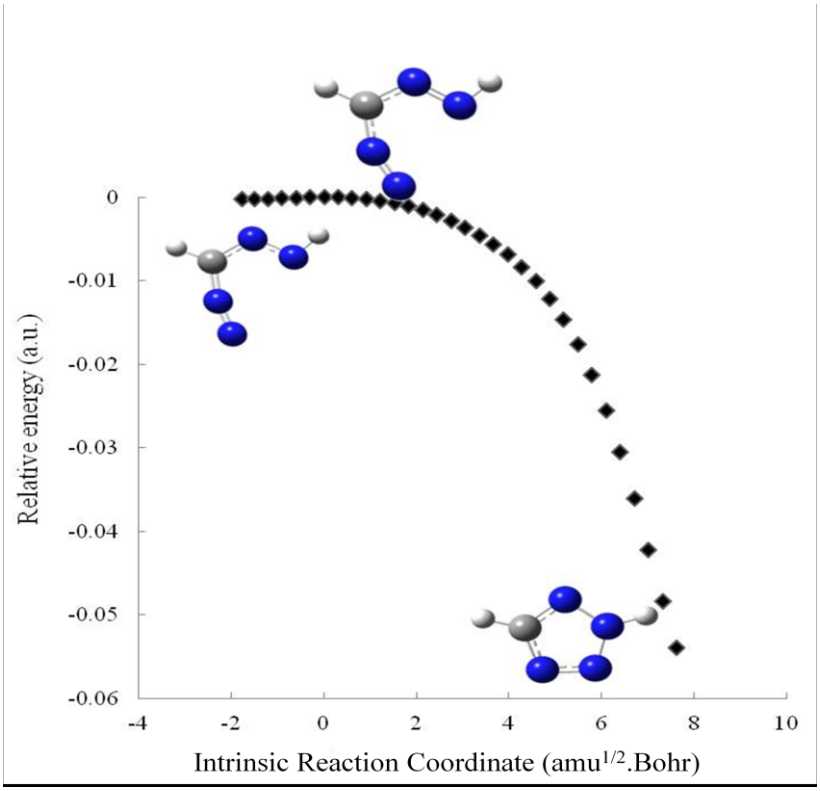

Figure 3-9. Intrinsic reaction coordinate for "TS1" of the decomposition of the unsubstituted tetrazole.

The N2–N3 bond on this path lengthens from 1.431 Å in the tetrazole to 2.824 in TS1 and 3.122 Å in the intermediate. In contrast, although "TS2" should correspond to C5–N4 bond cleavage, a visual inspection of its imaginary vibration mode is not helpful, because large movements are indicated for both C5–N4 and N2–N3 bonds, similar to what is expected in the transition state for a concerted fragmentation. The IRC path for "TS2" is given in Fig. 3-11 and illustrates that "TS2" is indeed the transition state for concerted tetrazole decomposition, as it links the products to the reactant, not the intermediate. Hence, "TS2" corresponds to the concerted mechanism. In an effort to locate the real TS2, the CN bond in the intermediate was gradually lengthened from 1.810 Å to 3.0 Å in 0.5 Å increments, but the concerted TS was obtained from this approach as well. This result suggests that the real TS2 is higher in energy than the concerted TS, and it was not pursued further.

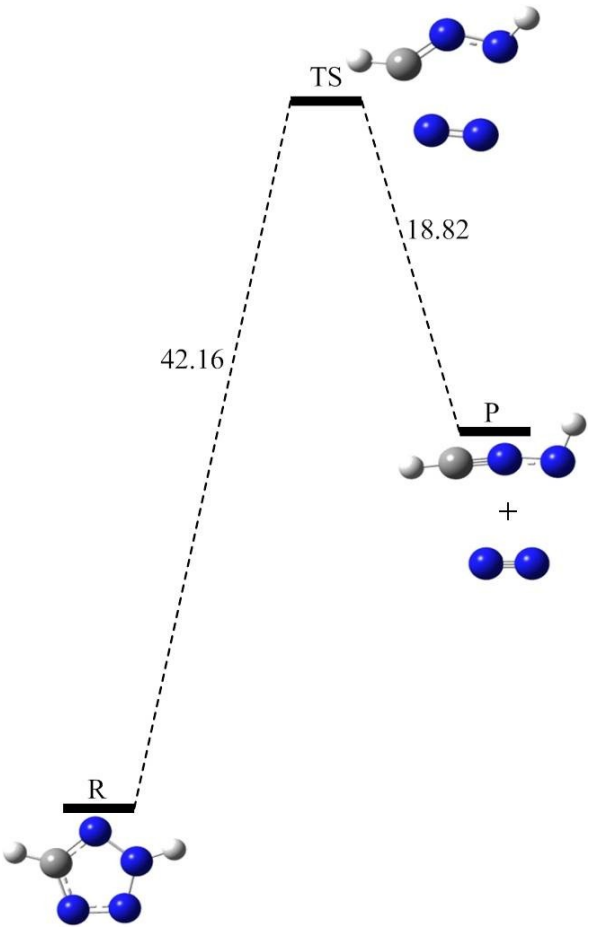

Figure 3-10. Energy (kcal mol^{-1}) profile for the decomposition of the unsubstituted tetrazole.

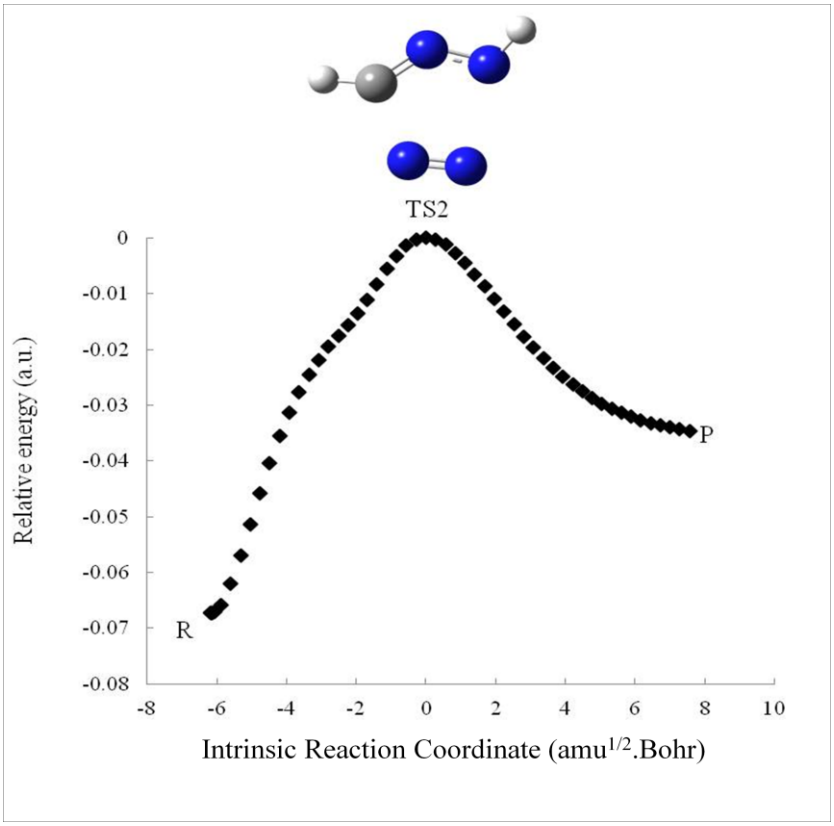

Figure 3-11. Intrinsic reaction coordinate for "TS2" of the decomposition of the unsubstituted tetrazole.

3.3.2.2. Decomposition of 2,5-Disubstituted Tetrazoles

From the selected twelve 2,5-disubstituted tetrazoles, an NBO analysis of the corresponding nitrilimines indicates that only six possess an electron lone pair on carbon, which could be indicative of a sizeable carbenic contribution to the valence-bond structure (results will be presented in Chapter 4). Based on this finding, the decomposition of the respective tetrazoles was investigated only. These tetrazoles can be grouped into possessing an electron withdrawing or electron donating group on carbon. Accordingly, to determine the effect of substituents on the thermal decomposition of tetrazoles, the mechanism of decomposition is examined with respect to C-substitution.

Figure 3-12 shows the decomposition path for a tetrazole with an electron withdrawing carboxyl group on carbon. Both TS1 for N2–N3 cleavage and TS2 for C5–N4 cleavage are located without difficulty, and the decomposition is clearly stepwise. In contrast, the concerted transition state could not be located, suggesting that it belongs to a high-energy path. The energy barrier to reach TS2 is 24.0 kcal mol^{-1}, which is substantially less than that (37.4 kcal mol^{-1}) required for decomposition of the unsubstituted tetrazole. Tetrazoles with CHO, NO_2 and F substitution on carbon similarly follow the stepwise pathway (Table 3-2). All activation barriers for TS2 are somewhat similar and relatively small. For difluoro substitution, TS1 becomes rate determining (Table 3-2).

In contrast to the above, Fig. 3-13 demonstrates that a tetrazole with an electron donating methoxyl group on carbon follows the concerted decomposition pathway, with the corresponding transition state TSc. The first step of the stepwise decomposition is included in Fig. 3-13, and it is apparent that the activation energy for concerted decomposition is less than that required for the first step in the stepwise fragmentation. For these particular substituents, the activation energy required for the lowest available, concerted pathway is prohibitively high, even substantially higher than that for the unsubstituted tetrazole. That the choice of substituents here is particularly crucial is illustrated in Table 3-3 with the 2,5-diaminotetrazole entry. Its activation energy for fragmentation is more in line with the remaining Table entries.

Finally, Figs. 3-12 and 3-13 clarify an earlier point, that of the nature of "TS2" in the unsubstituted tetrazole. In Fig. 3-12, TS2 has the expected orientation of nitrogen for extrusion, in particular, N3 does not seem to be moving back toward N2, i.e., back to the position it occupied in TS1. In fact, N3 in TS2 is not located in the former ring-plane any

longer. A comparison with the concerted TS in Fig. 3-13 and the questionable "TS2" in Fig. 3-11 clearly assigns "TS2" in the decomposition of the unsubstituted tetrazole as the transition state for the concerted pathway.

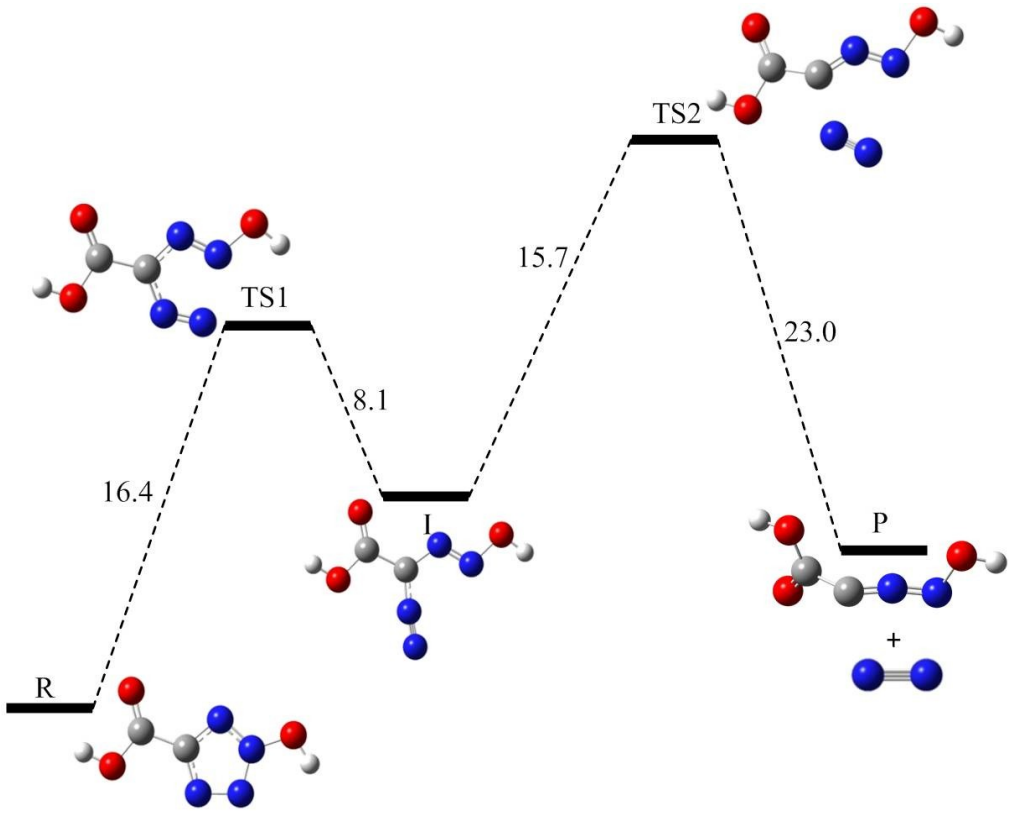

Figure 3-12. Energy (kcal mol^{-1}) profile for the decomposition of a disubstituted tetrazole with an electron withdrawing group on carbon.

Table 3-3. Activation energies[a] (kcal mol^{-1}) for decomposition of 2,5-disubstituted tetrazoles. Free energies of activation (kcal mol^{-1}) presented in parentheses.

R^1	R^2	TS1	TS2	TS1-I[b]	I-TS2[b]	TSc
COOH	OH	16.4 (16.4)	24.1 (23.0)	8.1	15.7	
CHO	OH	16.1 (16.1)	21.9 (20.6)	6.7	12.5	
NO_2	NH_2	19.0 (19.3)	28.9 (28.1)	6.9	16.8	
F	F	24.1 (28.1)	22.6 (21.0)	10.1	8.6	
NH_2	NH_2	33.4				29.3 (29.0)
OCH_3	CH_3	44.2				41.1 (40.3)

[a] Relative to the reactant tetrazole. [b] Activation energies to changes from the intermediate.

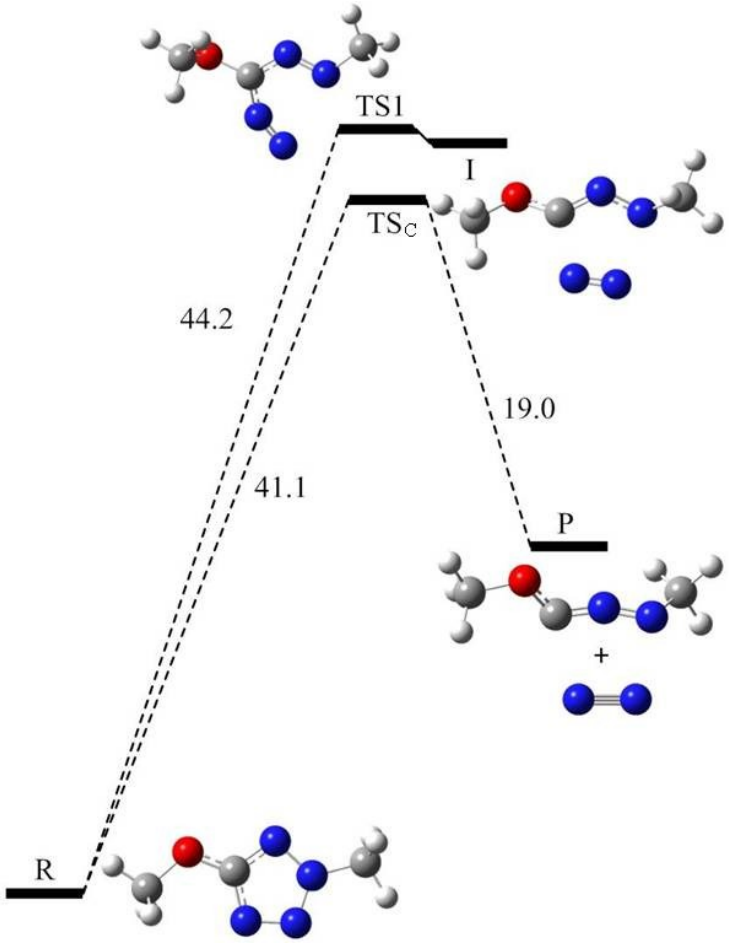

Figure 3-13. Energy (kcal mol^{-1}) profile for the decomposition of a disubstituted tetrazole with an electron donating group on carbon.

3.4. Conclusions

Tetrazoles with varying substitution were analyzed with respect to selected geometric parameters, aspects of their electronic structure, and decomposition behaviour. An examination of the substituent effect on the N–N bond length of a series of 2,5-disubstituted tetrazoles known in the literature shows that the π-effect of substituents on carbon is captured by Hammett σ^+ constants, and C-substituents substantially influence the N–N bond length. In particular, electron withdrawing groups on carbon cause an increase in the N–N bond length whereas electron donating groups have the opposite effect. Furthermore, the stabilization energy of C-substituents shows a good correlation with Hammett σ^+ constants and electron donating groups stabilize tetrazoles more than electron withdrawing groups.

It is found that thermal decomposition of 2H-tetrazole follows the concerted mechanism, based on simultaneous N–N and C–N bond cleavages in vibration modes as well as the intrinsic reaction coordinate connecting reactant and products. Even though this pathway requires more energy than the first transition state for stepwise decomposition, the transition state for the second step could not be located, presumably because it is much higher in energy. For 2,5-disubstituted tetrazoles, the mechanism of decomposition is controlled by C-substitution. In the case of electron withdrawing groups on the carbon atom, the mechanism follows the stepwise pathway and the total energy barrier in all cases is less than the activation barrier required for 2H-tetrazole decomposition. Electron donating groups on the carbon atom promote the concerted mechanism and the energy barrier can be prohibitively high.

Chapter 4.

Electronic Structure of Nitrilimines

4.1. Introduction

Nitrilimines were first generated by Huisgen in 1959 through thermolysis of 2,5-disubstituted tetrazoles or treatment of hyrazonyl chloride with triethylamine.[13] They are well-known as 1,3-dipoles undergoing 1,3-dipolar cycloaddition reactions which lead to the generation of heterocyclic compounds. Nitrilimines are highly reactive intermediates,[3-5, 10, 40] and therefore, little experimental evidence exists regarding their actual structure. Accordingly, theoretical methods have been employed to examine the electronic structure of nitrilimines.[10, 16, 20, 21, 110, 117]

Huisgen reported that nitrilimines could be described as a combination of several valence-bond structures, including sextet structure (e.g. 1,3-dipole, carbenic) and octet structure (e.g. propargylic, allenic) (Fig. 4-1).[12] Early computational studies revealed that a planar geometry corresponding to a propargylic structure is the lowest energy conformation of the parent nitrilimine.[2, 19, 20, 110] Houk and co-workers then claimed that a nonplanar, bent, allenic structure was another stable conformation of nitrilimine close in energy to the propargylic structure.[15, 16, 19] In all cases, the energy difference between the planar and nonplanar structures was small, and therefore nitrilimine was deemed a "floppy" molecule.[16] Inspection of the frontier molecular orbitals indicated that nitrilimine is indeed a flexible molecule which adopts its a minimum-energy geometry - planar or nonplanar – highly dependent on the basis set employed.[16] Further

investigations using high-level ab initio calculations revealed that the nonplanar allenic structure is preferred to the propargylic structure.[24] In 1987, Kahn et al. claimed that an hypervalent valence-bond structure was also possible, on the basis of calculated CN and NN bond lengths at the Hartee-Fock level of theory, 1.138 Å and 1.259 Å, respectively.[20] On the other hand, Kuhler and co-workers obtained bond lengths of 1.205 Å and 1.233 Å for the CN and NN bonds, respectively, and concluded that nitrilimine should be described as a mixture of allenic and propargylic valence-bond structures.[21] In 2004, Mawhinney et al. reported that the ground state of nitrilimine includes four major valence-bond forms with similar weights, according to natural resonance theory (NRT), namely the propargylic, allenic, carbenic and 1,3-dipolar structures.[22] However, two years later, Cargoni et al. claimed that the propargylic structure is predominant for nitrilimine.[17] All these studies focused on the unsubstituted nitrilimine. For substituted nitrilimines, some information was obtained from X-ray crystallography, demonstrating that nitrilimines have a bent and nonplanar structure corresponding to the allenic structure.[11] However, electron-withdrawing substituents change this geometry to one consistent with the propargylic structure. The electronic structure of substituted nitrilimines was examined theoretically using NRT, and in all cases the weight of the four major valence-bond structures, i.e. propargylic, allenic, 1,3-dipolar and carbenic, were used to describe the electronic structure of nitrilimines.[22]

To the best of our knowledge, the carbenic structure of nitrilimines has not been extensively inspected, and thus, in the following section, we examine the geometry of parent and substituted nitrilimines as well as the contribution of the major structures to their electronic structure using NRT.

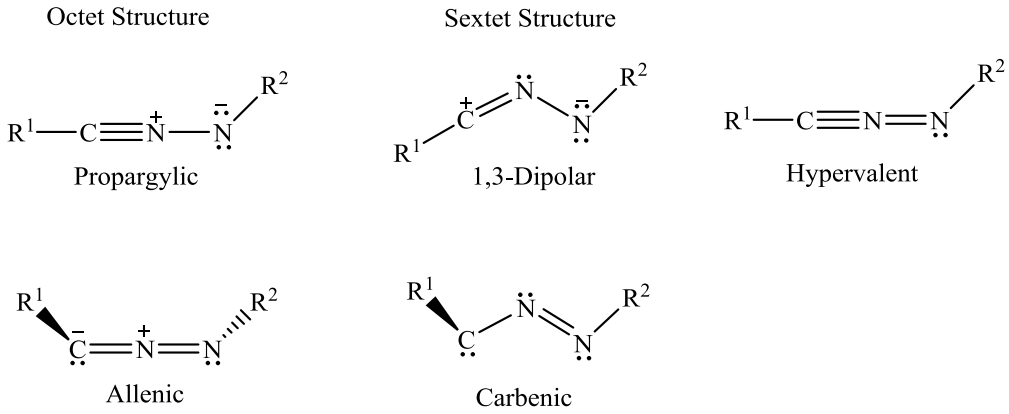

Figure 4-1. Major resonance structures of nitrilimines.

4.2. Computational Details

All calculations were performed using the Gaussian 03[174] and Gaussian 09[175] packages. Geometry optimization of the nitrilimines was carried out using the Becke 3-parameter Lee-Yang-Parr (B3LYP)[176-179] and Perdew-Burke-Ernzerhof[187, 188] (PBE0) hybrid density functionals with 6-31+G(d) and 6-311++G(2df,pd) basis sets, respectively. A vibrational analysis was used to characterize the nature of all stationary points, and all energies were corrected for zero-point energy. All geometries were confirmed to be minima. Unrestricted and restricted density-functional theory (DFT) calculations yielded the same results, implying the absence of additional stable diradical species. The NRT approach[189] was employed to determine the contributions of various resonance structures to the overall electronic structure using the program NOB5. In this chapter the results of PBE0/6-311++(2df,pd) is presented and the other results are provided in appendix B.

4.3. Results and Discussion

4.3.1. Geometries

The major geometric parameters of the nitrilimines are collected in Table 4-1. The results show a linear CNN backbone for the unsubstituted nitrilimine consistent with the propargylic (planar) structure, although the HCN bond angle is distorted. Another geometric feature of the nitrilimines is that the calculated CN bond length, 1.184 Å (PBE0/6-311++G(2df,pd)), is comparable to the experimental CN triple bond length of 1.093(4) Å in nitriles (R-CN)[190]. On the other hand, the calculated NN bond length, 1.231 Å (PBE0/6-311++G(2df,pd)), is similar to the experimental NN double bond length of 1.326(4) Å in R-N=N-R,[191] which is not consistent with a propargylic structure. However, inspection of the charge distributions demonstrates that the carbon atom carries a negative charge while the middle nitrogen atom carries a positive charge, leading to an allenic bent-type structure. Since nitrilimine is a transient compound, X-ray crystallography could not be used to charcaterize its structure, although X-ray crystal data are available for some stable substituted nitrilimines. For example, $((iPr)_2N)_2PS–CNN–P((iPr)_2N)_2$ was reported to have CN and NN bond lengths of 1.177(6) and 1.240(5) Å, respectively.[64, 161] It was suggested that this nitrilimine has a structure halfway between the planar and bent ones. The CN and NN bond lengths of $Ph_3C–CNN–CPh_3$ were reported to be 1.173(3) and 1.262(2) Å, respectively.[65] Thus, the calculated CN and NN bond lengths of nitrilimine (Table 4.1) are in accord with those reported for substituted nitrilimines in the solid state. Our results indicate that F–CCN–F and $NH_2–CNN–NH_2$ have bent structures. The optimized geometries of COOH–CNN–OH, CHO–CNN–OH,

$H_3CO–CNN–CH_3$, $NO_2–CNN–NH_2$, and $Si(CH_3)_3O–CNN–Si(CH_3)_3$ are consistent with an allenic structure while those of $CH_3–CNN–CH_3$, Ph–CNN–Ph, $H_3CS–CNN–SO_2N(CH_3)_2$, and $Si(CH_3)_3NH–CNN–Si(CH_3)_3$ are consistent with a propargylic structure, based on the CN bond lengths.

Table 4-1. Selected PBE0/6-311++G(2df,pd) bond lengths (Å) and bond angels (°) of nitrilimines ($R^1–CNN–R^2$)

	$R^1–C$	C–N	N–N	$N–R^2$	$R^1–C–N$	C–N–N	$N–N–R^2$
H–CNN–H	1.077	1.184	1.231	1.022	132.5	170.2	109.6
F–CNN–F	1.305	1.261	1.202	1.408	116.8	158.6	108.5
$NH_2–CNN–NH_2$	1.317	1.31	1.236	1.363	117.2	132	113.5
COOH–CNN–OH	1.456	1.201	1.216	1.398	131.1	170.8	109.5
CHO–CNN–OH	1.444	1.195	1.219	1.398	138.4	171.9	109.2
$H_3CO–CNN–CH_3$	1.327	1.222	1.223	1.458	123.7	164.6	114.9
$NO_2–CNN–NH_2$	1.457	1.227	1.214	1.354	116.2	165.5	116
Ph–CNN–Ph	1.409	1.163	1.249	1.394	177.8	173.6	117.1
$CH_3–CNN–CH_3$	1.468	1.183	1.234	1.456	140.7	171.6	113.8
$Si(CH_3)_3O–CNN–Si(CH_3)_3$	1.32	1.196	1.234	1.769	135.1	167.9	120.1
$H_3CS–CNN–SO_2N(CH_3)_2$	1.651	1.163	1.258	1.678	175.4	175.4	111.7
$Si(CH_3)_3NH–CNN–Si(CH_3)_3$	1.344	1.184	1.244	1.76	145.9	170.9	119.6

4.3.2. Energies and Frequencies

Among all nitrilimines considered, only a few have different conformers. For example, CHO–CNN–OH possesses four conformers (Figure 4-2). There are eight conformers for COOH–CNN–OH and two for $H_3CO–CNN–CH_3$ and $H_3CS–CNN–CH_3$ (Table and Fig. B-1). The lowest-energy conformer was used in further calculations. The total energy and geometry of all conformers are provided in Table B-2 and Figure B-1.

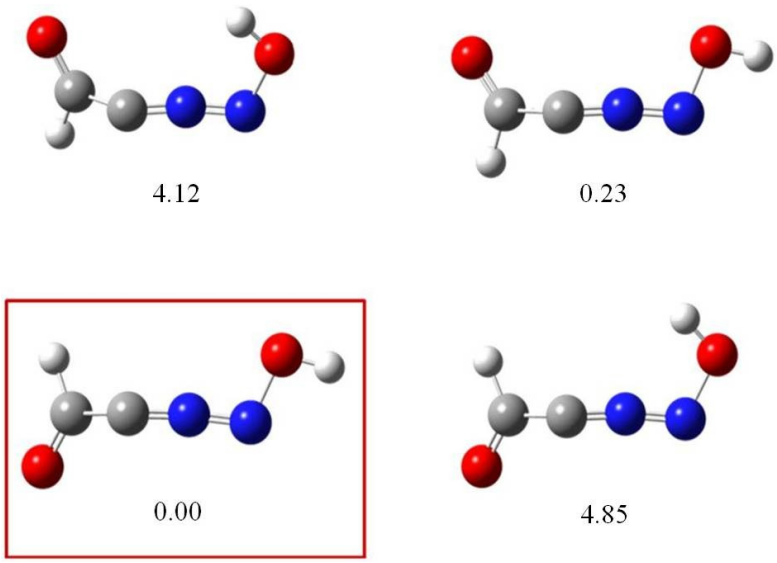

Figure 4-2. Conformers of CHO–CNN–OH and their relative energies (kcal mol^{-1})

4.3.3. Natural Resonance Theory (NRT) Analysis of Nitrilimines

In this section, we examine the effect of substitution on the electronic structure of nitrilimines using NRT analysis. Previous studies demonstrated that geometrical parameters in nitrilimines correspond to a superposition of three valence-bond structures: allenic, carbenic, and 1,3-dipolar,[192] and thus these three possible structures are considered in this section.

By default, NRT calculations consider octet structures (propargylic and allenic), and sextet structures must be specified as reference structures.[177, 180, 181] The carbenic structure was specified as a reference structure, since previous work showed that its inclusion as a reference best describes the changes in molecular structure caused by various substituents.[192, 193] As shown in Figure 4-3, there is a connection between the three resonance structures of nitrlimines: the allenic structure converts to the carbenic one by donation of the central-nitrogen electron lone pair to the empty carbon p-orbital;

meanwhile, the 1,3-dipolar structure can be obtained by donation of the carbon electron lone pair to the empty π^*_{NN} orbital.[193] Consequently, resonance contributions vary upon substitution.

Based on the tetrazoles found in the literature and natural bond orbital (NBO) calculations nitrilimines with a carbon lone pair were investigated (Table 4-2), as they are expected to show a potentially high carbenic character.

The normalized weights for the three valence-bond structures - allenic, 1,3-dipolar, and carbenic - from the NRT analysis are given in Table 4-2 along with the raw values. The results indicate that these three structures encompass 72-88% of the electronic structure for all nitrilimines studied. The residual 12-28% contribution corresponds to classic valence-bond ionic or cyclic structures. For example, valence-bond structures of unsubstituted nitrilimine with more than 1% contribution are shown in Figure 4-4, regardless of geometry. The total contribution of the carbenic character was evaluated by adding to the contribution of the original carbenic structure those of all its possible resonance structures (e.g. the resonance structure for a nitrogen lone pair and an empty carbon p–orbital in NH_2–CNN–NH_2 (Fig. B-3)).

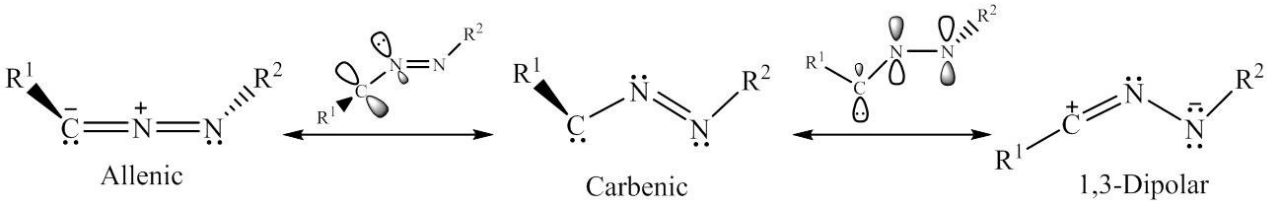

Figure 4-3. Three main valence-bond structures of nitrilimines: allenic, carbenic, and 1,3-dipolar

Table 4-2. Natural bond orbital calculations of nitrilimines with a carbon lone pair occupancy (R^1–CNN–R^2)

R^1	R^2	n_C occupancy
NH_2	NH_2	1.923
OCH_3	CH_3	1.553
COOH	OH	1.287
CHO	OH	1.280
NO_2	NH_2	1.999
F	F	1.686

Table 4-3. Normalized PBE0/6-311++G(2df,pd)values (%) of the valence-bond structure contributions according to NRT analysis (absolute values in parenthesis).

	allenic	1,3-dipolar	carbenic
H–CNN–H	41 (36)	43 (38)	16 (14)
F–CNN–F	26 (22)	19 (16)	55 (47)
NH_2–CNN–NH_2	14 (12)	13 (11)	73 (61)
COOH–CNN–OH	49 (33)	38 (26)	13 (9)
CHO–CNN–OH	48 (33)	39 (27)	13 (9)
H_3CO–CNN–CH_3	35 (29)	28 (23)	37 (31)
O_2N–CNN–NH_2	42 (30)	18 (13)	40 (29)

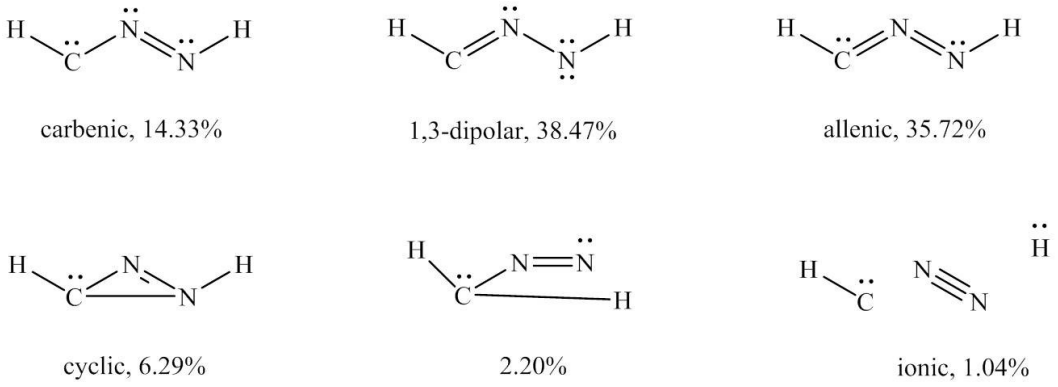

Figure 4-4. Valence-bond structures of unsubstituted nitrilimine with more than 1% contribution

As can be seen from Table 4-3, for H–CNN–H, the valence-bond structure of the allenic and 1,3-dipolar have similar weight, approximately 3 times that of the carbenic structure. The carbenic character is weak because of the interaction with the NN moiety, as shown in Figure 4-2. The results of NRT analysis using B3LYP/6-31+G(d) are presented in Table B-4.

For the nitrilimines with a π-electron donating substituent such as NH_2–CNN–NH_2, F–CNN–F and H_3CO–CNN–CH_3, the C-substitution lone pair is donated to the empty carbon p-orbital, and therefore, the resonance between the carbenic and allenic structure is reduced. On the other hand, electron withdrawing substituent inductive effects reduce the carbon lone pair density, and consequently, the resonance of the carbenic and 1,3-dipolar structures is diminished. The allenic contribution is enhanced by increase of the lone pair availability of the substituent, based on the electronegativities of the substituents. Along the series OCH_3, NH_2, and F, the electron donating effect decreases and the electron withdrawing effect increases. Since the amino group has an optimal combination of π-electron donating and σ-electron withdrawing abilities, it has the most dramatic effect on the nitrilimine electronic structure. Alternatively, for N-substitution, the substituent lone pair is donated to the π^*_{NN} orbital, resulting in a reduction of carbenic and 1,3-dipolar character. The electron withdrawing inductive effect reduces the nitrogen lone pair density, and hence the resonance of the carbenic and 1,3-dipolar structures is diminished. Substitution with the N-methyl group, an electron donating group, diminishes the availability of the π^*_{NN} orbital, resulting in a decrease in carbenic and 1,3-dipolar character. Accordingly, both C- and N-substitution affect the magnitude of the contributions of the valence-bond structures, and overall, NH_2–CNN–NH_2, F–CNN–F,

and $H_3CO–CNN–CH_3$ have a total carbenic contribution of 73, 55, and 37%, respectively.

In the case of $NO_2–CNN–NH_2$, the effect of the electron withdrawing nitro group is to reduce the carbon lone pair density, and consequently, the resonance of the carbenic to 1,3-dipolar structures diminishes. Moreover, the amine lone pair is donated to the π^*_{NN} orbital, also causing a decrease in the resonance of the carbenic to 1,3-dipolar structures. For COOH–CNN–OH and CHO–CNN–OH, although a similar behaviour could be expected, the carbenic contribution remains very low. The reason might be that C- and N-substituents cancel the effects of each other on the electronic structure and these nitrilimines exhibit the same behaviour as unsubstituted nitrilimine.

NRT calculations provided two new structures with lone pairs on their carbon atoms which might be also considered to have carbenic character. As shown in Figure 4-5(a), one of these structures is the resonance structure of carbenes in which the lone pair of electron donating groups on the carbon atom interacts with the empty p-orbital of carbon. The weight of the carbenic character of this resonance structure might be included when the total amount of carbenic contribution is calculated. This structure was observed in $NH_2–CNN–NH_2$, F–CNN–F and $CH_3O–CNN–CH_3$. However, in the second structure (Fig. 4-5(b)), which was observed in most cases, N-substituents are responsible for the resonance stabilization and the N-N bond order is different from the carbenic structure. Further investigation is required to verify whether the carbenic character of the second structure should be included in the total carbenic contribution. All predicted structures are provided in Figure B-3.

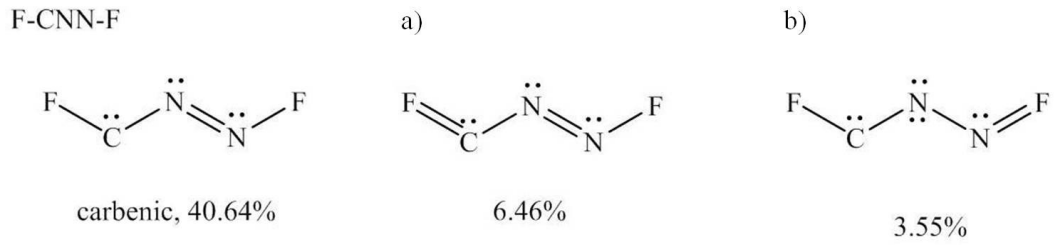

Figure 4-5. Example of nitrilimines structures analogue to carbenic structure. a) and b) resonance structures of carbenic structure regardless charges.

4.4. Conclusions

The results presented in this chapter demonstrate that the optimized geometry of nitrilimines varies upon substitution. All nitrilimines have a structure halfway between the planar (propargylic) and bent (allenic) one. However, a propargylic structure had been proposed for some of them on the basis of the CN bond lengths.

Natural resonance theory (NRT) analyses showed that three valence-bond structures - allenic, carbenic, and 1,3-dipolar - are important in the description of the electronic structure of nitrilimines, amounting to over 70% of the resonance structure contributions to the overall electronic structure. In H–CNN–H, the carbenic contribution is rather small and the allenic and 1,3-dipolar contributions are predominant. Substituents influence the resonance interactions between the allenic, carbenic, and 1,3-dipolar structures. C-electron donating substituents such as F and OCH_3 decrease the resonance of the carbenic to allenic structure, while their electron inductive effect diminishes the resonance of the carbenic to 1,3-dipolar structures, and therefore, the weight of carbenic structure is increased. On the other hand, C-electron withdrawing substituents such as NO_2 reduce

the resonance of VBS-C to VBS-D, and hence, the carbenic contribution is enhanced. Moreover, N-substitutions with either electron donating or electron withdrawing groups reduce the resonance of VBS-C to VBS-D. In some cases, N-substitutions may counteract the effect of C-substitutions or vice-versa.

Chapter 5.

Possible intermolecular carbene-type cycloaddition of nitrilimines

5.1. Introduction

Nitrilimines, R–CNN–R, have been widely used in 1,3-dipolar (or [3+2]) cycloadditions, in which they are added to a dipolarophile, typically an alkene or alkyne, to form 5-membered heterocyclic rings.[1] Nitrilimines as 1,3-dipoles are commonly prepared in situ as a transient species that can then readily react in the presence of a dipolarophile.[11] In fact, all nitrilimines studied experimentally undergo [3+2] cycloaddition reactions and their mechanism has been extensively studied.[6, 46, 50, 56, 194-196] Huisgen proposed a carbene as a resonance structure of a 1,3-dipole, however, he proposed that a carbene should only have a small contribution to the electronic structure of 1,3-dipoles due to the lack of octet stabilization.[1]

Six valence bond structures[1, 15-17, 19-22, 24] -propargylic, allenic, 1,3-dipolar, carbenic, reverse 1,3-dipolar, and hypervalent- have been used to describe the electronic structure of nitrilimines. A nitrilimine with some carbenic component can be expected to undergo [1+2] cycloaddition reactions in addition to the well-known [3+2] cycloaddition reactivity, based on the formation of cyclopropanes from carbenes and alkenes.[197-199] For nitrilimines, there are two factors to be considered in reaction control where a choice of [1+2] over [3+2] is desired. First, the CNN carbon atom needs to possess substantial

electrophilic character since a "stable" nitrilimine with too much nucleophilic character on carbon should not react with C=C (again based on carbine reactivity).[200] It has been shown that nitrilimines can be regarded as ambiphilic species reacting with both electron-poor and electron–rich alkenes.[201] Second, as suggested from the presence of six possible valence bond structures, the geometry of nitrilimines varies vastly depending on substitution. Correspondingly, through molecular orbital calculations, Houk and Caramella demonstrated that even nitrilimine itself is a flexible molecule that can adapt its geometry depending on the nature of the reaction.[15, 16]

Previously, our group examined [1+2] and [3+2] cycloaddition reaction pathways between ethene and a series of 13 nitrilimines.[202] The result of this study showed that the [3+2] reaction dominates in most cases, however, the [1+2] pathway can be obtained by varying the N-substituent. Ridge-bifurcation was proposed on the potential energy surface in the vicinity of the two transition states (TS), [1+2] and [3+2], for the reaction of the unsubstituted nitrilimine with ethene. It was suggested that the reaction initially started with a carbene-type attack of the nitrilimine, and that the [3+2] products would form after crossing the ridge-inflection region of the surface. Based on the potential energy surface, whose one parameter was the torsion angle between the nitrilimine CN and the alkene CC units, this is due to an energetically downhill torsion from 90º (in the [1+2] path) to 0º (as required in the [3+2] TS) as the two fragments approach the [1+2] TS. As a result, the formation of [3+2] products can be suppressed when this torsion is hindered. Such a geometrical dependence has been addressed before, and the literature exhibits "examples" of intramolecular [1+2] reactivity,[9, 61, 62, 203-208] which is supposed to occur when the p-orbital of the dipolarophile is limited to attack perpendicular to the

nitrilimine plane due to geometrical restrictions. It has recently been demonstrated, though, that these "literature examples" of [1+2] reactivity cannot be upheld under the scrutiny of modern computational methods, and that the products do not arise from a concerted cycloaddition.[58] To the best of our knowledge, observations of intermolecular [1+2] cycloaddition reactivity have not been claimed for nitrilimines. Yet, we expected that nitrilimines with large carbenic character should undergo [1+2] cycloadditions. The nitrilimines were chosen from the outcome of Chapter 4, and the results were compared to those for the parent, unsubstituted nitrilimine.

5.2. Computational Details

Gaussian 03[174] and Gaussian 09[175] program packages were used for transition state optimization and frequency calculations. Density functional theory calculations were performed with B3LYP (Becke3-Lee, Young and Parr)[176-179] hybrid density functional and a mid-sized Pople-style basis set (6-31+G(d)). In addition, PBE0 (Perdew-Burke-Ernzerhof)[187, 188] with a larger Pople-style basis set (6-311++G(2df,pd)) were employed for selected transition state calculations, from H–CNN–H, F–CNN–F, and NH_2–CNN–NH_2, to determine the effect of the model chemistry on activation energies and to allow comparisons to our earlier data.[202] The intrinsic reaction coordinate (IRC) procedure[180, 181] was applied to transition states to verify the nature of a proposed reaction mechanism. The Natural Resonance Theory (NRT) approach[209] was applied for the determination of the contribution of carbenic resonance structures to the overall electronic structure in transition states. Transition state theory (TST) was employed to calculate the reaction

rates.[210, 211] In this work, the results of B3LYP/6-31+G(d) is presented and the other results are provided in appendix C.

5.3. Results and Discussion

5.3.1. Reaction of Nitrilimines

Nitrilimines are described by six valence bond structures, namely, propargylic, allenic, 1,3-dipolar, carbenic, reverse 1,3-dipolar, and hypervalent. In particular, for the parent nitrilimine H–CNN–H, propargylic, allenic and 1,3-dipolar contributions to its electronic structure are predominant.[1, 22] The reactivity of nitrilimines can be varied based on the contributions of each resonance structure and on the electron density of the reaction partner. The schematic reactions of nitrilimines with alkenes are shown in Figure 5-1.

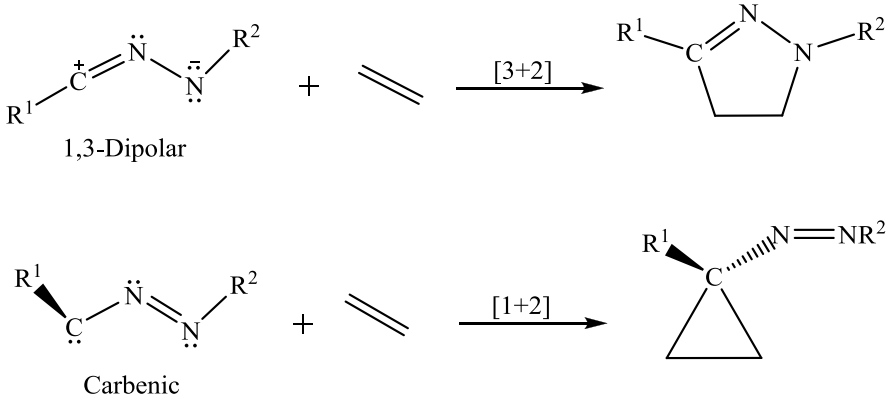

Figure 5-1. Schematic reactions of nitrilimines with alkenes.

5.3.1.1) With the electron-rich ethene

The two TS structures, for the [1+2] and [3+2] paths, are shown in Fig. 5-2. Since the unsubstituted nitrilimine only has a small carbenic character -16% where the carbenic

structure was used as reference structure in calculation[192, 212] while carbenic character for nitrilimine is reported 27% where the carbenic has not been employed as reference structure[22]-, [3+2] reactivity is indeed favoured in the reaction with ethene. As can be seen from Table 5-1, the relative activation barrier is 13.6 kcal mol^{-1} for the [1+2] path in contrast to only 9.9 kcal mol^{-1} for the [3+2] path. The conclusion is that, with the relatively electron-rich ethene, the [3+2] reaction path is preferred from this model chemistry. The results are in accord with previous work in our group using PBE0/6-311++G(2df,pd).[202] The small activation barrier and high exothermicity (as can be judged from the relative energy of the deeper minimum in both parts of Fig. 5-3) of the reaction in its [1+2] and [3+2] paths confirm the expected early transition states in accordance with the Hammond postulate.[213] As mentioned previously, apart from the closing C-C distance between the reaction partners, the torsion up to and in the two transition states is the main geometric parameter controlling the reaction. The main differences between the TS structures in [1+2] and [3+2] reactions are the length of the forming C3–C4 bond, which is slightly shorter in the [1+2] TS, as well as the C5–C4–C3–N2 dihedral angle (Table 5-2), which is nearly at 90º (perpendicular arrangement) in the [1+2] reaction compared to 0º (parallel arrangement) in the [3+2] reaction. These results are in accord with those previously obtained in our group using PBE0/6-311++G(2df,pd).[202]

Figure 5-3 shows the intrinsic reaction coordinate (IRC) for both the [1+2] and [3+2] paths in the cycloaddition nitrilimine with ethene, going from pre-reaction complexes over transition states to products with increasing reaction coordinate, and demonstrates the concerted nature of both mechanisms, in that only one transition state is located in each pathway.

Table 5-1. Activation energies (kcal mol^{-1}) for [1+2] and [3+2] cycloadditions of nitrilimines with ethene and tetrafluoroethene (free relative energies in parenthesis). Energies of reactants and transition states are provided in Appendix C.

	C_2H_4		C_2F_4	
	[1+2]	[3+2]	[1+2]	[3+2]
H–CNN–H	13.6 (23.4)	9.9 (20.1)	12.5 (22.6)	13.7 (24.5)
NH_2–CNN–NH_2	–	8.3 (19.4)	–	4.4 (15.7)
F–CNN–F	3.5 (14.1)	2.4 (13.1)	6.2 (17.4)	8.5 (19.8)
H_3CO–CNN–CH_3	10.8 (21.9)	7.0 (18.2)	10.0 (21.3)	8.5 (20.1)
NO_2–CNN–NH_2	7.6 (18.4)	5.1 (16.1)	9.1 (20.1)	9.9 (21.7)
COOH–CNN–OH	7.7 (18.1)	7.3 (18.7)	10.4 (21.9)	14.1 (25.8)
CHO–CNN–OH	4.0 (14.5)	6.2 (17.0)	9.2 (20.7)	14.5 (26.0)

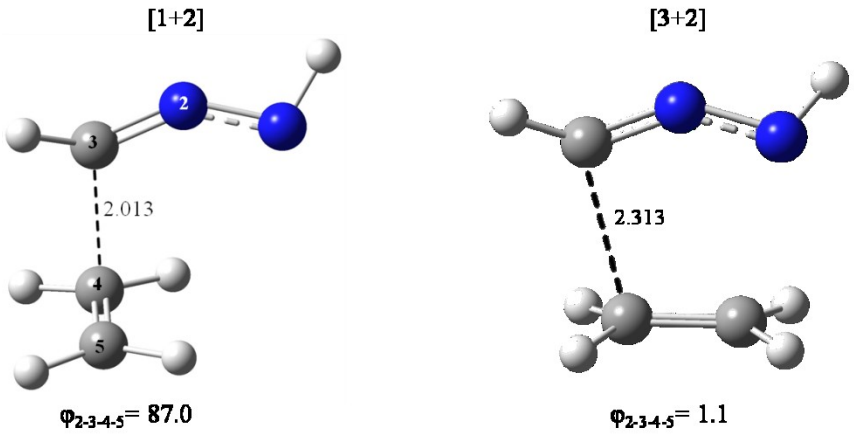

Figure 5-2. Geometries of [1+2] and [3+2] transition states in the cycloaddition of nitrilimine with ethene (distances in Å, torsion angles in degrees).

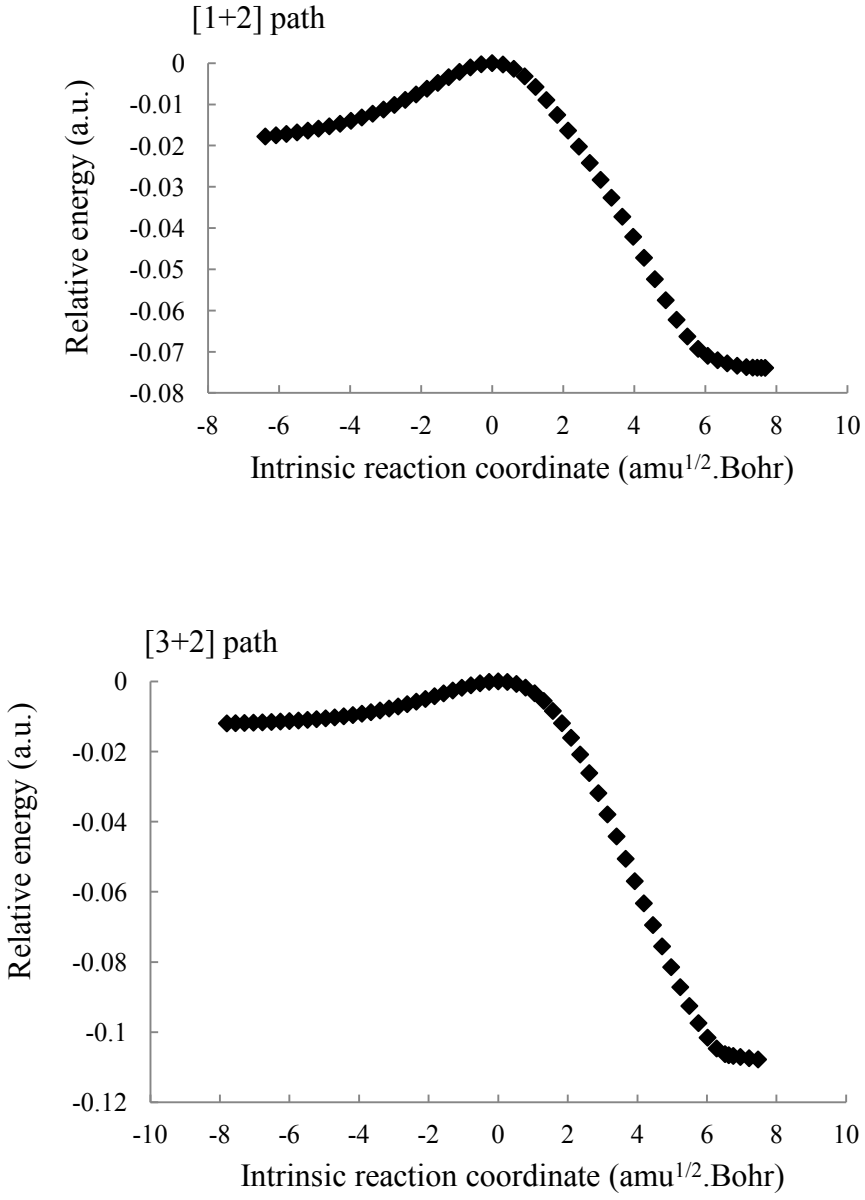

Figure 5-3. Intrinsic reaction coordinate (IRC) for [1+2] and [3+2] pathways in the cycloaddition reaction of nitrilimine with ethene. 1 a.u. = 627.5 kcal mol^{-1}.

In terms of frontier molecular orbital theory, interaction of the highest occupied molecular orbital (HOMO) of the dipole with the lowest unoccupied molecular orbital (LUMO) of the dipolarophile controls some 1,3-dipolar cycloaddition reactions, while others are controlled by the reverse interaction of $HOMO_{dipolarophile}$ with $LUMO_{dipole}$; in

some cases both combinations can be important.[214] As the nitrilimine could be an electrophile, nucleophile or ambiphile in the cycloaddition studied here, its philicity was inspected using the orbital energy differences between $HOMO_{C=C}$-$LUMO_{CNN}$ and $HOMO_{CNN}$-$LUMO_{C=C}$ (where C=C refers to ethene and CNN to nitrilimine). In the reaction of H–CNN–H with ethene, the orbital energy gaps of the two possible interactions are 6.9 and 6.6 eV, respectively (Table and Fig. 5-4). Figure 5-4 shows the orbitals on the two reaction partners in their orientations at the [3+2] transition state. The rather similar orbital energy gaps indicate that nitrilimine reacts as an ambiphilic species in this particular cycloaddition. Since the phases should match up in the bonding orbital, the LUMO+1 orbital is considered to overlap with HOMO of ethene. A picture and energy of LUMO is provided in Figure C-1 and Table C-5, appendix C.

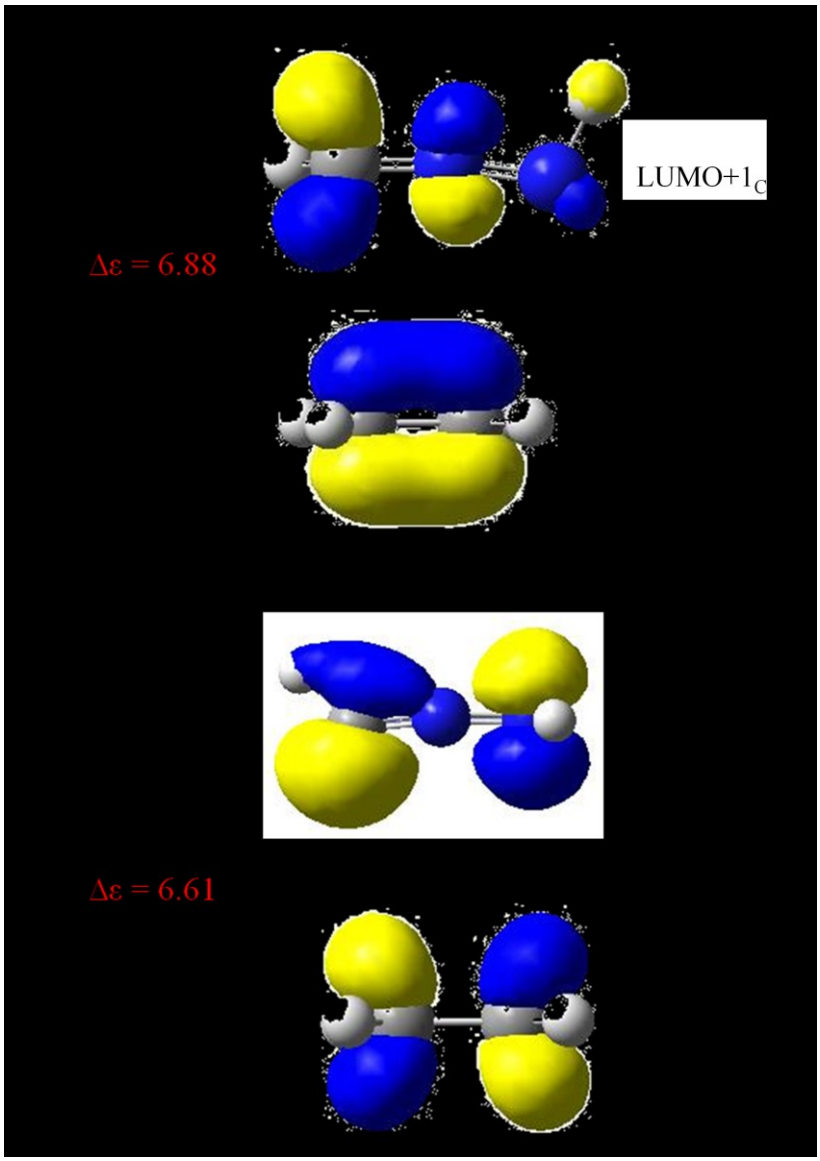

Figure 5-4. Ideal orientation of the frontier molecular orbitals in the [3+2] TS of the reaction of nitrilimine with ethene. a) dipole-LUMO controlled, and b) dipole-HOMO controlled. Orbital energies are provided for the non-interacting reactants.

Table 5-2. Selected bond lengths (Å), dihedral and bond angles (degrees) of [1+2] and [3+2] transition states in the cycloaddition between nitrilimines and ethene or tetrafluoroethene.

	C_2H_4			C_2F_4		
	C3–C4	N2–C3–C4–C5	C3N2N1	C3–C4	N2–C3–C4–C5	C3N2N1
[1+2] TS						
H–CNN–H	2.013	87	142.9	1.957	91.2	158.4
F–CNN–F	2.173	56.5	132.2	2.165	69.3	137.7
H_3CO–CNN–CH_3	2.066	71.9	134.4	2.086	83.7	142.3
NO_2–CNN–NH_2	2.202	55.2	137.6	2.095	73.2	143.7
COOH–CNN–OH	2.261	73.7	146.2	2.084	82.3	153.6
CHO–CNN–OH	2.384	80.7	149.9	2.11	86.3	154
[3+2] TS						
H–CNN–H	2.313	1.1	142.7	2.286	3.5	142.2
F–CNN–F	2.403	4.1	131.8	2.2	7.8	126.4
NH_2–CNN–NH_2	2.232	5.5	128.6	2.16	25.9	122.8
H_3CO–CNN–CH_3	2.436	0.4	138.7	2.334	7.8	134.5
NO_2–CNN–NH_2	2.328	4.9	135	2.3	3.8	130.3
COOH–CNN–OH	2.282	0.2	138.4	2.282	7	136.3
CHO–CNN–OH	2.269	5.9	139.8	2.268	5.4	136.4

Table 5-3. Energy differences (eV) between HOMO and LUMO of ethene or tetrafluoroethene and nitrilimines. Orbital energies are provided in Appendix C.

	C_2H_4		C_2F_4[a]	
	HO_{CNN}-$LU_{C=C}$	$HO_{C=C}$-LU_{CNN}	HO_{CNN}-$LU_{C=C}$	$HO_{C=C}$-LU_{CNN}
H–CNN–H	6.6	6.9[a]	7	7.0[a]
NH_2–CNN–NH_2	5.2	5.8	5.6	5.9
F–CNN–F	8.2	4.7[a]	8.5	4.8[a]
H_3CO–CNN–CH_3	6.2	7.6	6.5	7.7
NO_2–CNN–NH_2	7.1	5.9[b]	7.5	5.9[b]
CHO–CNN–OH	6.7	5.5	7.1	5.6
COOH–CNN–OH	6.8	5.6	7.1	5.7

[a] LUMO+1 is used instead of LUMO. [b] LUMO+2 is used instead of LUMO.

In order to investigate the expected product ratio, transition state theory[210] was employed to calculate the rate constants of both reaction paths in the range of low (77 K), room (298 K) and high (473 K) temperatures. Table 5-4 shows the calculated rate constants. As expected, due to the smaller activation energy, the magnitude of the reaction rate constant for the [3+2] cycloaddition is higher than that for the [1+2] reaction. Consequently, the [3+2] reaction will yield more product. As the temperature is elevated, all reaction rate constants are (dramatically) increased (Table 5-4). The ratio of [3+2] to [1+2] products, i.e., 5-membered versus 3-membered rings, was investigated using Equation 5-1. This ratio for the reaction of nitrilimine with ethene at 298 K was about 258 (Table 5-5). In other words, the cyclopropane is not formed.

Eq. 5-1

Table 5-4. Reaction rate constants (L mol^{-1} s^{-1}) for [1+2] and [3+2] paths in the cycloaddition reactions of nitrilimines with ethene at three different temperatures.

	Path	Temperature (K)		
		77	298	473
H–CNN–H	[1+2]	$5.09*10^{-32}$	$1.04*10^{-03}$	7.11
	[3+2]	$1.23*10^{-21}$	$2.68*10^{-01}$	$1.75*10^{+02}$
F–CNN–F	[1+2]	$4.74*10^{-04}$	$6.74*10^{+03}$	$1.01*10^{+05}$
	[3+2]	$4.92*10^{-01}$	$3.97*10^{+04}$	$2.91*10^{+05}$
H_3CO–CNN–CH_3	[1+2]	$4.55*10^{-25}$	$1.22*10^{-02}$	$1.58*10^{+01}$
	[3+2]	$2.30*10^{-14}$	7.33	$9.02*10^{+02}$
NO_2–CNN–NH_2	[1+2]	$6.56*10^{-16}$	$5.19*10^{0}$	$1.06*10^{+03}$
	[3+2]	$6.72*10^{-09}$	$2.17*10^{+02}$	$8.20*10^{+03}$
COOH–CNN–OH	[1+2]	$3.12*10^{-15}$	8	$1.47*10^{+03}$
	[3+2]	$2.23*10^{-16}$	2.84	$5.73*10^{+02}$
CHO–CNN–OH	[1+2]	$1.07*10^{-05}$	$3.38*10^{+03}$	$8.33*10^{+04}$
	[3+2]	$5.53*10^{-12}$	$5.40*10^{+01}$	$4.54*10^{+03}$

Table 5-5. Product ratio for the reaction of nitrilimines with ethene

	Temperature (K)		
	77	298	473
H–CNN–H	$2.42*10^{+01}$	$2.58*10^{+02}$	$2.46*10^{+01}$
F–CNN–F	$1.04*10^{+03}$	5.98	2.88
H_3CO–CNN–CH_3	$5.05*10^{+01}$	$6.01*10^{+02}$	$5.71*10^{+01}$
NO_2–CNN–NH_2	$1.02*10^{+07}$	$4.18*10^{+01}$	7.74
COOH–CNN–OH	$7.15*10^{-02}$	$3.55*10^{-01}$	$3.90*10^{-01}$
CHO–CNN–OH	$5.17*10^{-07}$	$1.60*10^{-02}$	$5.45*10^{-02}$

Six substituted nitrilimines with different carbenic character (as determined in Chapter 4) were employed to examine the possibility of the formation of [1+2] cycloaddition products (cyclopropanes). According to natural resonance theory (NRT)

results, NH_2–CNN–NH_2 shows a large carbenic character (70%)[22, 192, 212] and can be considered a stable carbene due to the presence of amino groups that stabilize the electron deficient carbon atom. This view is corroborated by the computational value of the ^{13}C chemical shift for NH_2–CNN–NH_2 (241 ppm),[193] which is in the known range of those for stable carbenes.[215] NH_2–CNN–NH_2 as a stable carbene and therefore nucleophilic species does not tend to react with dipolarophiles, and hence, is not expected to follow [1+2] reactions, despite its large carbenic character. Accordingly, the TS for the [1+2] reaction pathways could not be located, whereas it was readily located for the [3+2] reaction (8.3 kcal mol^{-1}, Table 5-1). This result is consistent with that previously obtained in our group using a different model chemistry, PBE0/6-311++G(2df,pd).[202] Interestingly, the inspection of the frontier molecular orbitals indicates that the energy gaps between $HOMO_{C=C}$-$LUMO_{CNN}$ and $HOMO_{CNN}$-$LUMO_{C=C}$ are 5.8 and 5.2 eV, respectively (Table 5-3), and the nucleophilic character is thus not observed from these values. For further clarification, the [1+2] reaction of NH_2–CNN–NH_2 with acetone as an unsymmetric double bond with electrophilic carbon atom was investigated. Here, the results meet the expectations, in that the energy gap is smaller for $HOMO_{CNN}$-$LUMO_{C=C}$ (4.7 eV) compared to $HOMO_{C=C}$-$LUMO_{CNN}$ (5.3 eV), demonstrating that NH_2–CNN–NH_2 reacts as a nucleophile in this cycloaddition reaction, and thus, does not tend to react with the more electron-rich C=C double bond of ethene. Results are provided in appendix C, Table C-6.

For F–CNN–F, NRT analysis predicts 57% carbenic character.[22, 212] In the reaction with ethene, the C3–C4 bond distance is shorter in the [1+2] TS and the dihedral angle is decreased to 56.5° (from the near-90° value for the unsubstituted nitrilimine) in contrast

to 4.1° in the [3+2] TS (Table 5-2). Considering the energy gaps between the frontier orbitals of ethene and F–CNN–F, cycloaddition reactions are controlled by the interaction of the HOMO of ethene with the LUMO+1 of F–CNN–F (Fig. C-1); the energy gap between $HOMO_{C=C}$-$LUMO_{CNN}$ is about 3.5 eV smaller than that between $HOMO_{CNN}$-$LUMO_{C=C}$ (Table 5-3), indicating that F–CNN–F reacts as an electrophile in these cycloaddition reactions. Similar to the reaction of unsubstituted nitrilimine with ethene, the reaction of F–CNN–F is exothermic and has a very low activation barrier, but overall, the activation barrier required for this reaction is much smaller than that needed for the reaction of the unsubstituted nitrilimine with ethene; consequently, F–CNN–F is much more reactive than H–CNN–H. More importantly, though, the activation barrier for the [3+2] path is only 1 kcal mol^{-1} smaller than that of the [1+2] path (Table 5-1). Accordingly, the product ratio at 298 K is small at about 6, unlike the reaction of unsubstituted nitrilimine with ethene, indicating that about 14% of the cyclopropane might be observed. The result shows the importance of the very substantial carbenic contribution of F–CNN–F in the overall reaction.

In conjunction with the above results, it was particularly interesting to evaluate the reactions of substituted nitrilimines with moderate carbenic characters, i.e. H_3CO–CNN–CH_3 and NO_2–CNN–NH_2. From the NRT analyses in Chapter 4, the two nitrilimines possess 37 and 40% carbenic character, respectively. The activation energies for reaction with ethene are shown in Table 5-1. In both cases, the [3+2] path is preferred, and the preference is larger than for F–CNN–F. In terms of reactivity, H_3CO–CNN–CH_3 and NO_2–CNN–NH_2 lie in between H–CNN–H and F–CNN–F. Inspection of the molecular orbitals indicates that H_3CO–CNN–CH_3 reacts as a nucleophile in these cycloaddition

reactions, whereas NO_2–CNN–NH_2 reacts with more electrophilic character, but much less so than F–CNN–F (Table 5-3). The product ratio at 298 K for H_3CO–CNN–OH is about 600, and therefore even more unfavourable than for H–CNN–H; it is about 42 for O_2N–CNN–NH_2, indicating that the formation of the [1+2] product does not only depend on the amount of carbenic character, but also on the philicity of the CNN carbon atom.

We finally evaluated reactions from substituted nitrilimines with only a small carbenic character, namely CHO–CNN–OH and COOH–CNN–OH. From the NRT analyses in Chapter 4, both nitrilimines show only 13% carbenic character, and if only the carbenic character was important, these would not undergo [1+2] cycloadditions. Table 5-1 shows, though, that the [1+2] path is clearly preferred for CHO–CNN–OH and that the two reaction barriers for COOH–CNN–OH are rather similar with an energy difference of only 0.4 kcal mol^{-1}. The reactivity of both nitrilimines is higher than that of the unsubstituted nitrilimine (Table 5-1), and both nitrilimines react as electrophiles in these cycloadditions (Table 5-3). For COOH–CNN–OH, where the two activation energies are within computational uncertainty and reaction rates should be comparable, a mixture of 3- and 5-membered rings not far from a 15:1 ratio could be expected. But the projected product ratio in the reaction of CHO–CNN–OH with ethene is about 0.02 at 298 K, i.e., the product mixture should consist to 98% of the cyclopropane! In order to investigate the reason why CHO–CNN–OH undergoes the [1+2] cycloaddition so readily, despite their small carbenic character, NRT calculations were performed on the nitrilimine in its TS-geometry. However, a significant increase in the magnitude of the carbenic contribution was not found, and therefore, the preferred [1+2] reaction is not yet understood.

5.3.1.2. With the electron-poor tetrafluoroethene

To explore the effect of alkene electron density on the pathway of the reaction, tetrafluoroethene was chosen as an electron-poor alkene due to the fact that carbene-type reactivity from the nitrilimine should be enhanced. The activation energies are included in Table 5-1. For the unsubstituted nitrilimine, and in comparison to the reaction with the unsubstituted ethene, the activation barriers decreases, by 1 kcal mol^{-1} for the [1+2] and increases by about 4 kcal mol^{-1} for the [3+2] path (Table 5-1). This shows that the electron-poor alkenes have a differential effect on the two paths.

As expected, the [1+2] path gains in importance, and for the reaction of nitrilimine with tetrafluoroethene the activation barrier for the [1+2] path is now about 1 kcal mol^{-1} lower than that for the [3+2] path. Similar to the cycloadditions with ethene, with tetrafluoroethene the forming C3–C4 bond is shorter in the [1+2] TS then in the [3+2] TS (Table 5-2), and the dihedral angle is nearly at 90° in the TS of the [1+2] cycloaddition (Fig. 5-5).

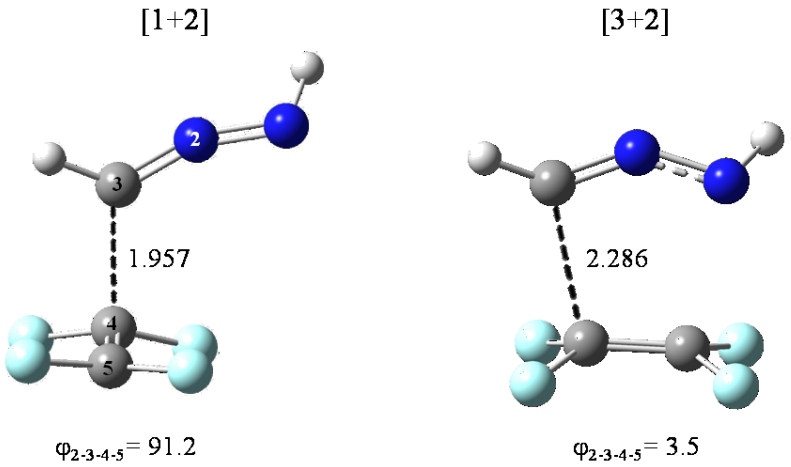

Figure 5-5. Geometries of [1+2] and [3+2] transition states in the cycloaddition of nitrilimine with tetrafluoroethene (distances in Å, torsion angles in degrees).

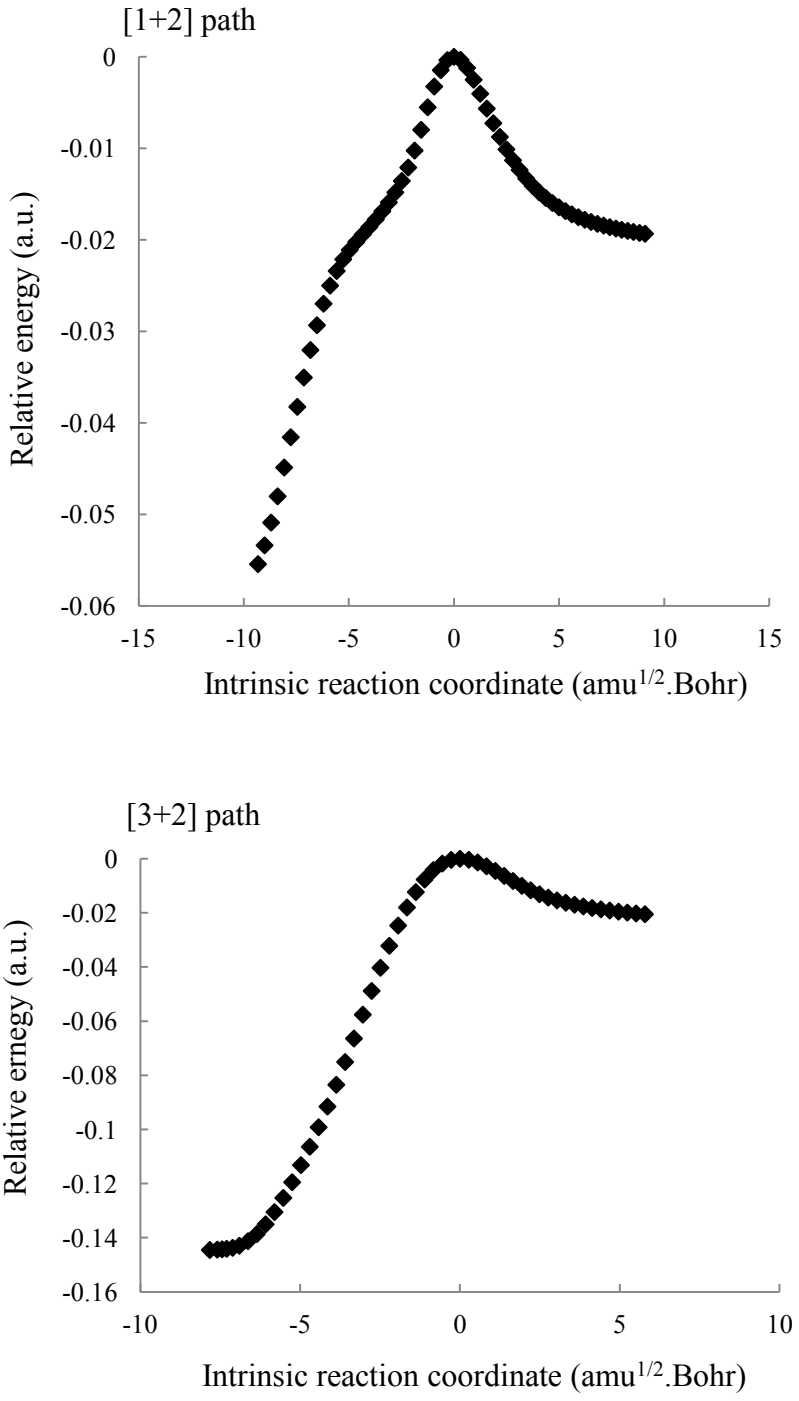

Figure 5-6. Intrinsic reaction coordinate (IRC) for [1+2] and [3+2] pathways in the cycloaddition reaction of nitrilimine with tetrafluoroethene. 1 a.u. = 627.5 kcal mol^{-1}.

The IRC results show that both paths again follow the concerted mechanism (Fig. 5-6). With the use of tetrafluoroethene, though, the IRC shows a shoulder on the product side of the [1+2] path, indicating a post-TS possible ridge-bifurcation,[216] but its significance will not be investigated here. Table 5-3 shows that nitrilimine reacts as an ambiphilic species in these cycloaddition reactions since the two energy gaps are identical. In order to match the phases of molecular orbitals, the LUMO+1 of alkene (Fig. C-1) was used in calculations. NRT evaluation of the geometry of H–CNN–H in the [1+2] transition state does not reveal a significantly enhanced carbenic character, and hence, tetrafluoroethene plays a major role in the promotion of the [1+2] reaction. NRT results are presented in Table C-7, appendix C. The calculated rate constants (Table 5-6) yield a product ratio of about 0.04, or 96% substituted cyclopropane in the product mixture (Table 5-7).

Table 5-6. Reaction rate constants (L mol^{-1} s^{-1}) for [1+2] and [3+2] paths in the cycloaddition reactions of nitrilimines with tetrafluoroethene at three different temperatures.

	Path	Temperature (K)		
		77	298	473
H–CNN–H	[1+2]	$1.47*10^{-29}$	$4.13*10^{-03}$	$2.03*10^{+01}$
	[3+2]	$1.95*10^{-33}$	$1.60*10^{-04}$	1.64
F–CNN–F	[1+2]	$8.23*10^{-13}$	$2.76*10^{+01}$	$3.32*10^{+03}$
	[3+2]	$2.82*10^{-19}$	$4.44*10^{-01}$	$2.01*10^{+02}$
H_3CO–CNN–CH_3	[1+2]	$1.10*10^{-23}$	$3.90*10^{-02}$	$5.05*10^{+01}$
	[3+2]	$1.46*10^{-19}$	$2.57*10^{-01}$	$1.78*10^{+02}$
NO_2–CNN–NH_2	[1+2]	$1.98*10^{-21}$	$1.18*10^{-01}$	$9.30*10^{+01}$
	[3+2]	$1.15*10^{-23}$	$1.76*10^{-02}$	$2.06*10^{+01}$
COOH–CNN–OH	[1+2]	$4.63*10^{-25}$	$1.26*10^{-02}$	$2.15*10^{+01}$
	[3+2]	$1.64*10^{-35}$	$1.87*10^{-05}$	$2.86*10^{-01}$
CHO–CNN–OH	[1+2]	$1.16*10^{-21}$	$9.69*10^{-02}$	$7.74*10^{+01}$
	[3+2]	$1.73*10^{-36}$	$1.23*10^{-05}$	$2.42*10^{-01}$

Table 5-7. Product ratio for the reaction of nitrilimines with tetrafluoroethene

	Temperature (K)		
	77	298	473
H–CNN–H	$1.33*10^{-04}$	$3.87*10^{-02}$	$8.08*10^{-02}$
F–CNN–F	$3.43*10^{-07}$	$1.61*10^{-02}$	$6.05*10^{-02}$
H_3CO–CNN–CH_3	$1.33*10^{+04}$	6.59	3.52
NO_2–CNN–NH_2	$5.81*10^{-03}$	$1.49*10^{-01}$	$2.22*10^{-01}$
COOH–CNN–OH	$3.54*10^{-11}$	$1.48*10^{-03}$	$1.33*10^{-02}$
CHO–CNN–OH	$1.49*10^{-15}$	$1.27*10^{-04}$	$3.13*10^{-03}$

For the reaction with NH_2–CNN–NH_2, tetrafluoroethene lowers the activation barrier about 4 kcal mol^{-1} in comparison to the reaction with ethene. Similar to the reaction with ethene, though, the [1+2] TS could not be located. The geometry of NH_2–CNN–NH_2 in

the [3+2] TS in the presence of tetrafluoroethene is similar to that in the reaction with ethene, but unexpectedly, the dihedral angle of NH_2–CNN–NH_2 with tetrafluoroethene is 25.9º, i.e., much higher than the normal range of this parameter for a [3+2] TS; with ethene it is 5.5º (Table 5-2). This larger torsion angle might lead to an explanation of why the [1+2] TS cannot be found, but this was not investigated further.

In general, the remaining nitrilimines do not present surprising features as to the transition state geometries (Table 5-2). All IRC calculations support the concerted mechanisms, and NRT calculations on TS geometries of those nitrilimines favouring the [1+2] reaction do not show any significant increase in their carbenic character.

Overall, there is no change in philicity of the nitrilimines with a change in reaction partner. Not surprisingly, the reaction barriers (Table 5-1) for all electrophilic nitrilimines (F–CNN–F, NO_2–CNN–NH_2, CHO–CNN–OH, COOH–CNN–OH) increase with the change to the electron-deficient alkene; the [1+2] path is affected less, by about 3-4 kcal mol^{-1}. This leads to a switch in preference in favour of the [1+2] path in those cases where it did not exist for the more electron-rich ethene, so that, with tetrafluoroethene, all electrophilic nitrilimines prefer the [1+2] path. From the rate constants at room temperature, cyclopropanes should be present in the product mixtures to high amounts. These could be as small as 87% (product ratio 0.15) for NO_2–CNN–NH_2 or as large as being basically quantitative (product ratio 0.0015) for COOH–CNN–OH. As discussed above, a similar differential destabilization is observed for the ambiphilic H–CNN–H, and this also leads to a switch in preference to the [1+2] path. General observations about the nucleophilic nitrilimines (NH_2–CNN–NH_2, H_3CO–CNN–CH_3) cannot be made (only two in the sample set, one out of four data points not available).

5.3.1.3 With the electron-poor butenone

In order to design an experimental procedure based on the above findings, both [1+2] and [3+2] paths of F–CNN–F were investigated with butenone, commonly used as an electron-deficient alkene in experimental work. Since butenone is not a symmetric alkene, two possible regioisomeric products, with their corresponding transition states, exist. For initial attack at the α-carbon, the [3+2] path is preferred, but the nitrilimine is selective for the β-carbon position,[19] which can be seen from the activation energies in Fig. 5-7. The activation energies as well as the thermal free energies of activation for both [1+2] and [3+2] paths are nearly the same (Fig. 5-7b). Accordingly, both products should be obtained experimentally, which would be the first time [1+2] reactivity from a nitrilimine was demonstrated. This shows that the nature of alkenes plays a major role in the control of the pathway of reaction.

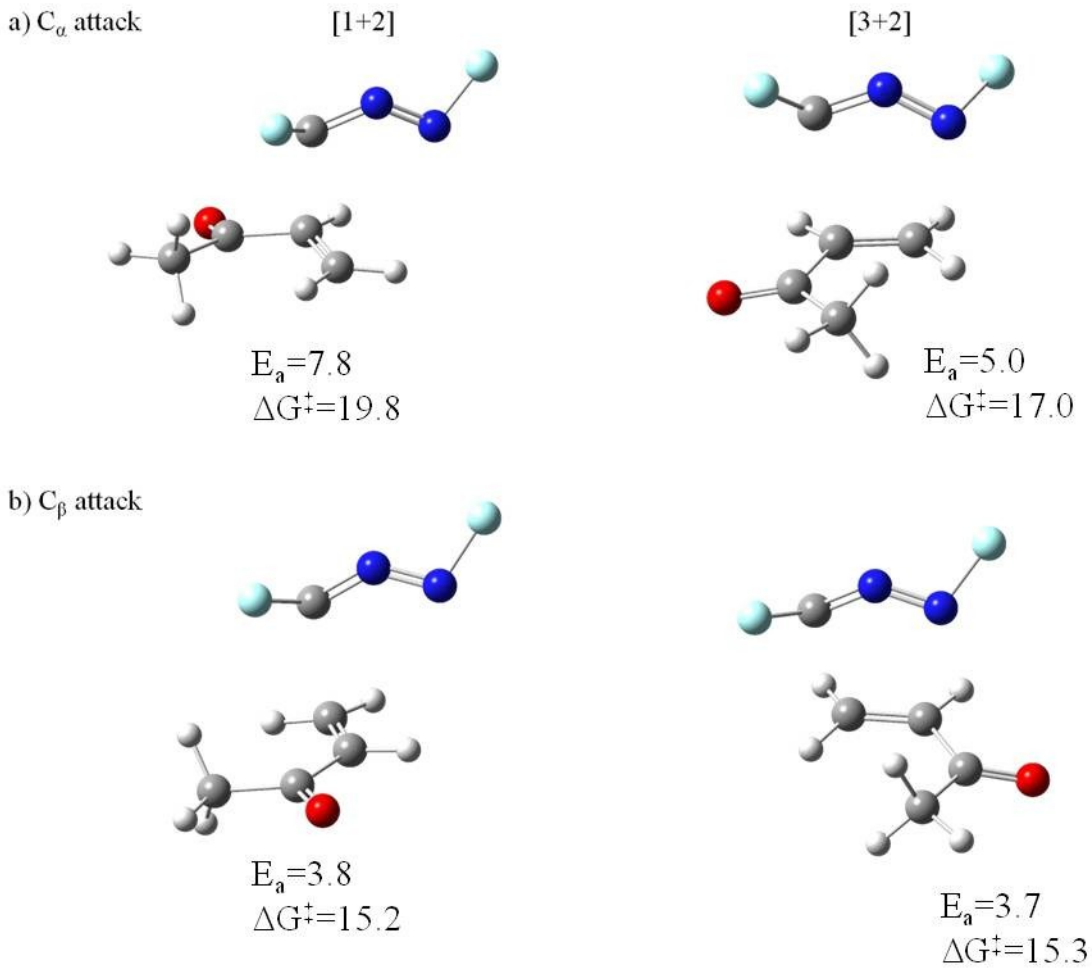

Figure 5-7. Transition states for [1+2] and [3+2] paths in the reaction of F–CNN–F with butenone. a) C_α attack, b) C_β attack (energies in kcal mol^{-1}).

5.4. Conclusions

The cycloaddition reactions, in the gas phase, of seven nitrilimines of varying carbenic character and philicity were investigated with electron-rich and -poor alkenes. The philicities of the nitrilimines were determined from a frontier molecular orbital approach. The electrophilic nitrilimines (F–CNN–F, NO_2–CNN–NH_2, CHO–CNN–OH, COOH–CNN–OH) are more reactive with ethene than with tetrafluoroethene. As a consequence, selectivity with respect to the preferred reaction path is increased with the

electron-poor alkene, and all electrophilic nitrilimines undergo preferentially the elusive [1+2] cycloaddition with tetrafluoroethene. The ambiphilic H–CNN–H also follows this pattern. The results suggest that electron-poor alkenes lead the reaction pathway towards the [1+2] cycloaddition by suppressing the [3+2] mechanism, and cyclopropanes as the reaction products from the [1+2] cycloaddition should be obtainable up to essentially quantitatively (COOH–CNN–OH plus tetrafluoroethene). Both nucleophilic nitrilimines (NH_2–CNN–NH_2, H_3CO–CNN–CH_3) prefer the [3+2] cycloaddition, and the change in alkene electron density seems irrelevant.

Finally, results from the reaction of F–CNN–F with butenone as a common electron-poor alkene show that the two possible cycloadditions involving the terminal unsaturated carbon atom have similar contributions to the overall reaction, implying that both the common 5-membered and the elusive 3-membered ring product should be obtained experimentally.

Chapter 6.

Conclusions and outlook

In the present computational work, we investigated the formation of nitrilimines through tetrazole decomposition, the contributions of three major valence bond structures of nitrilimines (allenic, carbenic and 1,3-dipolar) using natural resonance theory (NRT), and the possible reactions of nitrilimines with alkenes in [1+2] and [3+2] cycloaddition reactions.

Nitrilimines were generated through the decomposition of 2,5-disubstituted tetrazoles. Substituents influence the stability of tetrazoles, and subsequently, the mechanism of the decomposition pathway. In order to examine the effect of substituents on the NN bond length, the bond breaking first, Hammett substituent constants were employed since tetrazoles are aromatic compounds. Hammett plots showed that the π-effect of C-substitutions correlates well with the Hammett σ^+ constant while the σ-effect of N-substitution could not be captured by Hammett constants. C-electron donating substituents make the NN bond shorter whereas electron withdrawing groups cause an increase in the length of the same bond. Moreover, a good correlation exists between the stabilization energy for interaction of the C-substituent with ring of tetrazoles obtained by natural bond orbital analysis and Hammett substituent constants, indicating that electron donating groups on the carbon atom stabilize tetrazoles more than electron withdrawing groups. 2,5-disubstituted tetrazoles with electron withdrawing substituents on the carbon atom follow a stepwise mechanism while electron donating groups promote a concerted mechanism. Additionally, 2H-tetrazole follows a concerted mechanism although the first

step of the stepwise mechanism, NN bond breaking, was obtained with lower activation energy.

The electronic structure of nitrilimines has been the subject of several studies ever since they were first prepared. Six valence-bond structures, propargylic, allenic, 1,3-dipolar, carbenic, reverse 1,3-dipolar and hypervalent, were employed to describe the electronic structure of nitrilimines. Natural resonance theory analyses showed that allenic, carbenic and 1,3-dipolar structures have more than 70% contribution to the electronic structure of nitrilimines. It was shown earlier that there is a correlation between these three valence bond structures in resonance: the allenic structure converts to the carbenic structure by donation of the electron lone pair on the central nitrogen atom to the empty p-orbital on the carbon atom; the 1,3-dipolar structure is obtained by donation of the electron lone pair on the carbon atom to the empty π^*_{NN} orbital. Substituents influence the resonance of allenic, carbenic, and 1,3-dipolar structures. Electron donating groups on the carbon atom diminish the resonance of carbenic to allenic, and the withdrawing inductive effect of these groups reduces the resonance of carbenic to 1,3-dipolar. Thus, the contribution of the carbenic structure is increased. On the other hand, N-substituents, either electron donating or electron withdrawing, cause a decrease in the resonance of carbenic to 1,3-dipolar, and hence, the carbenic contribution is enhanced. In some cases, substituents cancel out the effect of one another and they behave like the parent nitrilimine with rather small carbenic contribution.

Nitrilimines are an important reagent in [3+2]cycloaddition reactions in the production of heterocyclic compounds. All nitrilimines studied experimentally undergo [3+2] cycloaddition reactions, presumably owing to their dominant 1,3-dipolar character,

while nitrilimines with reasonably large carbenic character are expected to undergo [1+2] cycloaddition reactions. Nitrilimines even with large carbenic character undergo the [3+2] reaction in the presence of ethene whereas tetrafluoroethene as an electron-poor alkene promotes [1+2] reactions. Therefore, the nature of alkenes plays a major role in control of the reaction pathway. For a specific nitrilimine, CHO–CNN–OH with small carbenic character, the [1+2] reaction is preferred with both ethene and tetrafluoroethene. The reason is not apparent although the carbenic character was examined in the transition structure using natural resonance theory and no changes were detected in its magnitude during the reaction.

References

1. Huisgen, R., *Angew. Chem. Int. Ed. Engl.* **1963,** *2*, 565-598.

2. Moffat, J. B., *J. Mol. Struct.* **1979,** *52*, 275-280.

3. Wentrup, C.; Fischer, S.; Maquestiau, A.; Flammang, R., *Angew. Chem. Int. Ed. Engl.* **1985,** *24*, 56-57.

4. Toubro, N. H.; Holm, A., *J. Am. Chem. Soc.* **1980,** *102*, 2093-2094.

5. Fischer, S.; Wentrup, C., *J. Chem. Soc., Chem. Commun.* **1980**, 502-503.

6. Garanti, L.; Sala, A.; Zecchi, G., *J. Org. Chem.* **1977,** *42*, 1389-1392.

7. Garanti, L.; Vigevani, A.; Zecchi, G., *Tetrahedron Lett.* **1976,** *17*, 1527-1528.

8. Schmitt, G.; Laude, B., *Tetrahedron Lett.* **1978,** *19*, 3727-3728.

9. Wentrup, C.; Damerius, A.; Reichen, W., *J. Org. Chem.* **1978,** *43*, 2037-2041.

10. Bock, H.; Dammel, R.; Fischer, S.; Wentrup, C., *Tetrahedron Lett.* **1987,** *28*, 617-620.

11. Bertrand, G.; Wentrup, C., *Angew. Chem. Int. Ed. Engl.* **1994,** *33*, 527-545.

12. Huisgen, R., *Angew. Chem. Int. Ed. Engl.* **1963,** *2*, 633-645.

13. Huisgen, R.; Seidel, M.; Sauer, J.; McFarland, J.; Wallbillich, G., *J. Org. Chem.* **1959,** *24*, 892-893.

14. Huisgen, R.; Seidel, M.; Wallbillich, G.; Knupfer, H., *Tetrahedron* **1962,** *17*, 3-29.

15. Caramella, P.; Gandour, R. W.; Hall, J. A.; Deville, C. G.; Houk, K. N., *J. Am. Chem. Soc.* **1977,** *99*, 385-392.

16. Caramella, P.; Houk, K. N., *J. Am. Chem. Soc.* **1976,** *98*, 6397-6399.

17. Cargnoni, F.; Molteni, G.; Cooper, D. L.; Raimondi, M.; Ponti, A., *Chem. Commun.* **2006**, 1030-1032.

18. Faure, J.; Reau, R.; Wong, M. W.; Koch, R.; Wentrup, C.; Bertrand, G., *J. Am. Chem. Soc.* **1997,** *119*, 2819-2824.

19. Houk, K. N.; Sims, J.; Duke, R. E.; Strozier, R. W.; George, J. K., *J. Am. Chem. Soc.* **1973,** *95*, 7287-7301.

20. Kahn, S. D.; Hehre, W. J.; Pople, J. A., *J. Am. Chem. Soc.* **1987,** *109*, 1871-1873.

21. Kuhler, K.; Palmer, R. T.; Wittkamp, B. L.; Hoffmann, M. R., *J. Mol. Struc. (THEOCHEM)* **1996,** *360*, 41-54.

22. Mawhinney, R. C.; Muchall, H. M.; Peslherbe, G. H., *Chem. Commun.* **2004**, 1862-1863.

23. Mawhinney, R. C.; Peslherbe, G. H.; Muchall, H. M., *J. Phys. Chem. B* **2007,** *112*, 650.

24. Wong, M. W.; Wentrup, C., *J. Am. Chem. Soc.* **1993,** *115*, 7743-7746.

25. Huisgen, R.; Seidel, M.; Wallbillich, G.; Knupfer, H., *Tetrahedron* **1962,** *17*, 3.

26. Padwa, A.; Caruso, T.; Nahm, S., *J. Org. Chem.* **1980,** *45*, 4065-4067.

27. Tanaka, K.; Igarashi, T.; Maeno, S.; Mitsuhashi, K., *Bull. Chem. Soc. Jpn.* **1984,** *57*, 2689-2690.

28. Sicard, G.; Baceiredo, A.; Bertrand, G., *J. Am. Chem. Soc.* **1988,** *110*, 2663-2664.

29. Castan, F.; Baceiredo, A.; Bertrand, G., *Angew. Chem. Int. Ed. Engl.* **1989,** *28*, 1250-1251.

30. Pierre, M.; Goodwin, H. P.; Baceiredo, A.; Dillon, K. B.; Bertrand, G., *Organometallics* **1991,** *10*, 3205-3210.

31. Castan, F.; Baceiredo, A.; Bigg, D.; Bertrand, G., *J. Org. Chem.* **1991,** *56*, 1801-1807.

32. Granier, M.; Baceiredo, A.; Bertrand, G., *Angew. Chem. Int. Ed. Engl.* **1988,** *27*, 1350-1351.

33. Granier, M.; Baceiredo, A.; Dartiguenave, Y.; Dartiguenave, M.; Menu, M. J.; Bertrand, G., *J. Am. Chem. Soc.* **1990,** *112*, 6277.

34. Foti, F.; Grassi, G.; Risitano, F., *Tetrahedron Lett.* **1999,** *40*, 2605-2606.

35. Wentrup, C.; Benedikt, J., *J. Org. Chem.* **1980,** *45*, 1407-1409.

36. Wentrup, C.; Damerius, A.; Reichen, W., *J. Org. Chem.* **1978,** *43*, 2037.

37. Padwa, A.; Caruso, T.; Nahm, S.; Rodriguez, A., *J. Am. Chem. Soc.* **1982,** *104*, 2865-2871.

38. Padwa, A.; Caruso, T.; Plache, D., *J. Chem. Soc., Chem. Commun.* **1980**, 1229-1230.

39. Ruccia, M.; Vivona, N., *Chim. Ind.* **1966,** *48*, 147.

40. Meier, H.; Heinzelmann, W.; Heimgartner, H., *Chimia* **1980,** *34*, 504-506.

41. Huisgen, R.; Sauer, J.; Seidel, M., *Chem. Ber.* **1961,** *94*, 2503–2509.

42. Huisgen, R.; Aufderhaar, E.; Wallbillich, G., *Chem. Ber.* **1965,** *98*, 1476-1486.

43. Bakavoli, M.; Moeinpour, F.; Davoodnia, A.; Morsali, A., *J. Mol. Struc.* **2010,** *969*, 139-144.

44. Del Buttero, P.; Molteni, G.; Pilati, T., *Tetrahedron* **2005,** *61*, 2413-2419.

45. Giorgio, M., *Tetrahedron: Asymmetry* **2004,** *15*, 1077-1079.

46. Pellissier, H., *Tetrahedron* **2007,** *63*, 3235-3285.

47. Krajsovszky, G.; Gaal, A.; Haider, N.; Matyus, P., *J. Mol. Struc. (THEOCHEM)* **2000,** *528*, 13-18.

48. Lauria, A.; Guarcello, A.; Macaluso, G.; Dattolo, G.; Almerico, A. M., *Tetrahedron Lett.* **2009,** *50*, 7333-7336.

49. Liu, B.; Wang, M.; Huang, Z., *Tetrahedron Lett.* **1999,** *40*, 7399-7402.

50. Molteni, G.; Ponti, A., *Tetrahedron* **2003,** *59*, 5225-5229.

51. Molteni, G.; Ponti, A., *Tetrahedron: Asymmetry* **2004,** *15*, 3711-3714.

52. Molteni, G.; Ponti, A., *Tetrahedron: Asymmetry* **2008,** *19*, 1381-1384.

53. Molteni, G.; Ponti, A.; Orlandi, M., *New J. Chem.* **2002,** *26*, 1340-1345.

54. Ponti, A.; Molteni, G., *J. Org. Chem.* **2001,** *66*, 5252-5255.

55. Ponti, A.; Molteni, G., *New J. Chem.* **2002,** *26*, 1346-1351.

56. Su, M.; Liao, H.; Chung, W.; Chu, S., *J. Org. Chem.* **1999,** *64*, 6710-6716.

57. Huisgen, R., *J. Org. Chem.* **1968,** *33*, 2291-2297.

58. Muchall, H. M., *J. Phys. Chem. A* **2011,** *115*, 13694-13705.

59. Lo Vecchio, G.; Grassi, G.; Risitano, F.; Foti, F., *Tetrahedron Lett.* **1973,** *14*, 3777-3780.

60. Padwa, A.; Carlsen, P. H. J., *J. Am. Chem. Soc.* **1975,** *97*, 3862-3864.

61. Padwa, A.; Nahm, S., *J. Org. Chem.* **1979,** *44*, 4746-4748.

62. Padwa, A.; Nahm, S., *J. Org. Chem.* **1981,** *46*, 1402-1409.

63. Brown, H. C.; Ford, T. M.; Hubbard, J. L., *J. Org. Chem.* **1980,** *45*, 4067-4068.

64. Granier, M.; Baceiredo, A.; Huch, V.; Veith, M.; Bertrand, G., *Inorg. Chem.* **1991,** *30*, 1161-1162.

65. Reau, R.; Veneziani, G.; Dahan, F.; Bertrand, G., *Angew. Chem. Int. Ed. Engl.* **1992,** *31*, 439-440.

66. Horchler von Locquenghien, K.; Baceiredo, A.; Boese, R.; Bertrand, G., *J. Am. Chem. Soc.* **1991,** *113*, 5062-5063.

67. Oh, L. M., *Tetrahedron Lett.* **2006,** *47*, 7943-7946.

68. Penning, T. D.; Talley, J. J.; Bertenshaw, S. R.; Carter, J. S.; Collins, P. W.; Docter, S.; Graneto, M. J.; Lee, L. F.; Malecha, J. W.; Miyashiro, J. M.; Rogers, R. S.; Rogier, D. J.; Yu, S. S.; Anderson, G. D.; Burton, E. G.; Cogburn, J. N.; Gregory, S. A.; Koboldt, C. M.; Perkins, W. E.; Seibert, K.; Veenhuizen, A. W.; Zhang, Y. Y.; Isakson, P. C., *J. Med. Chem.* **1997,** *40*, 1347-1365.

69. Donohue, S. R.; Halldin, C.; Pike, V. W., *Tetrahedron Lett.* **2008,** *49*, 2789-2791.

70. Pinto, D. J. P.; Orwat, M. J.; Wang, S.; Fevig, J. M.; Quan, M. L.; Amparo, E.; Cacciola, J.; Rossi, K. A.; Alexander, R. S.; Smallwood, A. M.; Luettgen, J. M.; Liang, L.; Aungst, B. J.; Wright, M. R.; Knabb, R. M.; Wong, P. C.; Wexler, R. R.; Lam, P. Y. S., *J. Med. Chem.* **2001,** *44*, 566-578.

71. Deeb, A.; El-Mariah, F.; Hosny, M., *Bioorg. Med. Chem. Lett.* **2004,** *14*, 5013-5017.

72. Rashad, A. E.; Hegab, M. I.; Abdel-Megeid, R. E.; Micky, J. A.; Abdel-Megeid, F. M. E., *Bioorg. Med. Chem. Lett.* **2008,** *16*, 7102-7106.

73. Cottineau, B.; Toto, P.; Marot, C.; Pipaud, A.; Chenault, J., *Bioorg. Med. Chem. Lett.* **2002,** *12*, 2105-2108.

74. McKeown, S. C.; Hall, A.; Giblin, G. M. P.; Lorthioir, O.; Blunt, R.; Lewell, X. Q.; Wilson, R. J.; Brown, S. H.; Chowdhury, A.; Coleman, T.; Watson, S. P.; Chessell, I. P.; Pipe, A.; Clayton, N.; Goldsmith, P., *Bioorg. Med. Chem. Lett.* **2006,** *16*, 4767-4771.

75. Brahma, K.; Sasmal, A. K.; Chowdhury, C., *Org. Biomol. Chem.* **2011,** *9*, 8422-8429.

76. Zhang, C.; Liu, X.; Wang, B.; Wang, S.; Li, Z., *Chem. Biol. Drug Des.* **2010,** *75*, 489-493.

77. Wang, L. Y.; Tseng, W. C.; Lin, H. Y.; Wong, F. F., *Synlett* **2011**, 1467-1471

78. Collin, X.; Sauleau, A.; Coulon, J., *Bioorg. Med. Chem. Lett.* **2003,** *13*, 2601-2605.

79. Lebouvier, N.; Giraud, F.; Corbin, T.; Na, Y. M.; Le Baut, G.; Marchand, P.; Le Borgne, M., *Tetrahedron Lett.* **2006,** *47*, 6479-6483.

80. Navidpour, L.; Shadnia, H.; Shafaroodi, H.; Amini, M.; Dehpour, A. R.; Shafiee, A., *Bioorg. Med. Chem.* **2007,** *15*, 1976-1982.

81. Naito, Y.; Akahoshi, F.; Takeda, S.; Okada, T.; Kajii, M.; Nishimura, H.; Sugiura, M.; Fukaya, C.; Kagitani, Y., *J. Med. Chem.* **1996,** *39*, 3019-3029.

82. Ouyang, X.; Chen, X.; Piatnitski, E. L.; Kiselyov, A. S.; He, H.-Y.; Mao, Y.; Pattaropong, V.; Yu, Y.; Kim, K. H.; Kincaid, J.; Smith Ii, L.; Wong, W. C.; Lee, S. P.; Milligan, D. L.; Malikzay, A.; Fleming, J.; Gerlak, J.; Deevi, D.; Doody, J. F.; Chiang, H.-H.; Patel, S. N.; Wang, Y.; Rolser, R. L.; Kussie, P.; Labelle, M.; Tuma, M. C., *Bioorg. Med. Chem. Lett.* **2005,** *15*, 5154-5159.

83. Saha, A. K.; Liu, L.; Simoneaux, R.; DeCorte, B.; Meyer, C.; Skrzat, S.; Breslin, H. J.; Kukla, M. J.; End, D. W., *Bioorg. Med. Chem. Lett.* **2005,** *15*, 5407-5411.

84. Hester, J. B.; Rudzik, A. D.; Kamdar, B. V., *J. Med. Chem.* **1971,** *14*, 1078-1081.

85. Del Buttero, P.; Molteni, G.; Pilati, T., *Tetrahedron: Asymmetry* **2010,** *21*, 2607-2611.

86. Del Buttero, P.; Molteni, G.; Pilati, T., *Tetrahedron: Asymmetry* **2010,** *21*, 2603-2606.

87. Del Buttero, P.; Molteni, G.; Pilati, T., *Tetrahedron Lett.* **2003,** *44*, 1425-1427.

88. Del Buttero, P.; Molteni, G.; Pilati, T., *Tetrahedron* **2005,** *61*, 2413.

89. Del Buttero, P.; Baldoli, C.; Molteni, G.; Pilati, T., *Tetrahedron: Asymmetry* **2000,** *11*, 1927-1941.

90. Del Buttero, P.; Molteni, G.; Papagni, A.; Miozzo, L., *Tetrahedron: Asymmetry* **2004,** *15*, 2555-2559.

91. Del Buttero, P.; Molteni, G.; Papagni, A.; Pilati, T., *Tetrahedron* **2003,** *59*, 5259-5263.

92. Broggini, G.; Garanti, L.; Molteni, G.; Zecchi, G., *Tetrahedron* **1998,** *54*, 14859-14868.

93. Tachikawa, R.; Miyadera, T.; Terada, A.; Fukunaga, M.; Kawano, Y.; Kamioka, T.; Tamura, C.; Takagi, H., *J. Med. Chem.* **1971,** *14*, 520-526.

94. Jimenez, R. M.; Alonso, R. M.; Oleaga, E.; Vicente, F.; Hernandez, L., *Fresenius J. Anal. Chem.* **1987,** *329*, 468-471.

95. Koldobskii, G. I.; Ostrovskii, V. A.; Gidaspov, B. V., *Chem. Heterocycl. Compd.* **1981,** *16*, 665.

96. Koldobskii, G. I.; Ostrovskii, V. A.; Popavskii, V. S., *Chem. Heterocycl. Compd.* **1982,** *17*, 965-988.

97. Gilman, H.; Yale, H. L., *J. Am. Chem. Soc.* **1951,** *73*, 4470-4471.

98. Henry, R. A., *J. Am. Chem. Soc.* **1951,** *73*, 4470.

99. Charton, M., *J. Chem. Soc. B* **1969**, 1240-1244.

100. Kaufman, M. H.; Ernsberger, F. M.; McEwan, W. S., *J. Am. Chem. Soc.* **1956,** *78*, 4197-4201.

101. Krugh, W. D.; Gold, L. P., *J. Mol. Spectros.* **1974,** *49*, 423-431.

102. Moore, D. W.; Whittaker, A. G., *J. Am. Chem. Soc.* **1960,** *82*, 5007.

103. Razynska, A.; Tempczyk, A.; Malinski, E.; Szafranek, J.; Grzonka, Z.; Hermann, P., *J. Chem. Soc., Perkin Trans. 2* **1983**, 379-383.

104. Witanowski, M.; Stefaniak, L.; Januszewski, H.; Grabowski, Z.; Webb, G. A., *Tetrahedron* **1972,** *28*, 637-653.

105. Wofford, D. S.; Forkey, D. M.; Russell, J. G., *J. Org. Chem.* **1982,** *47*, 5132-5137.

106. Van der Putten, N.; Meijdenrijk, D.; Schenk, H., *Cryst. Struct. Commun.* **1974,** *3*, 321.

107. Butler, R. N.; Garvin, V. C.; Lumbroso, H.; Liegeois, C., *J. Chem. Soc. Perkin Trans. 2* **1984**, 721-725.

108. Zhaoxu, C.; Heming, X., *J. Mol. Struc. (THEOCHEM)* **1998,** *453*, 65-70.

109. Fos, E.; Vilarrasa, J.; Fernandez, J., *J. Org. Chem.* **1985,** *50*, 4894-4899.

110. Guimon, C.; Khayar, S.; Gracian, F.; Begtrup, M.; Pfister-Guillouzo, G., *Chem. Phys.* **1989,** *138*, 157-171.

111. Kiselev, V. G.; Cheblakov, P. B.; Gritsan, N. P., *J. Phys. Chem. A* **2011,** *115*, 1743-1753.

112. Lumbroso, H.; Liegeois, C.; Pappalardo, G. C.; Grassi, A., *J. Mol. Struc.* **1982,** *82*, 283-294.

113. Mazurek, A. P.; Osman, R., *J. Phys. Chem.* **1985,** *89*, 460-463.

114. Mo, O.; De Paz, J. L. G.; Yanez, M., *J. Phys. Chem.* **1986,** *90*, 5597-5604.

115. Palmer, M. H.; Beveridge, A. J., *Chem. Phys.* **1987,** *111*, 249-261.

116. Wang, J.; Gu, J.; Tian, A., *Chem. Phys. Lett.* **2002,** *351*, 459-468.

117. Wong, M. W.; Leung-Toung, R.; Wentrup, C., *J. Am. Chem. Soc.* **1993,** *115*, 2465-2472.

118. Kishore, V.; Parmar, S. S.; Gildersleeve, D. L., *J. Heterocycl. Chem.* **1978,** *15*, 1335-1338.

119. Nohara, A.; Kuriki, H.; Ishiguro, T.; Saijo, T.; Ukawa, K.; Maki, Y.; Sanno, Y., *J. Med. Chem.* **1979,** *22*, 290-295.

120. Tomioka, S.; Kobayashi, Y., *Chem. Abstr.* **1980,** *92*, 16284.

121. Wheeler, W. J.; Preston, D. A.; Wright, W. E.; Huffman, G. W.; Osborne, H. E.; Howard, D. P., *J. Med. Chem.* **1979,** *22*, 657-661.

122. White, W. I.; Legg, J. I., *J. Am. Chem. Soc.* **1975,** *97*, 3937-3941.

123. Worsfold, M.; Marshall, M. J.; Ellis, E. B., *Anal. Biochem.* **1977,** *79*, 152-156.

124. Stawinski, J.; Hozumi, T.; Narang, S. A., *Can. J. Chem.* **1976,** *54*, 670-672.

125. Love, J. M.; Barden, J. A., *Chem. Abstr.* **1979,** *91*, 135451.

126. Bladin, J. A., *Ber.* **1885,** *18*, 2907-2912.

127. Bladin, J. A., *Ber.* **1892,** *25*, 1411-1413.

128. Dimroth, O.; Fester, G., *Ber.* **1910,** *43*, 2219–2223.

129. Arnold, C.; Thatcher, D. N., *J. Org. Chem.* **1969,** *34*, 1141-1142.

130. Brown, M.; Benson, R. E., *J. Org. Chem.* **1966,** *31*, 3849-3851.

131. Cantillo, D.; Gutmann, B.; Kappe, C. O., *J. Am. Chem. Soc.* **2011,** *133*, 4465-4475.

132. Shie, J.; Fang, J., *J. Org. Chem.* **2007,** *72*, 3141-3144.

133. Carpenter, W. R., *J. Org. Chem.* **1962,** *27*, 2085-2088.

134. Gilchrist, T. L.; Rees, C. W.; Thomas, C., *J. Chem. Soc., Perkin Trans. 1* **1975**, 12-18.

135. Joo, Y.; Shreeve, J. M., *Org. Lett.* **2008,** *10*, 4665-4667.

136. Kaim, L. E.; Grimaud, L.; Patil, P., *Org. Lett.* **2011,** *13*, 1261-1263.

137. Neilson, D. G.; Roger, R.; Heatlie, J. W. M.; Newlands, L. R., *Chem. Rev.* **1970,** *70*, 151-170.

138. Norris, W. P.; Finnegan, W. G., *J. Org. Chem.* **1966,** *31*, 3292-3295.

139. Gelleri, A.; Messmer, A., *Tetrahedron Lett.* **1973,** *14*, 4295-4298.

140. Hong, S. Y.; Baldwin, J. E., *Tetrahedron* **1968,** *24*, 3787-3794.

141. Kano, H.; Yamazaki, E., *Tetrahedron* **1964,** *20*, 461-464.

142. Yates, P.; Meresz, O., *Tetrahedron Lett.* **1967,** *8*, 77-81.

143. da Silva, G.; Bozzelli, J. W., *J. Org. Chem.* **2008,** *73*, 1343-1353.

144. Padwa, A.; Nahm, S.; Sato, E., *J. Org. Chem.* **1978,** *43*, 1664-1671.

145. Takach, N. E.; Holt, E. M.; Alcock, N. W.; Henry, R. A.; Nelson, J. H., *J. Am. Chem. Soc.* **1980,** *102*, 2968-2979.

146. Raap, R.; Howard, J., *Can. J. Chem.* **1969,** *47*, 813-819.

147. Bookser, B. C., *Tetrahedron Lett.* **2000,** *41*, 2805-2809.

148. Hammett, L. P., *Chem. Rev.* **1935,** *17*, 125-136.

149. Tomasik, P.; Johnson, C. D.; Katritzky, A. R.; Boulton, A. J., *Adv. Heterocycl. Chem.* **1976,** *20*, 1-64.

150. Isaacs, N. S., *Physical organic chemistry* Wiley: New York, 1987.

151. Hansch, C.; Leo, A., *Substituent constants for correlation analysis in chemistry and biology* Wiley: New York, 1979.

152. Brown, H. C.; Okamoto, Y., *J. Am. Chem. Soc.* **1958,** *80*, 4979-4987.

153. Okamoto, Y.; Brown, H. C., *J. Org. Chem.* **1957,** *22*, 485-494.

154. Knapp, S.; Hale, J. J.; Bastos, M.; Gibson, F. S., *Tetrahedron Lett.* **1990,** *31*, 2109-2112.

155. Streitwieser, A.; Perrin, C., *J. Am. Chem. Soc.* **1964,** *86*, 4938.

156. Taft, R. W., *J. Am. Chem. Soc.* **1952,** *74*, 3120-3128.

157. Charton, M., *J. Am. Chem. Soc.* **1969,** *91*, 615-618.

158. Charton, M., *J. Am. Chem. Soc.* **1969,** *91*, 619-623.

159. Charton, M., *J. Am. Chem. Soc.* **1975,** *97*, 1552.

160. Charton, M., *J. Am. Chem. Soc.* **1975,** *97*, 1552-1556.

161. Granier, M.; Baceiredo, A.; Dartiguenave, Y.; Dartiguenave, M.; Menu, M. J.; Bertrand, G., *J. Am. Chem. Soc.* **1990,** *112*, 6277-6285.

162. Lesnikovich, A. I.; Ivashkevich, O. A.; Lyutsko, V. A.; Printsev, G. V.; Kovalenko, K. K.; Gaponik, P. N.; Levchik, S. V., *Thermochim. Acta* **1989,** *145*, 195-202.

163. Lesnikovich, A. I.; Ivashkevich, O. A.; Printsev, G. V.; Gaponik, P. N.; Levchik, S. V., *Thermochim. Acta* **1990,** *171*, 207-213.

164. Baum, M. W.; Font, J. L.; Meislich, M. E.; Wentrup, C.; Jones, M., *J. Am. Chem. Soc.* **1987,** *109*, 2534-2536.

165. Elwood, J. K.; Gates, J. W., *J. Org. Chem.* **1967,** *32*, 2956-2959.

166. Lesnikovich, A. I.; Levchik, S. V.; Balabanovich, A. I.; Ivashkevich, O. A.; Gaponik, P. N., *Thermochim. Acta* **1992,** *200*, 427-441.

167. Wentrup, C.; Becker, J., *J. Am. Chem. Soc.* **1984,** *106*, 3705-3706.

168. Wentrup, C.; Becker, J., *J. Am. Chem. Soc.* **1984,** *106*, 3705.

169. Maier, G.; Eckwert, J.; Bothur, A.; Reisenauer, H. P.; Schmidt, C., *Liebigs Ann.* **1996,** *1996*, 1041-1053.

170. Vyazovkin, S. V.; Lesnikovich, A. I.; Lyutsko, V. A., *Thermochim. Acta* **1990,** *165*, 17-22.

171. Baldwin, J. E.; Hong, S. Y., *Chem. Commun. (London)* **1967**, 1136a.

172. Semenov, V. V.; Kanischev, M. I.; Shevelev, S. A.; Kiselyov, A. S., *Tetrahedron* **2009,** *65*, 3441-3445.

173. Luo, Y. R., *Handbook of bond dissociation energies in organic compounds*. Boca Raton, Fla. : CRC Press: 2003; p 254 and 258.

174. Gaussian 03, R. C., Frisch, M. J.; Trucks, G. W.; Schlegel, H. B.; Scuseria, G. E.; Robb, M. A.; Cheeseman, J. R.; Montgomery, Jr., J. A.; Vreven, T.; Kudin, K. N.; Burant, J. C.; Millam, J. M.; Iyengar, S. S.; Tomasi, J.; Barone, V.; Mennucci, B.; Cossi, M.; Scalmani, G.; Rega, N.; Petersson, G. A.; Nakatsuji, H.; Hada, M.; Ehara, M.; Toyota, K.; Fukuda, R.; Hasegawa, J.; Ishida, M.; Nakajima, T.; Honda, Y.; Kitao, O.; Nakai, H.; Klene, M.; Li, X.; Knox, J. E.; Hratchian, H. P.; Cross, J. B.; Bakken, V.; Adamo, C.; Jaramillo, J.; Gomperts, R.; Stratmann, R. E.; Yazyev, O.; Austin, A. J.;

Cammi, R.; Pomelli, C.; Ochterski, J. W.; Ayala, P. Y.; Morokuma, K.; Voth, G. A.; Salvador, P.; Dannenberg, J. J.; Zakrzewski, V. G.; Dapprich, S.; Daniels, A. D.; Strain, M. C.; Farkas, O.; Malick, D. K.; Rabuck, A. D.; Raghavachari, K.; Foresman, J. B.; Ortiz, J. V.; Cui, Q.; Baboul, A. G.; Clifford, S.; Cioslowski, J.; Stefanov, B. B.; Liu, G.; Liashenko, A.; Piskorz, P.; Komaromi, I.; Martin, R. L.; Fox, D. J.; Keith, T.; Al-Laham, M. A.; Peng, C. Y.; Nanayakkara, A.; Challacombe, M.; Gill, P. M. W.; Johnson, B.; Chen, W.; Wong, M. W.; Gonzalez, C.; and Pople, J. A, *Gaussian, Inc., Wallingford CT* **2004**.

175. Gaussian 09, R. A., Frisch, M. J.; Trucks, G. W.; Schlegel, H. B.; Scuseria, G. E.; Robb, M. A.; Cheeseman, J. R.; Scalmani, G.; Barone, V.; Mennucci, B.; Petersson, G. A.; Nakatsuji, H.; Caricato, M.; Li, X.; Hratchian, H. P.; Izmaylov, A. F.; Bloino, J.; Zheng, G.; Sonnenberg, J. L.; Hada, M.; Ehara, M.; Toyota, K.; Fukuda, R.; Hasegawa, J.; Ishida, M.; Nakajima, T.; Honda, Y.; Kitao, O.; Nakai, H.; Vreven, T.; Montgomery, Jr., J. A.; Peralta, J. E.; Ogliaro, F.; Bearpark, M.; Heyd, J. J.; Brothers, E.; Kudin, K. N.; Staroverov, V. N.; Kobayashi, R.; Normand, J.; Raghavachari, K.; Rendell, A.; Burant, J. C.; Iyengar, S. S.; Tomasi, J.; Cossi, M.; Rega, N.; Millam, N. J.; Klene, M.; Knox, J. E.; Cross, J. B.; Bakken, V.; Adamo, C.; Jaramillo, J.; Gomperts, R.; Stratmann, R. E.; Yazyev, O.; Austin, A. J.; Cammi, R.; Pomelli, C.; Ochterski, J. W.; Martin, R. L.; Morokuma, K.; Zakrzewski, V. G.; Voth, G. A.; Salvador, P.; Dannenberg, J. J.; Dapprich, S.; Daniels, A. D.; Farkas, Ö.; Foresman, J. B.; Ortiz, J. V.; Cioslowski, J.; Fox, D. J. , *Gaussian, Inc., Wallingford CT* **2009**.

176. Becke, A. D., *J. Chem. Phys.* **1993,** *98*, 5648-5652.

177. Becke, A. D., *J. Chem. Phys.* **1996,** *104*, 1040-1046.

178. Lee, C.; Yang, W.; Parr, R. G., *Phys. Rev. B* **1988,** *37*, 785-789.

179. Stephens, P. J.; Devlin, F. J.; Chabalowski, C. F.; Frisch, M. J., *J. Phys. Chem.* **1994,** *98*, 11623-11627.

180. Gonzalez, C.; Schlegel, H. B., *J. Chem. Phys.* **1989,** *90*, 2154-2161.

181. Gonzalez, C.; Schlegel, H. B., *J. Phys. Chem.* **1990,** *94*, 5523-5527.

182. Weinhold, F., *Encyclopedia of Computational Chemistry*. John Wiley and Sons: Chichester, 1998; Vol. 3, p 1792.

183. Klapotke, T. M.; Sabate, C. M.; Stierstorfer, J., *New J. Chem.* **2009,** *33*, 136-147.

184. Prokudin, V. G.; Poplavsky, V. S.; Ostrovskii, V. A., *Russ. Chem. Bull.* **1996,** *45*, 2094-2100.

185. Prokudin V. G.; Poplavsky V. S.; A., O. V., *Russ. Chem. Bull.* **1996,** *45*, 2101.

186. Prokudin , V. G.; Poplavsky, V. S.; Ostrovskii, V. A., *Russ. Chem. Bull.* **1996,** *45*, 2101-2104.

187. Perdew, J. P.; Burke, K.; Ernzerhof, M., *Phys. Rev. Lett.* **1996,** *77*, 3865-3868.

188. Perdew, J. P.; Ernzerhof, M.; Burke, K., *J. Chem. Phys.* **1996,** *105*, 9982-9985.

189. Glendening, E. D.; Weinhold, F., *J. Comput. Chem.* **1998,** *19*, 593.

190. Jones, P. G.; Roesky, H. W.; Schimkowiak, J., *J. Chem. Soc., Chem. Commun.* **1988**, 730.

191. Mallya, M. N.; Nagendrappa, G.; Shashidhara Prasad, J.; Sridhar, M. A.; Lokanath, N. K.; Begum, N. S., *Tetrahedron Lett.* **2001,** *42*, 2565-2568.

192. Mawhinney, R. C.; Peslherbe, G. H.; Muchall, H. M., *Unpublished results.*

193. Mawhinney, R. C.; Peslherbe, G. H.; Muchall, H. M., *J. Phys. Chem. B* **2008,** *112*, 650-665.

194. Aurell, M. J.; Domingo, L. R.; Perez, P.; Contreras, R., *Tetrahedron* **2004,** *60*, 11503-11509.

195. Perez, P.; Domingo, L. R.; Jose Aurell, M.; Contreras, R., *Tetrahedron* **2003,** *59*, 3117-3125.

196. Sakata, K., *J. Phys. Chem. A* **2000,** *104*, 10001-10008.

197. Bourissou, D.; Guerret, O.; Gabbai, F. P.; Bertrand, G., *Chem. Rev.* **1999,** *100*, 39.

198. Moss, R. A., *Acc. Chem. Res.* **1989,** *22*, 15-21.

199. von E. Doering, W.; Hoffmann, A. K., *J. Am. Chem. Soc.* **1954,** *76*, 6162-6165.

200. Jones, M., Jr.; Moss, R. A., *Singlet Carbenes. In Reactive Intermediate Chemistry*. Wiley-Interscience: Hoboken, NJ, 2004.

201. Moss, R. A., *Acc. Chem. Res.* **1980,** *13*, 58-64.

202. Mawhinney, R. C.; Muchall, H. M.; Peslherbe, G. H., *Can. J. Chem.* **2005,** *83*, 1615-1625.

203. Garanti, L.; Zecchi, G., *J. Chem. Soc., Perkin Trans. 1* **1977**, 2092-2095.

204. Padwa, A.; Carlsen, P. H. J., *J. Am. Chem. Soc.* **1977,** *99*, 1514-1523.

205. Padwa, A.; Carlsen, P. H. J.; Ku, A., *J. Am. Chem. Soc.* **1977,** *99*, 2798-2800.

206. Padwa, A.; Kamigata, N., *J. Am. Chem. Soc.* **1977,** *99*, 1871-1880.

207. Padwa, A.; Ku, A.; Mazzu, A.; Wetmore, S. I., *J. Am. Chem. Soc.* **1976,** *98*, 1048-1050.

208. Panfil, I.; Maciejewski, S.; Belzecki, C.; Chmielewski, M., *Tetrahedron Lett.* **1989,** *30*, 1527-1528.

209. Glendening, E. D.; Weinhold, F., *J. Comput. Chem.* **1998,** *19*, 593-609.

210. Jensen, F., *Introduction to Computational Chemistry*. John Wiley & Sons Ltd: Chichester, 2007.

211. Song, K.; Hase, W. L., *J. Chem. Phys.* **1999,** *110*, 6198-6207.

212. Mehrpajouh, S.; Peslherbe, G. H.; Muchall, H. M., *Unpublished results.*

213. Hammond, G. S., *J. Am. Chem. Soc.* **1955,** *77*, 334-338.

214. Fleming, I., *Frontier orbitals and organic chemical reactions*. Wiley: New York, 1977.

215. Bourissou, D.; Guerret, O.; Gabbai, F. P.; Bertrand, G., *Chem. Rev.* **2000,** *100*, 39-92.

216. Ess, D. H.; Wheeler, S. E.; Iafe, R. G.; Xu, L.; Celebi-Olcum, N.; Houk, K. N., *Angew. Chem. Int. Ed. Engl.* **2008,** *47*, 7592-7601.

Appendix A.

Supporting information for Chapter 3

Table A-1. Electronic energies, enthalpies, Gibbs free energies, and zero-point energy (ZPE) corrected energies (a.u.) of tetrazoles (CN_4), transition states (TS), and nitrilimines (CNN).

	E_{el}	H_{298}	G_{298}	E_{el}+ ZPE
H–CN_4–H	–258.267726	–258.215757	–258.246200	–258.220126
TS1	–258.208574	–258.160480	–258.192349	–258.165488
TS2	–258.200528	–258.154386	–258.187227	–258.159977
H–CNN–H	–148.706536	–148.670344	–148.698174	–148.674790
N_2	–109.529779	–109.520883	–109.542636	–109.524187
NH_2–CN_4–NH_2	–368.953082	–368.864861	–368.902215	–368.872099
TS1	–368.895366	–368.811213	–368.849227	–368.818803
TSc	–368.900910	–368.817476	–368.855951	–368.82539
NH_2–CNN–NH_2	–259.406915	–259.333116	–259.367861	–259.339662
F–CN_4–F	–456.654169	–456.618052	–456.652792	–456.623857
TS1	–456.611649	–456.578962	–456.615926	–456.585458
TS2	–456.611019	–456.580293	–456.619283	–456.587843
F–CNN–F	–347.114990	–347.093678	–347.127900	–347.099524
OCH_3–CN_4–CH_3	–412.116296	–411.999323	–412.040226	–412.007862
TS1	–412.040538	–411.928145	–411.971008	–411.937423
TSc	–412.044809	–411.932760	–411.975979	–411.942331
OCH_3–CNN–CH_3	–302.542112	–302.439960	–302.480633	–302.448494
NO_2–CN_4–NH_2	–518.080439	–518.006025	–518.047407	–518.014344

	E_{el}	H_{298}	G_{298}	E_{el}+ ZPE
TS1	–518.046931	–517.975692	–518.016587	–517.984040
TS2	–518.027880	–517.958646	–518.002659	–517.968224
NO_2–CNN–NH_2	–408.533812	–408.473692	–408.513176	–408.481555
COOH–CN_4–OH	–521.999773	–521.926297	–521.967576	–521.934738
TS1	–521.970715	–521.900042	–521.941375	–521.908584
TS2	–521.955418	–521.886513	–521.930941	–521.896363
COOH–CNN–OH	–412.460612	–412.400848	–412.440712	–412.408881
CHO–CN_4–OH	–446.749665	–446.682502	–446.721354	–446.690122
TS1	–446.721099	–446.656748	–446.695711	–446.664399
TS2	–446.708787	–446.646096	–446.688518	–446.655208
CHO–CNN–OH	–337.211036	–337.157555	–337.195182	–337.164890

Appendix B.

Supporting information for Chapter 4

Table B-1. Electronic and zero-point vibrational energy (ZPE) corrected energies (au) of nitrilimines using B3LYP/6-31+G(d) and PBE0/6-311++G(2df,pd). (The most stable conformers of nitrilimines are presented in Table B-2)

	E_{el}	E_{el}+ ZPE
B3LYP/6-31+G(d)		
H–CNN–H	–148.706536	–148.674790
NH_2–CNN–NH_2	–259.406915	–259.339662
F–CNN–F	–347.114990	–347.099524
OCH_3–CNN–CH_3	–302.542112	–302.448494
NO_2–CNN–NH_2	–408.533812	–408.481555
COOH–CNN–OH	–412.460612	–412.408881
CHO–CNN–OH	–337.211036	–337.164890
PBE0/6-311++G(2df,pd)		
H–CNN–H	–148.57896	–148.546933
NH_2–CNN–NH_2	–259.19299	–259.125206
F–CNN–F	–346.863685	–346.847488
OCH_3–CNN–CH_3	–302.278865	–302.185092
NO_2–CNN–NH_2	–408.224261	–408.170912
COOH–CNN–OH	–412.152386	–412.099361
CHO–CNN–OH	–336.945316	–336.898362

Table B-2. Electronic and zero-point vibrational energy (ZPE) corrected energies (a.u.) of various conformers of nitrilimines using PBE0/6-311++G(2df,pd).

	E_{el}	E_{el}+ ZPE
COOH–CNN–OH		
1	–412.145775	–412.093245
2	–412.152081	–412.099105
3	–412.145261	–412.092773
4	–412.152386	–412.099361
5	–412.140275	–412.087912
6	–412.146280	–412.093513
7	–412.138205	–412.086013
8	–412.147221	–412.094380
CHO–CNN–OH		
1	–336.938225	–336.891793
2	–336.944915	–336.897999
3	–336.945316	–336.898362
4	–336.936973	–336.890632
OCH_3–CNN–CH_3		
1	–302.278865	–302.185092
2	–302.275735	–302.182049
SCH_3–CNN–SO_2NMe_2		
1	–1268.187515	–1268.040488
2	–1268.186910	–1268.039871

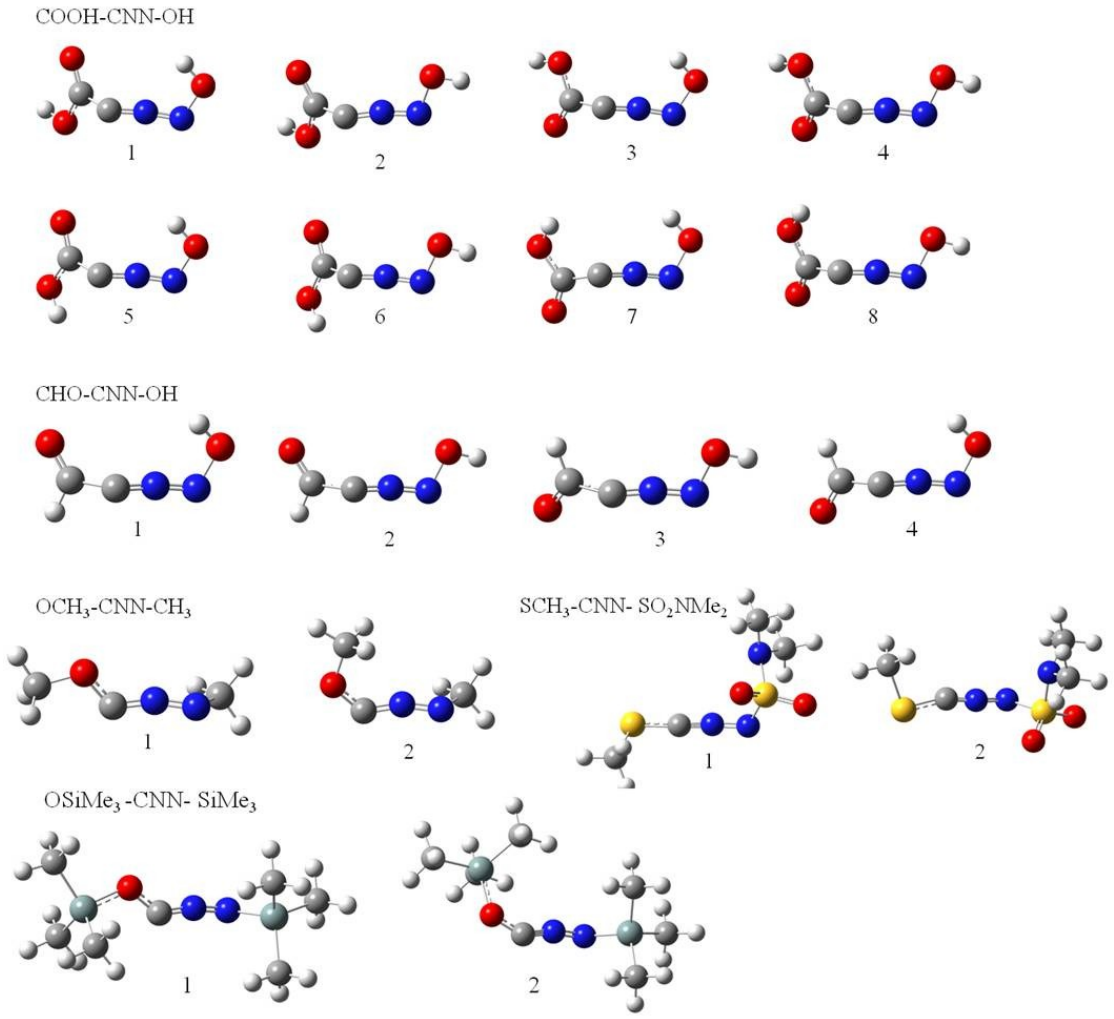

Figure B-1. Optimized structure of nitrilimines and their conformers using PBE0/6-311++G(2df,pd).

Table B-3. Coordinates of nitrilimines (Å) using PBE0/6-311++G(2df,pd). (centre numbers are provided in Figure B-2)

Center Number	Atomic Number	Coordinates		
		X	Y	Z
	H–CNN–H			
1	7	0.053960	0.012000	0.013391
2	7	-1.167853	-0.136623	0.018987
3	1	-1.624234	0.777306	0.011706
4	6	1.228695	0.010907	-0.133561
5	1	2.049318	0.029617	0.563020
	NH_2–CNN–NH_2			
1	7	-0.021721	-0.138379	0.268789
2	7	-1.002144	-0.177049	-0.482816
3	6	1.205663	-0.575405	0.130999
4	7	-2.176247	0.124034	0.141014
5	7	2.146044	0.325489	-0.064609
6	1	1.963459	1.313899	-0.214309
7	1	3.108005	0.035149	-0.065482
8	1	-2.081301	0.686408	0.981482
9	1	-2.845663	0.478302	-0.524332
	F–CNN–F			
1	6	1.133966	0.146870	0.525598
2	7	0.000509	0.239095	-0.018420
3	7	-1.132696	0.601925	-0.189196
4	9	2.116295	-0.262578	-0.228891
5	9	-1.991682	-0.489462	0.039972
	OCH_3–CNN–CH_3			
1	7	0.610410	-0.290820	-0.023215
2	7	1.785807	-0.612428	0.074500

Center Number	Atomic Number	Coordinates		
		X	Y	Z
3	6	-0.559109	-0.190491	-0.363825
4	6	2.733790	0.491404	-0.023914
5	1	3.467293	0.242238	-0.794786
6	1	2.249412	1.442540	-0.262253
7	1	3.270025	0.579509	0.924866
8	8	-1.551438	0.064743	0.479416
9	6	-2.824538	0.182082	-0.145632
10	1	-3.536622	0.374551	0.655440
11	1	-2.828066	1.011902	-0.855348
12	1	-3.084916	-0.743917	-0.662017
	NO_2–CNN–NH_2			
1	7	0.744172	-0.357976	0.204298
2	7	1.880161	-0.598979	-0.150390
3	6	-0.317170	-0.273313	0.814316
4	7	-1.490136	0.068581	0.020536
5	8	-1.744959	1.247986	-0.072839
6	8	-2.145674	-0.856993	-0.393929
7	7	2.746714	0.440437	-0.110910
8	1	3.520807	0.278986	-0.736263
9	1	2.340905	1.368516	-0.160240
	COOH–CNN–OH			
1	7	0.877250	-0.318531	0.223363
2	7	2.017605	-0.586697	-0.102584
3	6	-0.224778	-0.186793	0.681620
4	8	2.767713	0.589352	-0.188263
5	1	3.631725	0.255958	-0.452388
6	6	-1.522763	-0.061740	0.034344

Center Number	Atomic Number	Coordinates		
		X	Y	Z
7	8	-2.171340	-1.006310	-0.321951
8	8	-1.921402	1.212193	-0.024896
9	1	-2.810231	1.209948	-0.407966
	CHO–CNN–OH			
1	7	0.514438	-0.196387	0.201918
2	7	1.628748	-0.626312	-0.043092
3	6	-0.585946	0.103251	0.559852
4	8	2.514023	0.446207	-0.187611
5	1	3.343327	-0.004050	-0.379974
6	6	-1.855524	0.453808	-0.032141
7	8	-2.729226	-0.337013	-0.279056
8	1	-1.975186	1.547039	-0.164740

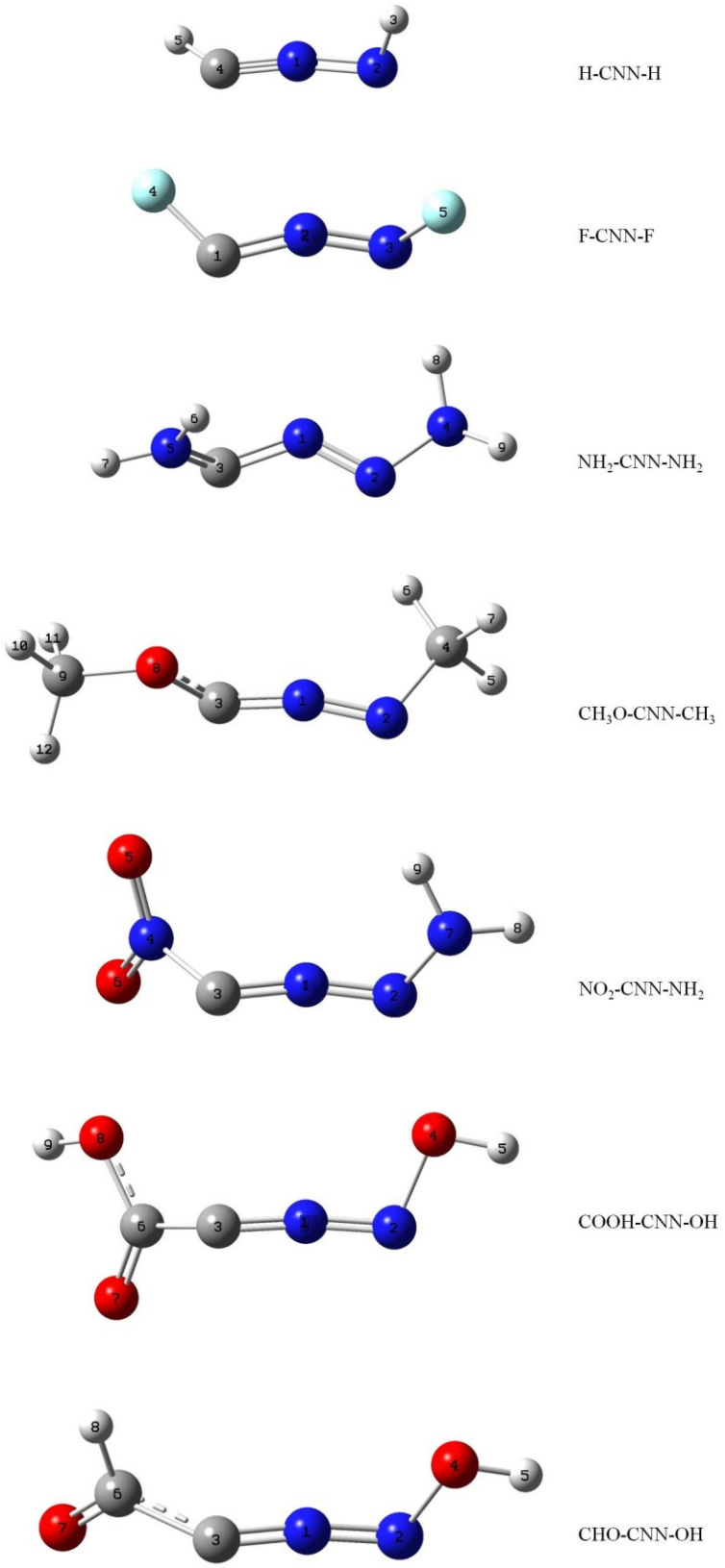

Figure B-2. Optimized structure of nitrilimines with center number using PBE0/6-311++G(2df,pd). (Lowest energy conformers are presented)

Table B-4. Absolute B3LYP/6-31+G(d) values (%) of the valence-bond structure contributions according to NRT analysis.

	allenic	1,3-dipolar	carbenic
H-CNN-H	38	38	15
F-CNN-F	21	15	48
NH_2-CNN-NH_2	10	10	63
COOH-CNN-OH	33	26	9
CHO-CNN-OH	32	27	10
H_3CO-CNN-CH_3	29	22	36
O_2N-CNN-NH_2	31	14	31

NH_2-CNN-NH_2

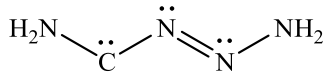

carbenic, 41.76%

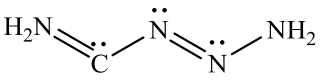

carbenic, 17.60%

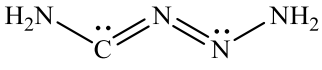

allenic, 11.89%

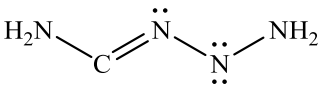

1,3-dipolar, 10.47%

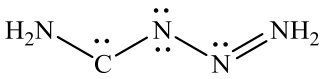

8.03%

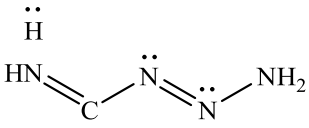

ionic, 2.41%

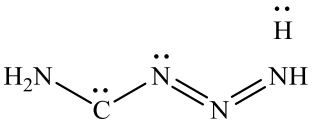

ionic, 1.48%

Figure B-2. Valence-bond structures of nitrilimines with more than 1% contribution using PBE0/6-311++G(2df,pd). (Lowest energy conformers are presented)

F-CNN-F

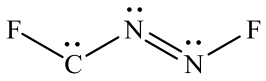

carbenic, 40.64%

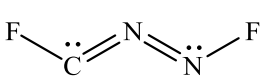

allenic, 21.91%

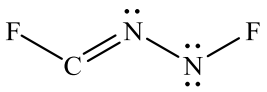

1,3-dipolar, 16.24%

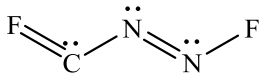

carbenic, 6.46%

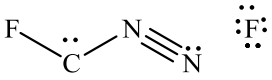

ionic, 5.01%

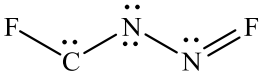

3.55%

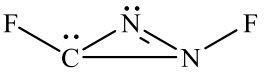

cyclic, 2.13%

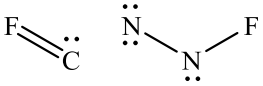

ionic, 1.26%

Figure B-3. Valence-bond structures of nitrilimines with more than 1% contribution (continued).

CH_3O-CNN-CH_3

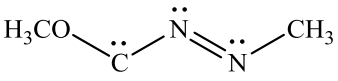

carbenic, 24.53%

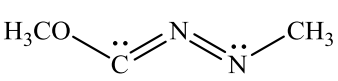

allenic, 28.70%

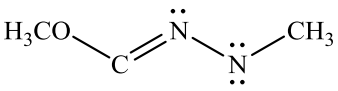

1,3-dipolar, 23.25%

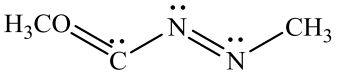

carbenic, 6.30%

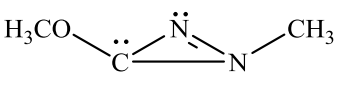

cyclic, 4.39%

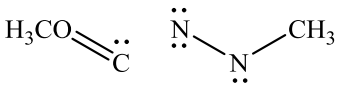

ionic, 1.52%

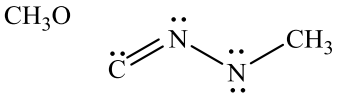

ionic, 1.13%

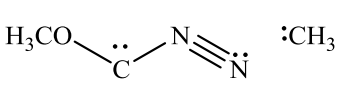

ionic, 1.03%

Figure B-3. Valence-bond structures of nitrilimines with more than 1% contribution (continued).

O_2N-CNN-NH_2

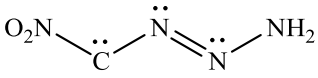

carbenic, 29.22%

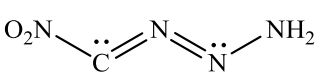

allenic, 29.90%

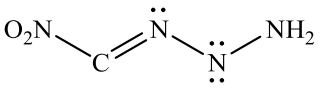

1,3-dipolar, 13.26%

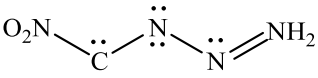

8.13%

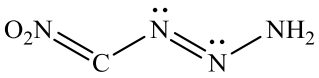

4.79%

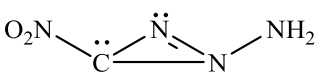

cyclic, 3.44%

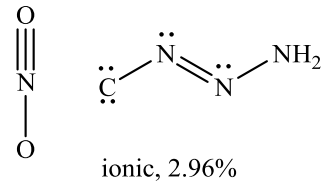

ionic, 2.96%

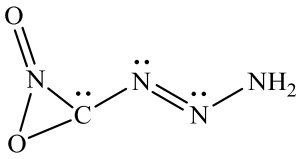

2.44%

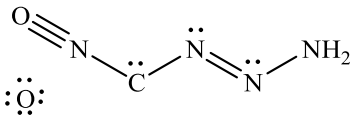

ionic, 1.54%

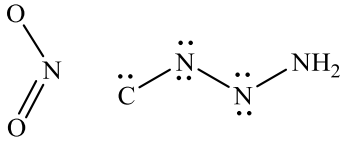

ionic, 1.52%

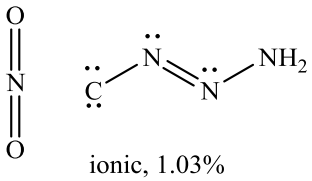

ionic, 1.03%

Figure B-3. Valence-bond structures of nitrilimines with more than 1% contribution (continued).

HOOC-CNN-OH

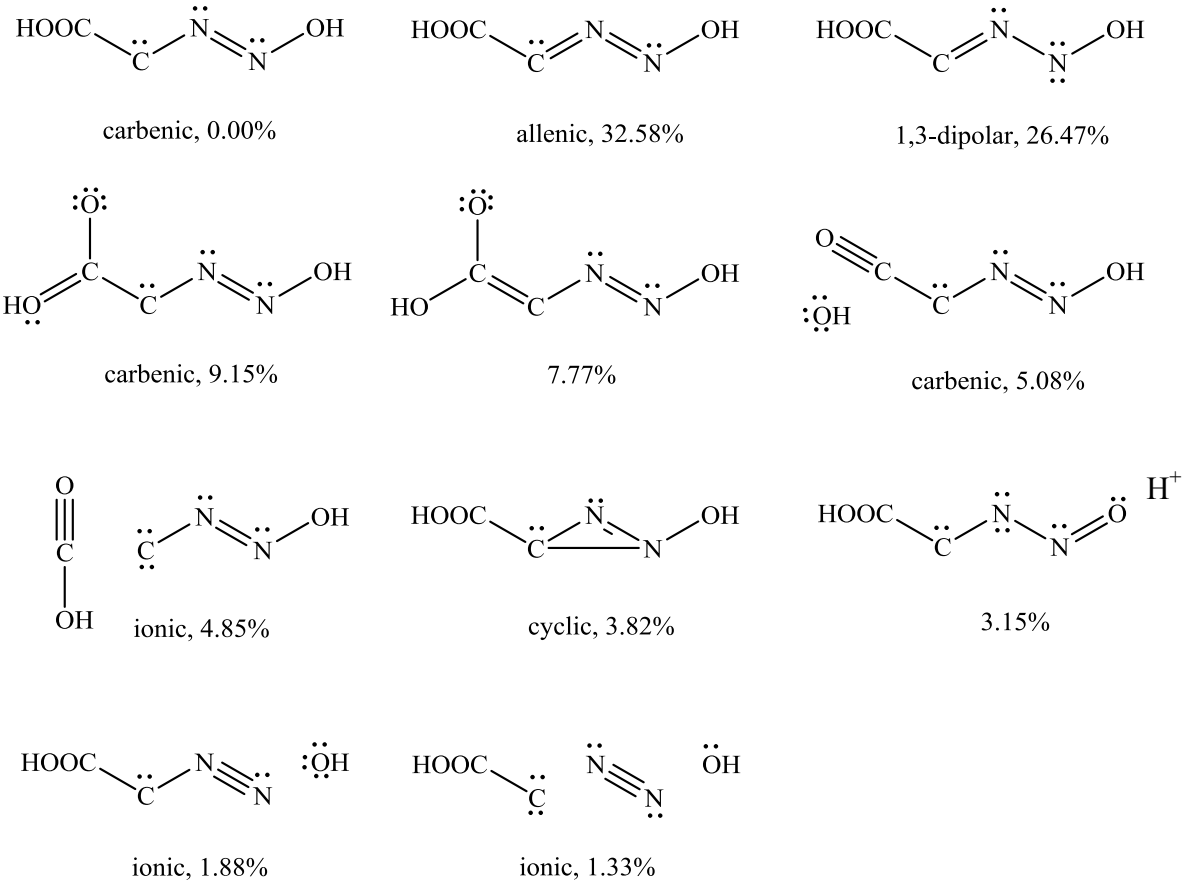

Figure B-3. Valence-bond structures of nitrilimines with more than 1% contribution (continued).

CHO-CNN-OH

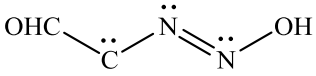

carbenic, 8.76%

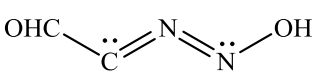

allenic, 32.57%

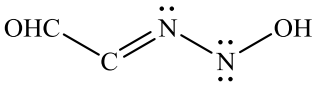

1,3-dipolar, 27.08%

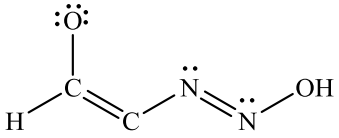

10.17%

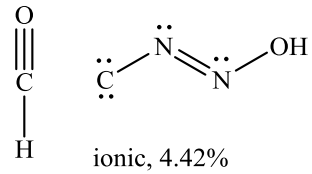

ionic, 4.42%

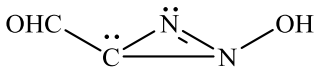

cyclic, 3.66%

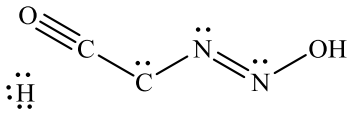

carbenic, 3.46%

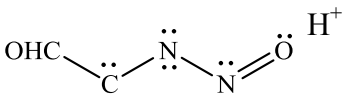

3.46%

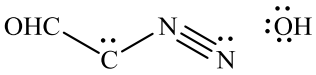

ionic, 1.98%

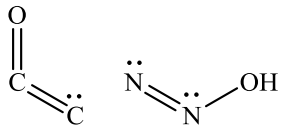

ionic, 1.25%

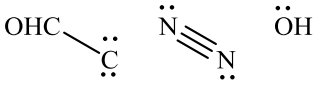

ionic, 1.24%

Figure B-3. Valence-bond structures of nitrilimines with more than 1% contribution (continued).

Appendix C.

Supporting information for Chapter 5

Table C-1. Electronic energies, enthalpies, Gibbs free energies, and zero-point energy (ZPE) corrected energies (a.u.) of nitrilimines, ethene and transition states using B3LYP/6-31+G(d).

	E_{el}	H_{298}	G_{298}	E_{el}+ ZPE
CH_2=CH_2	-78.593269	-78.538184	-78.563705	-78.54217
H–CNN–H	-148.706536	-148.670344	-148.698174	-148.674790
TS [1+2]	-227.281366	-227.188381	-227.224579	-227.195306
TS [3+2]	-227.287031	-227.194424	-227.229819	-227.201207
NH_2–CNN–NH_2	-259.406915	-259.333116	-259.367861	-259.339662
TS [3+2]	-337.989514	-337.859478	-337.900679	-337.868592
F–CNN–F	-347.114990	-347.093678	-347.127900	-347.099524
TS [1+2]	-425.705037	-425.627455	-425.669107	-425.636172
TS [3+2]	-425.706951	-425.629234	-425.670767	-425.637816
OCH_3–CNN–CH_3	-302.542112	-302.43996	-302.480633	-302.448494
TS [1+2]	-381.120141	-380.962326	-381.00936	-380.973457
TS [3+2]	-381.12642	-380.968332	-381.015392	-380.979445
NO_2–CNN–NH_2	-408.533812	-408.473692	-408.513176	-408.481555
TS [1+2]	-487.116916	-487.000795	-487.047626	-487.011638
TS [3+2]	-487.121426	-487.005061	-487.051162	-487.015621

	E_{el}	H_{298}	G_{298}	E_{el}+ ZPE
COOH–CNN–OH	-412.460612	-412.400848	-412.440712	-412.408881
TS [1+2]	-491.043999	-490.928251	-490.975562	-490.939392
TS [3+2]	-491.0438271	-490.927951	-490.974573	-490.938727
CHO–CNN–OH	-337.211036	-337.157555	-337.195182	-337.164890
TS [1+2]	-415.799546	-415.690096	-415.735726	-415.700648
TS [3+2]	-415.796344	-415.686921	-415.731827	-415.697116

Table C-2. Electronic energies, enthalpies, Gibbs free energies, and zero-point energy (ZPE) corrected energies (a.u.) of nitrilimines, tetrafluoroethene, and transition states using B3LYP/6-31+G(d).

	E_{el}	H_{298}	G_{298}	E_{el}+ ZPE
CF_2=CF_2	-475.536440	-475.508906	-475.543028	-475.515141
H–CNN–H	-148.706536	-148.670344	-148.698174	-148.674790
TS [1+2]	-624.224251	-624.160055	-624.205193	-624.170085
TS [3+2]	-624.222395	-624.158201	-624.202127	-624.168063
NH_2–CNN–NH_2	-259.406915	-259.333116	-259.367861	-259.339662
TS [3+2]	-734.937033	-734.835384	-734.885923	-734.847778
F–CNN–F	-347.114990	-347.093678	-347.127900	-347.099524
TS [1+2]	-822.642141	-822.592943	-822.643238	-822.604789
TS [3+2]	-822.638789	-822.58953	-822.639343	-822.601155
OCH_3–CNN–CH_3	-302.542112	-302.43996	-302.480633	-302.448494
TS [1+2]	-778.062520	-777.933176	-777.989784	-777.947709
TS [3+2]	-778.065557	-777.935789	-777.991559	-777.950096
NO_2–CNN–NH_2	-408.533812	-408.473692	-408.513176	-408.481555
TS [1+2]	-884.055747	-883.968164	-884.023379	-883.982155

	E_{el}	H_{298}	G_{298}	E_{el}+ ZPE
TS [3+2]	-884.054826	-883.967157	-884.021596	-883.980989
COOH–CNN–OH	-412.460612	-412.400848	-412.440712	-412.408881
TS [1+2]	-887.980634	-887.893363	-887.948796	-887.907470
TS [3+2]	-887.975150	-887.887713	-887.942641	-887.901615
CHO–CNN–OH	-337.211036	-337.157555	-337.195182	-337.164890
TS [1+2]	-812.732992	-812.651978	-812.705174	-812.665298
TS [3+2]	-812.724747	-812.643786	-812.696711	-812.656979

Table C-3. Electronic energies, enthalpies, Gibbs free energies, and zero-point energy (ZPE) corrected energies (a.u.) of nitrilimines, ethene and transition states using PBE0/6-311++G(2df,pd).

	E_{el}	H_{298}	G_{298}	E_{el}+ ZPE
CH_2=CH_2	-78.508423	-78.453367	-78.478871	-78.457353
H–CNN–H	-148.57896	-148.542497	-148.570268	-148.546933
TS [1+2]	-227.070421	-226.977379	-227.013556	-226.984308
TS [3+2]	-227.076974	-226.984186	-227.019414	-226.990921
NH_2–CNN–NH_2	-259.19299	-259.118584	-259.153598	-259.125206
TS [3+2]	-337.697386	-337.566933	-337.608231	-337.576079
F–CNN–F	-346.863685	-346.841787	-346.875559	-346.847488
TS [1+2]	-425.371349	-425.293438	-425.33531	-425.30219
TS [3+2]	-425.372637	-425.294593	-425.336457	-425.30326

Table C-4. Electronic energies, enthalpies, Gibbs free energies, and zero-point energy (ZPE) corrected energies (a.u.) of nitrilimines, tetrafluoroethene and transition states using PBE0/6-311++G(2df,pd).

	E_{el}	H_{298}	G_{298}	E_{el}+ ZPE
CF_2=CF_2	-475.227369	-475.199199	-475.23307	-475.205304
H–CNN–H	-148.57896	-148.542497	-148.570268	-148.546933
TS [1+2]	-623.788317	-623.723202	-623.767863	-623.733054
TS [3+2]	-623.786645	-623.72155	-623.764994	-623.731218
F–CNN–F	-346.863685	-346.841787	-346.875559	-346.847488
TS [1+2]	-822.086628	-822.036224	-822.085929	-822.047841
TS [3+2]	-822.082891	-822.032474	-822.081734	-822.043875

Table C-5. Selected molecular orbital energies (eV) of nitrilimines, ethene, and tetrafluoroethene from B3LYP/6-31+G(d).

	HOMO	LUMO	LUMO+1	LUMO+2
CH_2=CH_2	–7.55	–0.22		
CF_2=CF_2	–7.63		0.13	
H–CNN–H	–6.83		–0.67	
NH_2–CNN–NH_2	–5.45	–1.76		
F–CNN–F	–8.40		–2.84	
OCH_3–CNN–CH_3	–6.37	0.05		
NO_2–CNN–NH_2	–7.33			–1.69
COOH–CNN–OH	–7.00	–1.98		
CHO–CNN–OH	–6.96	–2.03		

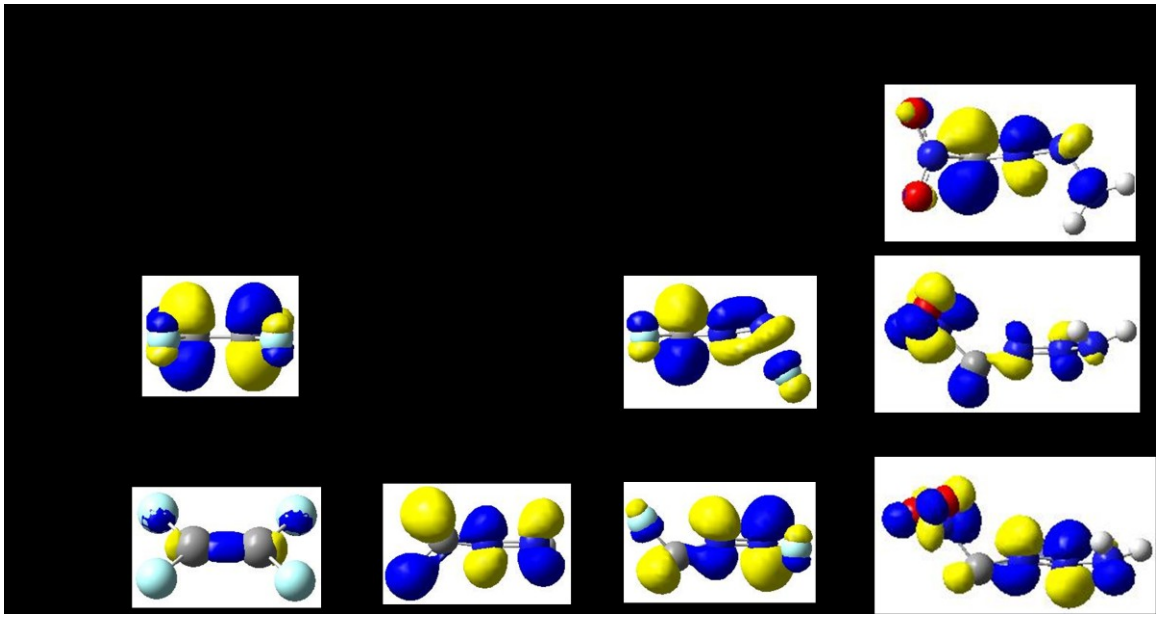

Figure C-1. Lowest unoccupied molecular orbital of nitrilimines with proper phase for molecular bonding.

Table C-6. Electronic energies, enthalpies, Gibbs free energies, and zero-point energy (ZPE) corrected energies (a.u.) of diaminonitrilimine, acetone, and transition state using B3LYP/6-31+G(d).

	E_{el}	H_{298}	G_{298}	E_{el}+ ZPE
CH_3COCH_3	-193.1662608	-193.07602	-193.110494	-193.08233
NH_2–CNN–NH_2	-259.406915	-259.333116	-259.367861	-259.339662
TS [1+2]	-452.5605452	-452.395485	-452.442869	-452.40706

	HOMO	LUMO
CH_3COCH_3	-7.03	-0.75

Table C-7. Absolute value of carbenic contribution in the [1+2] cycloaddition in transition states and ground state using B3LYP/6-31+G(d).

	ethene	4F-ethene	
	[1+2]	[1+2]	Ground State
H–CNN–H	19	17	15
CHO–CNN–OH	7	12	10